Technical Report

TR-00-22

Long term test of buffer material

Final report on the pilot parcels

Ola Karnland, Torbjörn Sandén, Lars-Erik Johannesson
Clay Technology AB

Trygve E Eriksen, Mats Jansson, Susanna Wold
Royal Institute of Technology

Karsten Pedersen, Mehrdad Motamedi
Göteborg University

Bo Rosborg
Studsvik Material AB

December 2000

Svensk Kärnbränslehantering AB
Swedish Nuclear Fuel
and Waste Management Co
Box 5864
SE-102 40 Stockholm Sweden
Tel 08-459 84 00
+46 8 459 84 00
Fax 08-661 57 19
+46 8 661 57 19

Long term test of buffer material

Final report on the pilot parcels

Ola Karnland, Torbjörn Sandén, Lars-Erik Johannesson
Clay Technology AB

Trygve E Eriksen, Mats Jansson, Susanna Wold
Royal Institute of Technology

Karsten Pedersen, Mehrdad Motamedi
Göteborg University

Bo Rosborg
Studsvik Material AB

December 2000

Keywords: bacteria, bentonite, buffer, clay, copper, corrosion, diffusion, field experiment, LOT, mineralogy, montmorillonite, physical properties, repository, Äspö.

Abstract

The "Long Term Test of Buffer Material" (LOT) series at the Äspö HRL aims at checking models and hypotheses for a bentonite buffer material under conditions similar to those in a KBS3 repository. The test series comprises seven test parcels, which are exposed to repository conditions for 1, 5 and 20 years. This report concerns the two completed pilot tests (1-year tests) with respect to construction, field data and laboratory results. Four research groups were engaged in this part of the project working on physical properties - mineralogy, cation diffusion, bacteria and copper corrosion, respectively.

The experimental layout was to place parcels containing heater, central copper tube, pre-compacted bentonite blocks and instruments in vertical boreholes in crystalline rock. The heaters were used for simulating the decay power from spent nuclear fuel at standard KBS3 conditions (S1 parcel, 90°C) and to give adverse conditions (A1 parcel, 130°C). The latter was used in order to accelerate possible processes. Temperature, total pressure, water pressure and water content were measured during the heating period. The two pilot tests were terminated after approximately 12 months of heating, and the parcels were extracted by overlapping core drilling outside the original borehole. The entire 4.5 m long S1-parcel with approximately 20 cm rock cover was successfully lifted in one piece from the rock, whereas the central part of the A1 parcel was lost during drilling. The upper and lower parts were however retrieved.

Reference and exposed bentonite material were analysed with respect to physical properties (triaxial, beam and oedometer tests), and to mineralogical properties (XRD, CEC, ICP-AES and SEM analyses) according to a defined test program. Some precipitation , mainly gypsum, was found in the warmest part of the parcels, and the only unpredicted change was minor uptake of Cu into the clay matrix. An overarching conclusion is that no degrading processes, with respect to buffer performance, were found in the major part of the bentonite as a consequence of the water saturation process and heating for one year. Bentonite plugs containing ^{134}Cs and ^{60}Co, with an activity of 1 MBq, respectively, were placed at defined positions in the bentonite in order to study cation diffusion. Transport in unsaturated bentonite was confirmed to be minimal. The apparent diffusivity of cobalt in the saturated bentonite was measured to be about 2×10^{-9} cm^2 s^{-1}, which is in good agreement with previous experiments. The caesium results, on the other hand, were not possible to accommodate to a diffusion profile, and further investigation will therefore be made. Large numbers of microorganisms, in the range of 10^7–10^9 cells gdw^{-1} clay, were introduced into two blocks as starting concentrations. The material was analysed immediately after mixing, after 72 hours, and after termination of the experiment. All bacteria except for the spore-forming species were eliminated below the detection limits in the exposed parcel material. Small well-characterised copper coupons were placed in the bentonite at a few locations. The coupons were of the same copper quality as proposed for the KBS3 canisters. The mean corrosion rate was calculated to be 3×10^{-6} m per year, which is well in accordance with previous modeling results for oxic conditions. Optical and SEM analyses did not reveal any signs of pitting. A higher copper content was noticed in the bentonite in the vicinity of the copper coupons. Valuable experiences concerning the construction and handling of the test system have been gained during the pilot tests, which are now used in the long-term tests and in the planning of the full-scale tests at Äspö HRL.

Sammanfattning

Försöksserien "Long Term Test of Buffer Material" (LOT) vid Äspölaboratoriet syftar till att utvärdera modeller och hypoteser om fysikaliska egenskaper och mineralogi hos en bentonitbuffert vid förhållanden som kan förväntas råda i ett KBS3-förvar. Testserien omfattar sju försökspaket, vilka utsätts för förvarsförhållanden under 1, 5 och 20 år. Denna rapport avser de två avslutade pilotförsöken (1-årsförsök) med avseende på konstruktion, fältdata och laboratorieresultat. Fyra forskargrupper med respektive inriktning på fysikaliska egenskaper/ mineralogi, katjondiffusion, bakterieaktivitet samt kopparkorrosion var engagerade i denna inledande del av projektet.

Försöksuppställningen var att placera paket innehållande värmare, kopparrör, förkompakterade bentonitblock och instrument i vertikala borrhål i kristallint berg. Värmarna användes för att simulera resteffekten från utbränt kärnbränsle och styrdes till att ge KBS3-förhållanden (S1 paketet, max 90°C), samt för att ge mer aggressiva förhållanden (A1 paketet, ~130°C). Det senare för att accelerera tänkbara processer i bufferten. Under försöket registrerades temperatur, tryck och fuktinnehåll i bentoniten. Pilottesterna avslutades efter cirka 12 månaders värmning, och försökspaketen lösgjordes genom överlappande kärnborrning utanför det ursprungliga borrhålet. Hela det 4.5 m långa S1-paketet och cirka 20 cm bergtäckning lyftes i ett stycke från berget. Den centrala delen av A1-paketet förlorades under friborrningen emedan den undre och övre delen kunde återtas.

Referens och exponerat bentonitmaterial analyserades med avseende på fysikaliska egenskaper (triaxial, balk, och ödometer-tester), och mineralogiska egenskaper (XRD, CEC, ICP-AES och SEM-analyser) enligt ett fastlagt testprogram. Begränsad utfällning, huvudsakligen av gips, noterades i den varmaste delen av försökspaketen. Den enda oförutsedda förändringen var ett litet upptag av koppar i lermatrisen. En övergripande slutsats är att inga degraderande processer, med avseende på bufferfunktion, har kunnat upptäckas i merparten av bentoniten som följd av vattenmättnad och värmepåverkan under ett års tid. Bentonit dopad med ^{134}Cs and ^{60}Co, till en respektive aktivitet på 1 MBq, placerades i bentoniten för att studera katjondiffusion. Försöken bekräftade att transport i omättad bentonit är obetydlig. Den apparenta diffusiviteten för kobolt i den mättade bentoniten uppmättes till omkring 2×10^{-9} cm^2 s^{-1}, vilket är i god överensstämmelse med tidigare försök. Cesiumresultaten däremot var inte möjliga att anpassa till en diffusionsprofil, varför fortsatta undersökningar kommer att genomföras. Ett stort antal mikroorganismer, mellan 10^7 - 10^9 celler per gram torrvikt lera, introducerades i två bentonitblock som startkoncentrationer. Materialet analyserades direkt efter blandning, efter 72 h och efter avslutat försök. Alla bakterier utom sporbildande arter försvann under detektionsgränser i det fältexponerade materialet. Små välkarakteriserade kopparkuponger placerades i bentoniten på några utvalda platser. Kupongerna var av samma kopparkvalitet som föreslås till KBS3-kapseln. Medelkorrosionen efter försöket uppmättes till 3×10^{-6} m/år, vilket är i god överensstämmelse med tidigare modellering av oxiderande förhållanden, och inga tecken på gropfrätning noterades. En förhöjd kopparhalt i bentoniten uppmättes i kopparprovens omedelbara närheten. Värdefulla erfarenheter angående konstruktion och handhavande av testsystemet har erhållits under pilotförsökens genomförande, vilka nu används i långtidsförsöken och vid planeringen av fullskaleförsöken vid Äspö HRL.

Executive summary

Background

Bentonite clay has been proposed as buffer material in several concepts for nuclear high level waste repositories. The favourable bentonite properties are closely related to the interaction between the main mineral montmorillonite and the groundwater. A number of laboratory test series, made by different research groups, have resulted in various buffer performance and alteration models. According to the latter, no major alteration is expected to take place in the buffer at the prevailing conditions in a KBS3 repository neither during, nor after water saturation. The "Long Term Test of Buffer Material" (LOT) series aims at validating models and hypotheses concerning bentonite mineral stability, physical properties and related processes regarding mineralogy, microbiology, cation transport, copper corrosion and gas transport under conditions similar to those in a Swedish KBS3 repository.

The total LOT test series comprises seven test parcels, which will be run for 1, 5 and 20 years. This report concerns the two completed pilot tests (1-year tests) with respect to construction, field data and laboratory results.

Objectives

Four research groups were engaged in the pilot test series in order to study buffer properties and alteration, cation diffusion, bacteria survival, and copper corrosion, respectively. The general objectives of the LOT project may be summarised in the following items:

- Check models concerning buffer performance under quasi-steady state conditions after water saturation, e.g. swelling pressure and cation exchange capacity.
- Produce data concerning gas penetration pressure and gas transport capacity in the buffer.
- Check models on buffer degrading processes, e.g. illitisation and salt enrichment
- Check models for cation diffusion in bentonite.
- Check models concerning survival, activity and migration of bacteria in the buffer.
- Check of models for copper corrosion, and information regarding type of corrosion.

In addition, the pilot tests had the aim to provide experience concerning clay preparation, choice of instruments and materials, data acquisition and evaluation, etc. in order to improve the design of the long term parcels and to serve the Retrieval and Prototype repository projects with information.

Field experimental concept

The test layout was aimed to give as realistic repository conditions as possible except for the smaller scale and the controlled "adverse" conditions in four tests parcels. Adverse conditions in this context refer to high temperatures, high temperature

gradients over the buffer, and additional accessory minerals leading to i.a. high pH and high potassium concentration in clay pore water.

The two pilot parcels were composed of a central heater surrounded by a copper-tube, which in turn was surrounded by approximately 40 highly compacted bentonite cylinder rings in which gauges and various additives were placed (Figure 3-3 p.16). The parcels were placed in core-drilled boreholes with a diameter of 300 mm and a depth of 4 m in diorite rock at a depth of 450 m below ground at the Äspö HRL. The axially compressed cylinder rings had a water ratio of 10%, an initial bulk density of 2080 kg/cm^3, outer diameter of 280 mm, and a height of 100 mm, which give a total bentonite mass of approximately 400 kg in each parcel. The final density of the bentonite clay, at full saturation and after swelling in the test holes, was calculated to be 2000 kg/m^3.

The lower 2 m of the parcels were equipped with heaters, which had a power output of 600 W in one parcel (S1) and of 1000 W in the other (A1). In warmest sections the bentonite temperature was 90°C at the interface with the copper tube and 50°C at the interface with the rock in the S1 parcel, and the corresponding values in the A1 parcel were 130 and 80 C°. In the uppermost part of the 2 parcels the temperature was close to background.

Temperature, total pressure, water pressure and water content were measured during the heating period. Each parcel contained 25 thermocouples, 4 total pressure gauges, 3 water pressure gauges, and 3 relative humidity sensors. The thermocouples were jacketed by Inconel 600 tubing and all other equipment was made of titanium. The sensors were connected to a standard PC-based data acquisition system, and registrations were made regularly every hour.

The two pilot tests were terminated after approximately 12 month of heating, and extracted by overlapping core drilling outside the original borehole. The entire 4.5 m long S1-parcel together with approximately 20 cm rock cover was successfully lifted in one piece from the rock, whereas the central part of the A1 parcel was lost during drilling. The upper and lower parts were however retrieved.

Tests and analyses

The lowest part of the parcels were cut off and transported in one piece to the Department of Chemistry, Nuclear Chemistry, Royal Institute of Technology, Stockholm for tracer analysis. The remaining parts of the parcels were approximately divided up into the original blocks at the test site and placed in airtight plastics. The bacteria inoculated blocks were promptly transported to an un-aerobic box, in which samples were prepared for further transport to the Department of Cell and Molecular Biology, Microbiology, Göteborg University. Blocks containing copper coupons were delivered to Studsvik Material AB, Nyköping, and the remaining blocks were transported to Clay Technology AB, Lund, and further split into test specimens according to a defined test program.

Bentonite mineralogy and physical properties

The loss of material in the A1 parcel precluded the planned analyses concerning combined effects of high temperature and additives, but the tests and analyses concerning material exposed to high and low temperature and cation diffusion were possible to accomplish. The total realised program for the two parcels included the following physical tests and mineralogical analyses (total number within brackets):

- Water ratio of parcel material (210).
- Density of parcel material (75).
- Hydraulic conductivity of reference (10) and parcel material (20).
- Swelling pressure of reference (10) and parcel material (20).
- Tensile strength of reference (10) and parcel material (19).
- Shear strength of reference (1) and parcel material (3).

- ICP-AES element analyses of total and clay fraction, reference (20) and parcel material (50).
- Cation exchange capacity of reference (10) and parcel material (20).
- ICP-AES element analyses of extractable ions of reference (10) and parcel material (20).
- XRD analyses of total and clay fraction, reference (20) and parcel material (50).
- SEM microstructure and element analyses (spot and mapping).

Both water saturation and heat exposure were expected to give relatively small effects on the bentonite. The quality of the analyses with respect to accuracy, precision and generality was therefore important in order to discriminate between small changes and non-detected changes in the exposed material. Much effort was consequently spent on improving the test techniques and to interpret the results.

The data from the reference material show that the natural variation in general is small both with respect to physical properties and mineralogy. Exceptions are significant content variations in illite/mica, feldspar and quartz as measured by XRD analyses. The quality and number of analyses from the original material are believed to be sufficient and to give a solid background for comparison with parcel material.

The most important finding concerning the parcel bentonite is that no degrading processes, with respect to mineralogy and thereby also buffer performance, were found in the major part of the bentonite as a consequence of the water saturation process and heating for one year. However, small but significant changes were found in part of the parcel material. The changes are considered to be results of the water saturation process and no conclusions concerning the effects of long-term exposure to repository conditions can be drawn before data from the ongoing long-term tests are at hand. The main results of the present study may be summarised in the following items:

- No signs of montmorillonite alteration.
- No significant changes in physical properties.
- Minor redistribution of elements along the temperature gradient, e.g. silicon and magnesium.

- Minor increase/decrease of elements in general e.g. sodium, calcium, potassium and copper, indicating ion-exchange processes.
- Precipitation, mainly gypsum, on the copper tube in the warmest section.
- Increase of minerals, mainly gypsum, in the innermost millimetres of the bentonite in the warmest 2 m section.

Observations, which were not related to basic aims with the project:

- The water saturation process in the bentonite seems qualitatively to have taken place in accordance with previous laboratory experiments.
- The rock around the core-drilled test-holes did not effectively distribute water for saturation as shown by the unsaturated lower part of parcel S1.

An overarching conclusion is that no unpredicted changes were found as a result of the exposure to 90 and 130 C° with the exception for a minor uptake of Cu into the clay matrix.

Cation diffusion

Bentonite material containing ^{134}Cs and ^{60}Co, with an activity of 1 MBq, respectively, was placed close to the copper tube in the lower part of the parcels. Both tracers were placed in two diametric positions in block 5, which was located half a meter from bottom of the parcels and exposed to a maximum temperature of approximately 65°C in the S1 parcel and 90°C in the A1 parcel.

The diffusion test volume in the S1 parcel had at termination only slightly higher water content than at test start, i.e. the bentonite was relatively dry with a water activity of around 0.6. The diffusion under such conditions is expected to be very slow and the experiment confirmed that both caesium and cobalt in principle were immobile.

The A1 parcel was fully water saturated and the results significantly different. The cobalt transport was limited, which was to be expected based on the relatively high K_d-values and low diffusivity coefficients found in previous investigations. The values fit well with calculated profiles, indicating that the apparent diffusivity, D_a, was about 2×10^{-9} cm^2 s^{-1}, which is in good agreement with apparent diffusivities obtained in laboratory as well as in CHEMLAB experiments.

The caesium results, on the other hand, were not possible to accommodate to a diffusion profile. Whereas the activity peak in the distance range 0 to 25 mm indicates an apparent diffusivity of 5×10^{-8} cm^2 s^{-1}, the widely spread level of 200-300 Bq/g clearly shows that part of the activity has been more dispersed than expected. Several different explanations to the caesium behaviour have been proposed by the different research groups, e.g. high caesium vapour pressure, intra-layer ionic diffusion, mechanical and geometrical conditions in the bentonite, water evaporating close to the copper tube dragging caesium away.

Most of these explanations are rather far fetched, and no final conclusions should be drawn from this single experiment. The result was though interesting and was one of the main reasons for a repetition of the experiment. Laboratory experiments have also been

started in order to study caesium diffusion at elevated temperature and in a partly saturated bentonite exposed to a temperature gradient.

Bacteria

Microorganisms can grow over a large range of water activities (a_w) down to 0.75, but most favour an a_w of seawater (0.98) or above. The final conditions after water saturation in the LOT bentonite was calculated to have an a_w of 0.96. The water content of the LOT plugs directly after preparation was, however, much lower; only 10% corresponding to an a_w of around 0.75.

Results from previously performed laboratory experiments with Sulphate Reducing Bacteria (SRB) show that the environmental conditions in compacted bentonite clay reduce the number of cultivable SRB by many orders of degree over a 60-day test period (Motamedi et al., 1996). A high reduction rate of cultivable microorganisms was therefore expected in the LOT material.

The original bentonite material, used to produce the bacteria doped plugs, was heat-treated before mixing with bacteria. The clay was analysed before the treatment in order to determine the natural occurring bacteria and after the treatment to get the test starting numbers. The following major results were obtained:

- The natural occurring numbers of cultivable cells were 3.4 x10^4, and <100 cells per gram dry weight (gdw^{-1}), isolated at 30°C, and 65°C, respectively. The bacteria isolated from the clay included a new species of *Bacillus* sp. (CCUG 36961), *Bacillus cereus* (CCUG 36963), *Pseudomonas stutzeri* (CCUG 36965), *Bacillus subtilis* (CCUG 36967) and *Breviabacillus brevis* (CCUG 36969).
- The number of cultivable aerobic bacteria in the heat-treated clay was 1.1 x 10^2, and <100 cells gdw^{-1} determined at 30°C and at 65°C, respectively.
- No SRB were found, neither in the heat-treated, nor in the non-heat-treated clay.

Large numbers of microorganisms, in the range of 10^7–10^9 cells gdw^{-1} clay, were introduced into two blocks as starting concentrations to counteract the harsh conditions in the clay and the hostile conditions during plug preparation. The material was analysed immediately after mixing and the plugs after 72 hours. The following test start conditions were measured:

- Up to 10% of the introduced aerobic bacteria could be cultured from the clay immediately after preparation.
- The cultivability of SRB differed markedly, depending on the species. The best cultivability was observed for *D. nigrificans. D. salexigens* could not be cultivated from the clay and the number of *D. aespoeensis* was down to 7.5% of the initial population.
- Sampling after 72 hours showed that only *D. radiophilus* and the spore-forming species *B. subtilis*, *B. stearothermophilus* and *D. nigrificans* were cultivable.

The number of cultivable cells of aerobic bacteria consequently decreased dramatically after preparation of the plugs, most probably due to the very desiccated and therefore harsh environmental conditions in the plugs. With the exception of *D. radiophilus*, only

spore-forming bacteria could be detected after 72 hours, showing the intolerance of non-spore-forming bacteria to a low a_w.

During the experiment the two blocks were exposed to temperatures ranging from 50–80 °C and around 25°C, respectively. The initial water activity value was 0.75 and the final value was around 0.97. Temperature and water activity co-operated to give a harsher environment in the inner part of the blocks, since water uptake started from the outer mantel surface. After 15 months' exposure of the plugs to the test conditions the following results were obtained:

- All bacteria except for the spore-forming species were eliminated below the detection limits.
- The numbers of cultivable aerobic bacteria from the plugs in the high temperature block were below detection limit (< 100 cells gdw^{-1}) for all investigated species.
- *B. subtilis* and *B. stearothermophilus* could be isolated from the plugs originally containing aerobic bacteria in the low temperature block and *B. subtilis* was also cultivated from one of the plugs in the high temperature block.
- In the plugs containing SRB, only *D. nigrificans* could be cultured.

High temperature obviously added a significant constraint to the cultivability of the introduced microorganisms, i.e. the spores.

The viability of bacterial spores generally show a specific declination rate that may be large or negligible, as a function of a range of spore and environmental characteristics. The results in this study have given detailed information on the interaction between bacteria and the buffer material under repository like conditions.

Copper corrosion

Small well-characterised copper coupons were placed in the bentonite at a few locations. The coupons were of the same copper quality as proposed for the canisters. In total 12 copper coupons were used for the study; 4 were placed in parcel S1, 4 in parcel A1, and 4 were kept as reference.

The visual inspection after field exposure did not reveal any significant differences between the surfaces of the copper tubes and the copper coupons, with the exception of the mineral precipitation on the warmest parts of the tubes. The following basic observations were made concerning the copper coupons:

- The entire plate surface was affected.
- The corrosion attack was uneven.
- The optical and SEM micrographs did, however, not reveal any signs of pitting.

The mean corrosion rate was calculated to be 3×10^{-6} m/y, based on the mass loss of an exposed sample and a reference sample after removal of corrosion products. This is well in accordance with previous modeling, indicating conservative corrosion rates of 2×10^{-8} and 7×10^{-6} m/y for anoxic and oxic conditions, respectively.

The corrosion pattern was rather complicated and several types of corrosion products were present e.g. Cuprite (Cu_2O), and Malachite, ($Cu_2CO_3(OH)_2$). A detailed XRD analysis is therefore planned for on the coupons placed in the A0 parcel.

A higher copper content was noticed in the bentonite in the vicinity of the copper coupons. A significant increase in copper content was found a few microns from the copper surface. Indication of an increase compared to reference samples was found tens of microns from coupon A according to SEM analyses. The ICP/AES analyses of the solid total material showed a maximum copper content in the first centimetre of up to 100 ppm and a mean value of around 25 ppm at a distance of 3 cm from the tube.

An uptake of copper into the bentonite, of the order and character found in this study, is expected to be negligible for both the canister and the buffer material.

Additional

Valuable experiences concerning the construction and handling have been gained during the pilot tests, which now are used in the long-term tests and in the planning of the full-scale tests. The most important items may be summarised in the following way:

- Unintentionally the large-scale effect of high salinity and reduced mechanical support for the bentonite was experienced in the release operation of the A1 parcel which led to a major loss of material during the drilling operation.
- Alloys, which are corrosion resistant under oxic conditions, are not necessarily well suited for the buffer conditions.
- Corrosion problems can be avoided by the use of titanium. Machining of titanium sensors have been developed.
- Technique for preparation, handling and instrumentation of bentonite blocks has been developed.
- The Datascan hardware and Orchestrater software data collection system have been adapted to the needs and found sufficient for most instruments and for alarm functions.
- A system for data handling and presentation of field data has been developed.

Contents

List of figures

List of tables

1 Background

1.1 General

Bentonite clay has been proposed as buffer material in several concepts for HLW repositories. In the Swedish KBS3 concept the demands on the bentonite buffer are to serve as mechanical support for the canister, reduce the effects on the canister of a possible rock displacement, and minimise water flow over the deposition holes. The transport through the buffer is expected to be reduced principally to diffusion, both with respect to corrosive components in the groundwater and to corrosion products and escaping radionuclides in case of a canister failure.

Comprehensive research and development work has been carried out during the last twenty years in order to determine the basic behaviour of unaltered bentonite material. The results have been reported in technical reports, and tentative computer codes concerning both unsaturated and saturated buffer conditions are at hand (e.g. Börgesson et al. 1995). The models are believed to well describe the function of an unaltered MX-80 bentonite buffer after water saturation with respect to physical properties, e.g. swelling pressure, hydraulic conductivity and rheological behaviour. Further, techniques for bentonite block production and application have been developed in order to fulfil the requirements concerning density, homogeneity, handling etc. (Johannesson 1995).

The decaying power from the spent fuel in the HLW canisters will increase temperature and initially give rise to a thermal gradient over the bentonite buffer by which original water will be redistributed parallel to an uptake of water from the surrounding rock. A number of laboratory test series, made by different research groups, have resulted in various buffer alteration models. According to these models no significant alteration of the buffer is expected to take place at the prevailing physico-chemical conditions in a KBS3 repository neither during nor after water saturation. The models may to a certain degree be validated in long term field tests. Former large scale field tests in Sweden, Canada, Switzerland and Japan have in different respects deviated from possible KBS3 repository conditions and the testing periods have generally been dominated by initial processes, i.e. water uptake and temperature increase.

The present test series is consequently focused on the long term performance of the bentonite buffer, i.e. the conditions after water saturation, and on buffer related processes in a water saturated bentonite buffer concerning microbiology, cation transport, copper corrosion and gas transport. Long term in this context does of course not refer to the full time span of a repository. However, a considerable part of the heating period in a KBS3 repository is being covered with respect to kinetic reactions by the use of adverse conditions in four of the test parcels.

This report concerns the two pilot tests, A1 and S1, with respect to:

- Background
- Construction
- Field tests
- Laboratory tests and analyses of bentonite
- Cation diffusion test

- Bacteria test
- Copper corrosion test

1.2 Organisation

The project was initiated and fully financed by SKB and has been a co-operation between the following four groups:

- Bentonite, construction and project management; Ola Karnland, Torbjörn Sandén, Lars-Erik Johannesson, Harald Hökmark, Reza Goudarzi and David Gunnarsson, Clay Technology AB, Lund, Mikael Erlström, SGU, Lund, and John Algers, Inorganic Chemistry, Lund University.

- Bacteria; Karsten Pedersen, Mehrdad Mutamedi, Farideh Taherinejad, Agneta Welin, Nadi Jahromi and Berit Ertman Ericsson, Department of Cell and Molecular Biology, Microbiology, Göteborg University.

- Cation diffusion; Trygve Eriksen, Kjell Svärdström, Mats Jansson and Susanna Wold, Department of Chemistry, Nuclear Chemistry, Royal Institute of Technology (KTH), Stockholm.

- Copper corrosion; Bo Rosborg, Hans Erikssson, Jiaxin Chen, Camilla Hansson and Kurt Norrgård, Studsvik Material AB, Nyköping.

Gunnar Ramqvist was on-site coordinator, Tomas Karlsson was responsible for the field data acquisition system, Ebbe Eriksson for data handling and Masueto Morosino for contacts with authorities concerning the radioactive tests, all stationed at Äspö HRL.

At test site Kjell Svärdström, KTH and Nils-Göran Myrén, NCC carried out indispensable work, and the project management also like to give prominence to the entire staff at the Äspö HRL, who in different ways have contributed to the project.

2 Objectives

2.1 General

The bentonite buffer material in the KBS3 concept is a natural mixture of smectite and several common minerals, e.g. quartz, feldspar, calcite, siderite and pyrite. A fundamental demand on the buffer is that the desirable physico-chemical properties are preserved to a large extent during the lifetime of the repository. These properties e.g. low hydraulic conductivity, swelling ability and suitable rheological behaviour, are mainly determined by the interaction between water and the smectite component in bentonite, which usually is montmorillonite. The stability of the montmorillonite mineral is therefore of vital importance for the buffer performance and the main aim with this study.

The test layout also made it possible to study other important processes in the canister-buffer-rock system, such as bacteria activity, tracer element transport, copper corrosion and gas transport.

Description of specific issues is given in the following sections. The general objectives may be summarised in the following items:

- Data for validation of models concerning buffer performance under quasi-steady state conditions after water saturation, e.g. swelling pressure, hydraulic conductivity and rheological properties.
- Check of existing models concerning buffer degrading processes, e.g. illitisation and salt enrichment.
- Produce data concerning "critical gas penetration pressure" and gas transport capacity.
- Check of existing models concerning cation diffusion in bentonite.
- Information concerning survival, activity and migration of bacteria in bentonite.
- Check of calculated data concerning copper corrosion, and information regarding type of corrosion.
- Information, which may facilitate the realisation of the full-scale test series (e.g. the Prototype project) with respect to clay preparation, instrumentation, data handling and evaluation.

The results from the present two "pilot tests" are not expected to give information on all of the above items, but more, together with the reference material, serve as a starting point with which the following long-term tests result will be compared.

2.2 Physical buffer properties

The clay/water system in a KBS3-type repository is expected to have well known physical properties. Vital properties for the buffer function are swelling pressure, hydraulic conductivity and plasticity. These properties are mainly determined by the interaction between the montmorillonite part of the buffer and water, and the properties may be expressed as a function of the final density of the buffer. A large number of data

from laboratory tests are available in reports produced by SKB and corresponding organisations in other counties (e.g. NAGRA, AECL, ENRESA, PNC).

The main hypotheses in the pilot part of the project are that initial swelling pressure, hydraulic conductivity and plasticity of the water saturated bentonite material are well described and possible to predict for a KBS3-like construction by present models. Main aspects of tests and analyses are to check that compaction, placement and water saturation in a KBS3-type construction do not significantly change the physical properties of the buffer.

2.3 Buffer stability

2.3.1 General

The clay/water system in a KBS3-type repository can not generally be supposed to be in chemical equilibrium with the surrounding groundwater in crystalline rock. The elevated temperature and temperature gradients during the initial period will also affect the equilibrium conditions in the buffer/water system. Consequently, different alteration processes have been studied with respect to repository conditions, but also with respect to other applications, especially in oil industry and a large number of data have been published over the last 50 years.

The concept of buffer alteration may be divided into the following three quite different categories:

- Clay mineral (montmorillonite) alteration
- Clay surface reactions
- Accessory mineral alteration

Depending on the overall conditions all three types of alteration may result in changed physical properties.

The clay mineral reactions in a KBS3-repository system are generally considered to be very slow in relation to the lifetime of a repository, and no major changes are expected, neither in clay mineral structure nor in physical properties. The following possible alteration processes have been of special interest for repository conditions, and have previously been intensively studied in both laboratory tests and in natural analogues.

2.3.2 Smectite-to-illite conversion

Depending on the conditions, alteration of minerals in the smectite group may take place and form a number of related minerals, e.g. illite, chlorite or zeolites. In nature the most common smectite alteration at elevated temperature is transformation into illite. This type of conversion has also been considered as the most probable, or rather least improbable, under repository conditions. Fortunately the smectite-to-illite reaction has been extensively studied for several decades because of its relevance to oil prospecting. Different parameters have been proposed as kinetic controlling factors but there is no basic consensus on the reactions involved in the conversion. Based on geological

analogues and laboratory experiments i.a. the following factors have been proposed as kinetic controlling factors (no ranking):

- Overburden pressure (Weaver 1959)
- Temperature (Perry and Hower 1970)
- Potassium activity (Hower 1976)
- Aluminium activity (Boles and Frank 1979)
- pH (Eberl 1993)
- Dehydration (Couture 1985, Karnland 1994)
- Silica activity (Abercrombie 1994)

According to the Huang, Longo and Pevear model (1993), the overall kinetics of the smectite-to-illite reaction can be described by the equation:

$$-dS/dt = A\cdot[K^+]\cdot S^2 \cdot \exp(-E_a/RT)\ , \qquad 2\text{-}1$$

where S is the smectite fraction in the illite/smectite material, A is frequency factor, E_a is activation energy and R is the universal gas constant, and T is temperature. After integration of eq. 2-1, the smectite content at a certain time can be calculated if the temperature and potassium concentration in the pore water are known. The potassium concentrations in the Äspö groundwater are measured to be in the range of a few ppm up to 80 ppm (Nilsson 1994). According to the model, practically no clay conversion is possible in a KBS3-type repository at these conditions as shown in Figure 2-1.

However, the reaction relationship and the constants are determined from relatively short-term laboratory experiments at temperatures significantly higher than repository conditions (250-325°C), and from geological analogues, which differ from repository conditions in several aspects. The uncertainty in calculated conversion increases with the difference in temperature between test condition and calculated condition (Karnland 1995). Maximum conservative constants as evaluated from the Huang et al. experiments and a very high potassium concentration was used to calculate the conversion in Figure 2-2. The conservative high potassium concentration 0.1M was calculated as a free release from potassium feldspar at pH 4 according to Aagard (1983). The hypothetic low pH was based on discussion by Grauer 1986 and laboratory tests with MX-80 bentonite at high temperatures (Pusch 1991).

The present tests aim at checking the model constants (activation energy and frequency factor) in experiments performed at ”as repository like conditions” as possible. No changes are expected at repository conditions and the main aim is to check that the reaction is not substantially faster than predicted by the model by use of moderate temperature increase (130°C) and high potassium concentration.

In order to avoid misunderstandings it should be mentioned that the transport of potassium, which is considered as one of the major hindrances for illitisation, is leaped over by the technique to add potassium used in the adverse condition tests (Hökmark 1995, Karnland 1995).

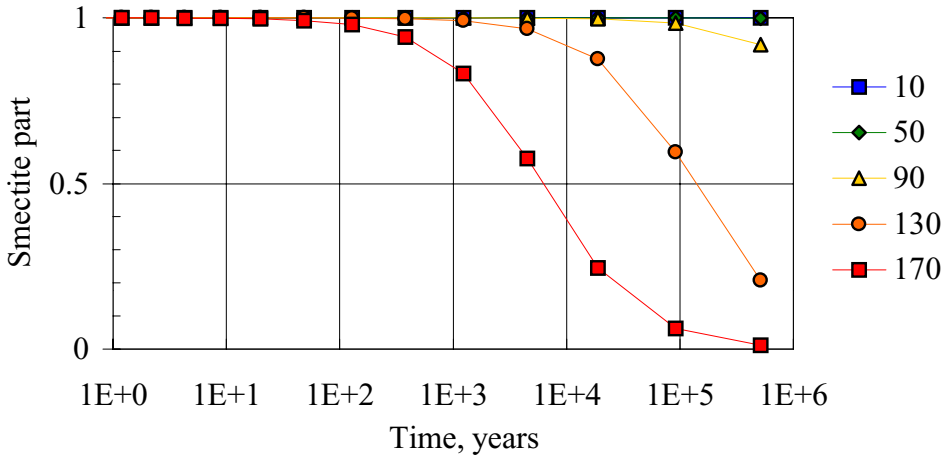

Figure 2-1 *Remaining smectite part for different temperatures in a hydrothermal system with $[K^+]$ = 0.002 mole/litre (80 ppm) according to the Huang et al. kinetic model and laboratory determined constants (E_a = 27.4 kcal/mole and A = 8.5E4).*

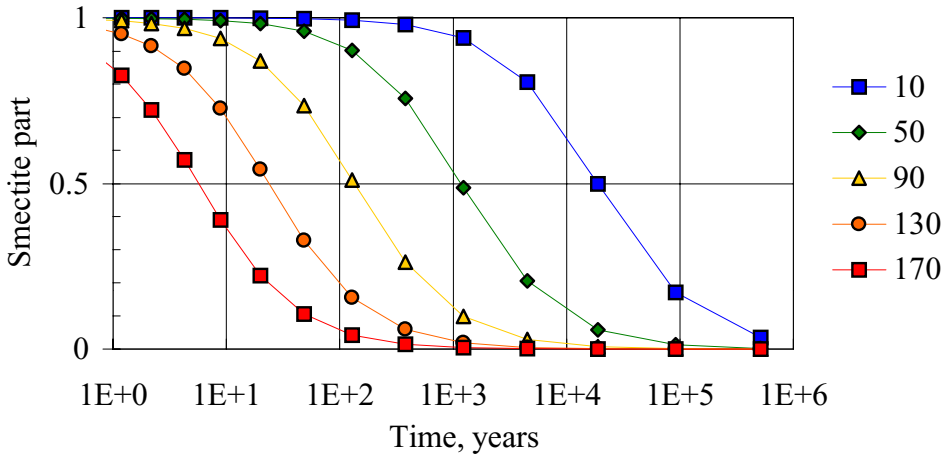

Figure 2-2 *Remaining smectite part for different temperatures in a hydrothermal system with $[K^+]$ = 0.1 mole/litre according to the Huang et al. kinetic model and maximum conservative constants according to laboratory tests (E_a = 12.6 kcal/mole and A = 0.095.)*

Table 2-1 **Calculated smectite-to-illite conversion at high K^+ concentration (0.1M), according to the Huang et al. model, by use of proposed constants and evaluated maximum conservative constants according to Karnland 1995. Result figures are expressed in % illite.**

Constants	Time	Temperature			
	years	50°C	90°C	130°C	170°C
Proposed	1	0.0	0.0	0.0	0.0
	5	0.0	0.0	0.0	0.1
	10	0.0	0.0	0.0	0.2
Conservative	1	0.1	0.7	4.1	15.0
	5	0.4	3.6	17.5	46.8
	10	0.8	6.9	29.7	63.7

2.3.3 Dissolution and neoformation of accessory minerals

The temperature gradient, which prevails over the buffer during the first part of the deposition period, may affect the buffer functions by different enrichment processes of dissolved substances, with e.g. changed rheological properties (cementation) as a consequence (Pusch 1992). One such process is ion transport parallel to water uptake from the outer cooler parts of the bentonite, or from the surrounding groundwater, to the wetting front in the originally unsaturated bentonite. The transport is assumed to take place by a cyclic evaporation/condensation process in which water is sucked in from cooler parts, evaporates at the wetting front, and is partly redistributed in the form of steam. Dissolved salts will thereby be deposited at the wetting front.

A second possible process is precipitation of specimens, which have lower solubility at higher temperature, e.g. calcium sulphate (gypsum) and calcium carbonate (calcite). This process may take place also in a fully saturated bentonite and the potential problem is consequently larger. If the buffer material is the source of the original pore water concentration, the process will come to a standstill after a limited enrichment, which is easily calculated. On the other hand, if the surrounding groundwater is the cause of the pore water concentration, the enrichment process may continue until a major part of the pore volume is filled by the neoformed mineral.

According to laboratory experiments the following conditions reduces enrichment of easily dissolved minerals in a bentonite buffer (Karnland 1995:2).

- High buffer density, no enrichment at buffer conditions (2000 kg/m^3),
- Low content of accessory minerals in the buffer,
- Low electrolyte content in the surrounding water,
- High water pressure.

The use of pre-saturated bentonite blocks, supply of low electrolyte water in open slots, and a fast restoration of the hydrostatic pressure are consequently considered in a KBS3-repository in order to reduce mineral redistribution and enrichment.

In the present test series the initial water content has not been increased and the slots were filled with groundwater in order to have conservative test conditions. The conditions varied partly by controlled actions, and partly by the natural variation in boundary conditions. Temperature, content of accessory minerals and salinity have been controlled and higher compared to KBS3 conditions in the adverse condition parcels.

The hypotheses are that precipitation will be negligible and that no major cementation processes will take place at normal repository conditions. The tests and analyses were expected to give qualitative and quantitative data concerning possible precipitation and changes in rheology.

2.3.4 Effects of cement pore water

Possible effects on the bentonite of an exposure to cement pore water are believed to be (Eberl 1993, Karnland 1997):

- Replacement of the original charge balancing cation i.e. sodium against calcium.
- Cementation of the bentonite due to precipitation of cement matter (e.g. calcium-silica-hydrates and calcite) in clay pore space.
- Attack on the accessory minerals (cristobalite) in the bentonite.
- Alteration of clay mineral lattice due to the induced high pH.

The hypothesis is that bentonite under repository conditions resists short-term attack from cement pore water without major alteration. The main aspect is to confirm results from laboratory experiments showing ion exchange, minor mineral dissolution-neoformation and no clay lattice alteration (Karnland 1997).

2.4 Microbiology

The survival of bacteria in bentonite has been suggested to depend on the water activity (a_w). Laboratory tests have shown that two different species of sulphate reducing bacteria were killed when the a_w was decreased to 0.96, corresponding to the conditions in an unpressurised and fully saturated clay at a density of 2000 kg/m^3 (Motamedi et al, 1995). It may, however, be argued that other, more halotolerant sulphate reducing bacteria could survive and be active.

The main hypothesis is that bacterial survival is governed by water activity/induced swelling pressure. The low water activity/high swelling pressure in compacted bentonite around waste canisters is expected to act as a strong limiting factor for bacterial survival and activity, thereby reducing or eliminating the risk for bacterial production of gas and corrosive metabolic products.

It has been argued that bacteria should be able to colonise the buffer from the groundwater. The presence of viable bacteria in deep clay sediment is usually interpreted as if the bacteria were mixed in with the clay during burial. Theoretically, the pore size of compacted bentonite is far to small for bacteria but convincing evidence is missing. The pore size is in the nanometer range, which makes contamination of a compacted buffer with microorganisms, migrating into the buffer from groundwater, improbable.

2.5 Cation migration

The diffusion of radionuclides in compacted bentonite has been studied rather extensively in laboratory experiments with synthetic groundwater. The pore water diffusion model, generally used to interpret the experimental data, is based on the assumption that diffusion takes place in pore water and is retarded by sorption of the diffusing species on the solid phase. This model is adequate for cations sorbed on the solid phase by surface compexation mechanisms, e.g. Co^{2+}. For cationic species sorbed by ion exchange, e.g. Cs^+ and Sr^{2+}, experimental data indicate an additional diffusion

mechanism in which migration takes place within the electrical double layers next to the mineral surface. The diffusivities of Cs^+ and Co^{2+} in compacted bentonite saturated with groundwater of different ionic strength (salinity) are rather well documented at room temperature and, in principle, it should be possible to model the diffusive transport of these cations in the actual bentonite system.

The main hypothesis is that cation transport may take place by two different transport mechanisms i.e. solely by diffusion in the pore water and by an additional migration within the electrical double layers next to the mineral surface.

A difference in diffusive transport is expected between cations sorbed by surface complexation mechanisms e.g. Co^{2+} and cationic species sorbed by ion exchange e.g. Cs^+ and Sr^{2+}. A faster transport is therefore expected to take place for the latter cations.

2.6 Copper corrosion

The corrosion rate of the canister is in principle determined by the chemical reactivity at the canister surface and the mass transfer from and to this surface. For a specific canister, the rate depends on the geochemical conditions of the nearfield, i.e. the type, content and mobility of dissolved constituents in the surrounding bentonite buffer. Thermodynamic calculations show that alteration products of copper are stable and that the corrosion process is expected to be affected by the redox conditions of the clay medium (Wersin, 1993).

In general there are different types of uncertainties associated with estimation of the corrosion rate of copper in bentonite:

- Model validity
- Time scale of oxic/anoxic transition
- Pitting factor
- Transport properties of the clay

Modelling which takes into account diffusive transport in addition to flow, equilibrium reactions and kinetic processes at the bentonite-canister interface has been made (Wersin 1994). The results indicate conservative corrosion rates of 2×10^{-8} and 7×10^{-6} m/y for anoxic and oxic conditions, respectively. A sensitivity analysis indicates that the main uncertainties arise from the diffusion properties of the clay.

The testing aims at determining the mean corrosion rate, and identify possible pitting and corrosion products. The main hypothesis is that the mean corrosion rate under oxic conditions will be less than $7\cdot10^{-6}$ m/y.

2.7 Gas transport

No gas pressure tests were included in the pilot tests because of the short time between full water saturation and termination of the tests.

3 Experimental concept

3.1 General

3.1.1 Principles

The LOT test series may be described as a multi-task experiment in which test parcels are exposed to conditions similar to those in a KBS3-repository and to conditions, which accelerate alteration processes, respectively. The test parcels contain prefabricated bentonite blocks placed around a copper tube, which are placed in vertical boreholes in a granitic rock structure. At tests termination the parcels are extracted by overlapping core drilling around the original borehole, and the parcels are lifted and partitioned. Material from defined positions in the test parcels and reference material are thereafter examined by a general, well-defined set of tests and analyses in order to provide data for the different objectives.

The dimensions of the parcels are kept considerably smaller, especially the diameter, compared to a KBS3 deposition hole in order to:

- Shorten the water saturation period and thereby have saturated condition during a substantial part of the test period
- Get a higher temperature gradient over the buffer material
- Facilitate sampling, i.e. release and lift the exposed test parcel in one piece

3.1.2 Adverse conditions

Mineralogical stability of the bentonite clay is one of the grounds for the choice of bentonite as buffer material. Nevertheless, alteration processes will take place in the buffer but are predicted to be very slow under KBS3 repository conditions. In order to study expected processes, and to search for overlooked processes, in the relatively short duration time of the experiments, the following accelerating conditions compared to KBS3 conditions are used:

- Higher temperature,
- Higher temperature gradient,
- Higher content of accessory minerals (calcite, gypsum, K-feldspar),
- Introduction of new substances (Portland cement).

The expected effect of these accelerating conditions (buffer adverse conditions) may be summarised in the following discussion.

The initial reaction rate of a reaction

$$aA + bB \rightarrow \text{products} \qquad 3\text{-}1$$

can be described by the standard rate law

$$\text{Rate} = k\,[A]^n\,[B]^m \qquad 3\text{-}2$$

where n and m are constants, and k is a rate constant which can be expressed by the Arrhenius relationship

$$k = zp \cdot \exp(-E_a / RT) , \qquad 3\text{-}3$$

where z is the collision frequency factor, p is the steric factor, and E_a is activation energy and R is the gas constant.

This reaction rate theory consequently implies:

- Reaction rate increases with increasing concentration of a reactant,
- Reaction rate increases with increasing temperature,
- Temperature increase effect is reduced with increasing temperature,
- Temperature effect increases with increasing activation energy.

A rule of thumb is that a temperature increase of 10K gives a doubled reaction rate. A slow reaction rate is normally due to high activation energy, which means that the effect of temperature is more pronounced for slow reactions. E.g. in the case of illitisation a rather high activation energy is measured by Huang et al. (114700 J/mole), and a temperature increase of 10 K results in a close to tripled reaction rate. The increase from maximum temperature in the KBS3 buffer to the maximum temperature in the adverse conditions parcels (130°C) leads to an increased illitisation reaction rate of around 40 times. Further, hundred years after deposition the most conservative assumption (uppermost curve in Figure 3-1) concerning water saturation gives a calculated maximum temperature increase of around 60°C in a KBS3 repository, and the corresponding temperature after 1000 years is 40°C (Arfvidsson, in print). A comparison between the 130°C in the adverse condition parcel and a constant bentonite temperature of 70°C (60°C increase plus background) gives a reaction rate factor of almost 400 times. In a KBS3 repository outermost part of the bentonite will be exposed temperatures shown in the lowermost curve in Figure 3-1, i.e. substantially lower temperatures. In a 5-year test, only the effect of increased temperature in the A parcels will accordingly simulate the major period of elevated temperature in a KBS3 repository, with respect to kinetically governed processes.

Consequently, the LOT tests can be expected to show the effects of processes governed by the kinetics of the involved reactions. The introduction of additional substances and increased temperature gradients is made in order to accelerate also processes, which are governed by transport of substances. The effect of the temperature gradient is, however, not possible to describe in an, as simple and general way, as the effect of increased temperature and concentrations of reactants.

The adverse conditions do not accelerate possible reactions, which contain elements that are not present in the buffer or in the introduced substances. The reaction rate will then be governed by the diffusive transport of the substances into the reaction zone. A special case is also possible reactions governed by the concentration of the reaction products. The kinetics of product precipitation or the diffusive transport of the products from the reaction zone governs such reactions. The adverse conditions do not accelerate such processes generally, although this likely is the case for e.g. quartz precipitation due to the higher temperature.

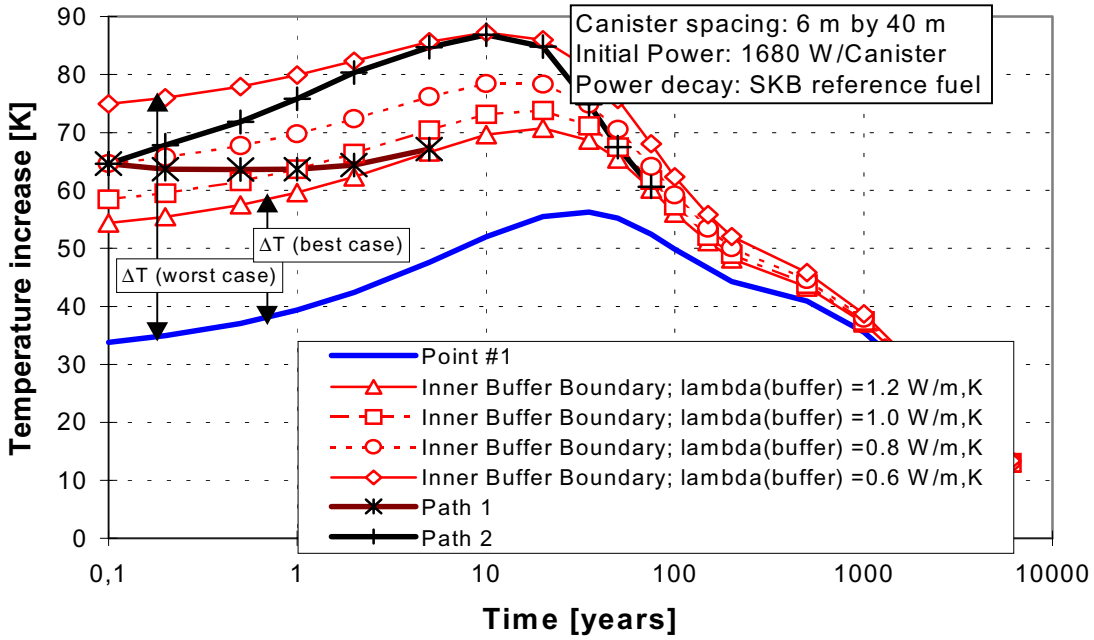

Figure 3-1 *Temperature evolution in the buffer in a KBS3 repository for a number of assumptions regarding the effective buffer heat conductivity according to Arfvidsson. Point #1 represents outer buffer boundary (rock side).*

3.2 Experimental configuration

3.2.1 Test program

In total, the test series includes 7 test parcels (Table 3-1) of which 3 are exposed to standard KBS-3 conditions, mainly in order to study unaltered buffer material, and 4 test parcels which are exposed to adverse conditions mainly in order to check models for buffer alteration. This section concerns the construction of the two pilot test parcels A1 and S1.

Table 3-1 **Test program for the ”Long Term Test of Buffer Material” series.**

A = adverse conditions
T = temperature
pH = high pH from cement
S = standard conditions
$[K^+]$ = potassium concentration
am = accessory minerals added

Type	No.	max T, °C	Controlled parameter	Time, years	Remark
A	**1**	**130**	**T, $[K^+]$, pH, am**	**1**	**pilot test**
A	0	120-150	T, $[K^+]$, pH, am	1	main test
A	2	120-150	T, $[K^+]$, pH, am	5	main test
A	3	120-150	T	5	main test
S	**1**	**90**	**T**	**1**	**pilot test**
S	2	90	T	5	main test
S	3	90	T	>>5	main test

3.3 Test site

3.3.1 General

The niche on the south side of the TBM tunnel at 3385 m from the tunnel entrance, i.e. opposite side of the TBM tunnel from the lowest elevator stop was used for the 2 one year pilot tests (Figure 3-2). The depth from surface is around 450 m and the rock consists mainly of Äspö diorite and greenstone, which are crossed by some pegmatite and bands of fine-grained granite. Several visible water-bearing fractures make the area relatively wet. Approximately 3 m of the eastern part of the niche was cleaned from filling material and the surface was levelled off by use of concrete in order to support a drilling machine.

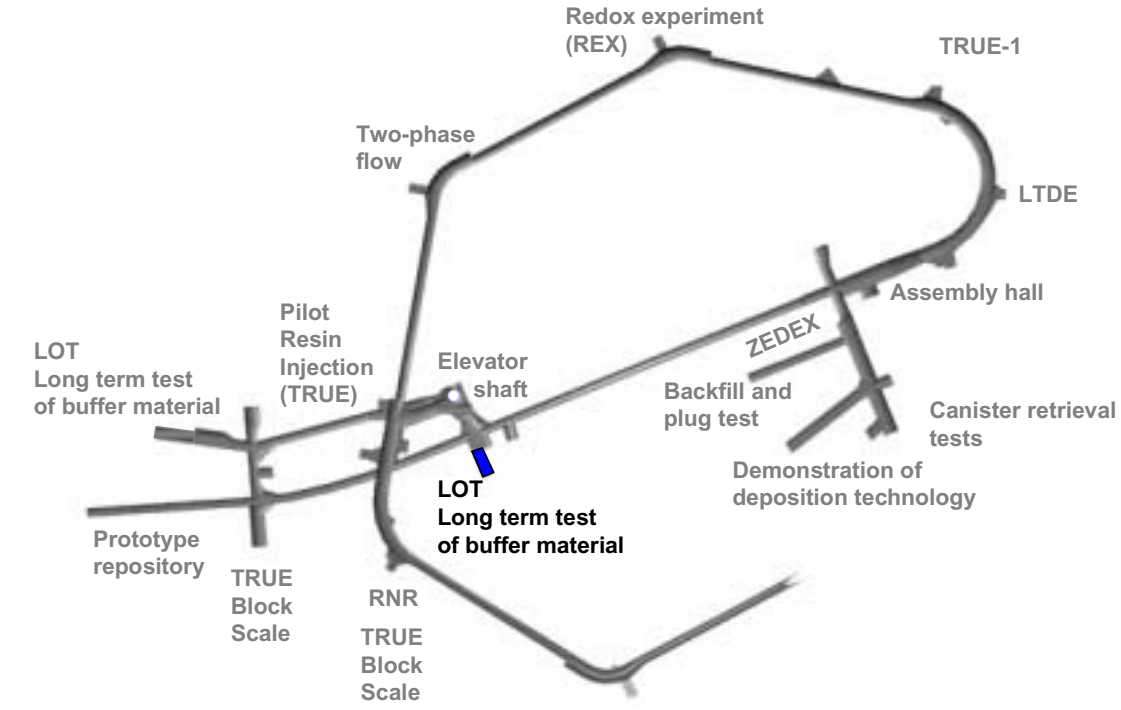

Figure 3-2 Test sites in the lower part of the Äspö tunnel. The pilot test site is shown in the centre.

3.3.2 Pilot holes

Two 86 mm pilot holes were drilled to a depth of approximately 5.7 m in order to check the suitability of the rock with respect to water flow and water pressure. The holes were placed approximately 2 m from the eastern wall and a relative distance of approximately 3 m. The holes were named 1 (northern hole) and 2 (southern hole).

No suitability criteria were defined but the water pressure in the lower part of the holes had to be higher than the vapour pressure at the chosen test temperature. Further, water inflow had to be sufficiently low to allow the emplacement of the test parcels and to exclude the risk of piping and erosion after closure. A reasonable guess was that an inflow of 1 litre per minute could be accepted provided that the water pressure could be kept low in the upper part of the test hole. Packers, mechanical manometers and

graduated glass were used to determine the water flow and pressure. An obvious interaction between the two holes was noticed, which was not considered as a major problem since it was expected to give conservative (lower) values with respect to water pressure compared to the test conditions.

In pilot hole no 1 the water pressure was approximately 1000 kPa below a packer position at 2.15 m under the upper concrete surface, and above this position values from 250 to 0 kPa were found. The total inflow below the lower packer position was approximately 50 ml/minute. In pilot hole no 2 the water pressure was 600 kPa below a packer position down at 1.8 m and 540 kPa below a packer position down at 1.4 m. The total water inflow below the lower packer position was approximately 470 ml/minute.

Core examinations were made and showed that several water-bearing fractures were present in both holes. The general conclusions from the examinations were that the holes were possible to use, and that hole no 2 likely was most suited for the A1 test since the water pressure was sufficiently high (above 300 kPa at 2 m depth) and that the pressure drop took place at a higher level than in hole no 1.

3.3.3 Test holes

The two pilot holes were over-cored by core drilling in order to give test holes with a diameter of 300 mm to a depth of 4 m. The test holes were named as follows according to the standard Äspö database nomenclature:

KXBLOTS1 (pilot hole no 1) and KXBLOTA1 (pilot hole no 2),

where K stands for core drilled hole, X for experiment, B for bentonite/buffer type of experiment, LOT for the experimental series, A for adverse test conditions and S for standard conditions, and finally 1 for the first experiment of the type.

The cores were compared with the pilot cores and the test holes were inspected by use of core television technique (BIPS). The diameter and the straightness of the test holes were checked and found sufficient. The upper part of the holes had a diameter, which exceeded 300 mm by up to 10 mm.

The inflow in hole KXBLOTA1 was checked in conjunction with the emplacement of the A1 parcel. A mean inflow rate of 2 litres per minute was measured during natural filling of the hole, which accordingly was significantly higher than in the pilot 86 mm hole.

Additional information is given in the SKB report PR HRL-97-30 concerning the bibs-data, fractures, mineralogy, core sample pictures, etc.

3.4 Test parcel construction

3.4.1 General

The basic demand for the test parcel construction was to keep a defined maximum temperature in the central part of the clay column during the test time span. An important part of the system was therefore the temperature measurement and power regulation system. A central heater inside an open tube was chosen, since this allows for heater change during the test period in case of a failure. The central tube was made of copper in order to have the system as similar as possible to the KBS3 concept with respect to chemical conditions.

The two pilot test parcels (S1 and A1) were in principle identical constructions, except for a number of different additives at specific locations in the bentonite blocks in the A1 parcel (Figure 3-3 and 3-4). The heater, central tubes, bentonite blocks and instrumentation are individually described in the forthcoming sections.

3.4.2 Heater

Specially designed electric heaters from Backer Elektro-värme AB, Sösdala, were used. The total length was 4650 mm, and the active bottom part had a length of 2000 mm. Three individual stainless steel (SS2348) elements with a diameter of 14 mm were brazed into a stainless steel (SS2343) flange, which was designed in order to let the heater hang down from the support of the upper part of the copper tube. The maximum power was decided to be 2 kW (230/400 V, AC), i.e. each element has a maximum power of 667 W (230 V) corresponding to 0.7 W/cm^2. The expected power need was based on scoping calculations made by MICROFIELD finite element computer code performed by Harald Hökmark. The calculations were made by applying axi-symetric geometry and a thermal conductivity of the bentonite in the range of 0.8 to 1.5 W/mK (dry and wet conditions), 3.0 W/mK for the rock and 390 W/mK for copper. The calculations were made both for adiabatic conditions and for fixed boundary conditions in 3 m radius geometry.

3.4.3 Central tubes

The canister simulating copper tube (SS 5015-04) had a length of 4700 mm, an inner diameter of 100 mm and a wall thickness of 4 mm. At the bottom end a copper plate and 4 copper reinforcement elements were brazed by use of soldering silver. A detachable lifting device was placed at the top of the tube during the placement. The possible external pressure acting on the outside of the central tube was expected to be less than 10 MPa (bentonite swelling pressure plus hydrostatic water pressure), which correspond to a maximum compression stress of 140 MPa acting at the inner radius. The used hard-drawn copper quality has a yield point exceeding 200 MPa, which consequently was sufficient. Still an inner steel tube (SS1650) was placed inside the copper tube, because of the uncertainty of the effects of the brazing, and of the relatively high test temperatures. The purpose was to protect the heater from mechanical damage in case of unexpected buckling of the copper tube.

It was of vital importance for the heater/tube function and for the mass transport that no leakage into the tube takes place. The impenetrability was therefore tested after the soldering by use of a helium source inside the copper tube and an external detector.

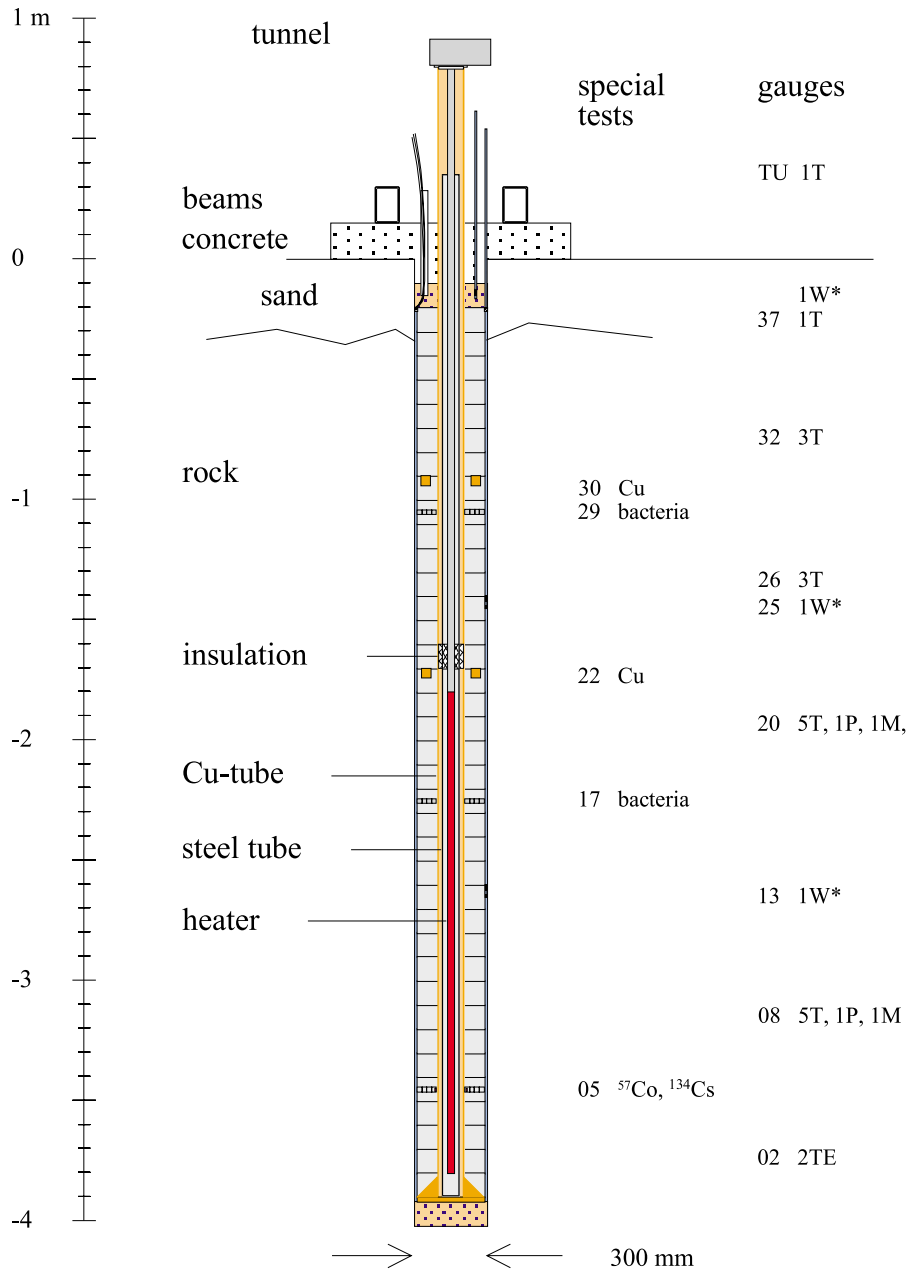

Figure 3-3 Explanatory sketch of the S1 parcel. Abbreviations are explained in section 3.5.

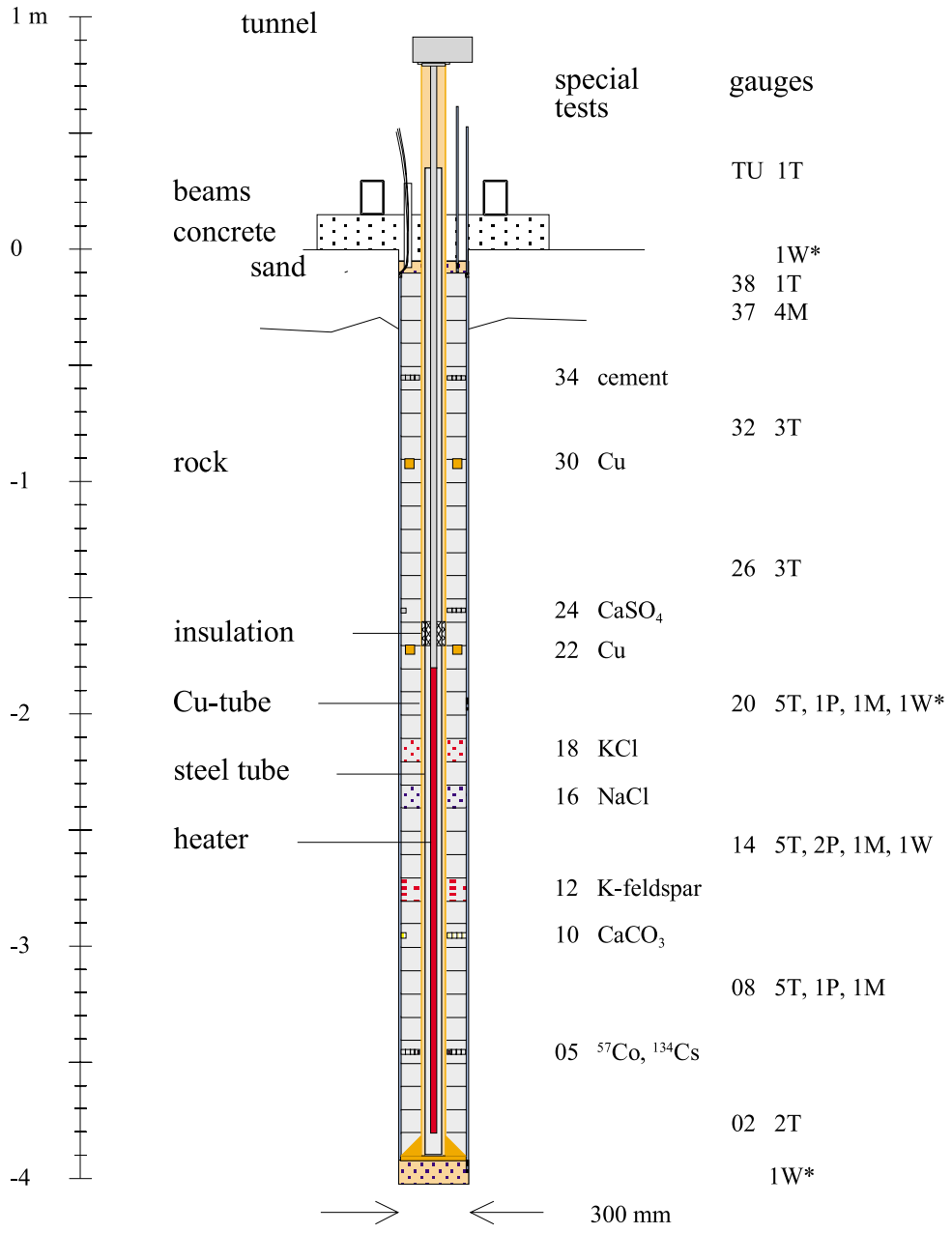

Figure 3-4 *Explanatory sketch of the A1 test parcel. Abbreviations are explained in section 3.5.*

3.4.4 Blocks

Wyoming bentonite sold under the commercial name MX-80 was the source material for all bentonite components in the system. It was delivered by Askania AB and produced by Volclay LTD, Mersyside, UK. The material was delivered in 25 kg sacks in one consignment.

The material is dominated by natural sodium montmorillonite clay (~ 75% by weight), which is responsible for the desired physical properties. The rest consists of quartz (~15%), feldspars (~7%), carbonates (~1.4%) sulphides (~0.3%), organic carbon (~0.4%). Dispersed in distilled water the clay fraction (d < 2 μm), make up around 80%, of which 90-95% are in the minus 0.2 μm fraction after active dispersion. The mean mineralogical composition of the montmorillonite part is given by:

$(Al_{3.10}\ Fe^{3+}_{0.4}\ Fe^{2+}_{0.02}\ Mg_{0.48})$	$(Si_{7.92}\ Al_{0.08})$	$O_{20}\ (OH)_4$	$Na_{0.48}\ Ca_{0.04}\ Mg_{0.02}$
octahedral cations	tetrahedral cations	structural O/OH	exchangeable cations

The cation exchange capacity is around 0.8 eq/kg bulk material and around 1.1 eq/kg clay in the minus 2μm fraction. The natural exchangeable cations are sodium (~85%), calcium (~10%), magnesium (~4%) and small amounts of potassium (~0.3%). The specific surface area is around 550 m^2/gram material and the grain density is around 2.75 g/cm^3 (Müller-Vonmoos, 1983).

The different blocks and plugs, which were used, may be divided in the following groups:

- Standard blocks with maximum diameter of 281 mm and a height of 100 mm.
- Special blocks, which were prepared from standard blocks, with excavations for reinforcements, instruments, copper plates or 20 mm test plugs.
- Special blocks with additives, in which the bentonite was mixed with different additives in the entire block and compacted to the same density as the standard blocks.
- 20 mm diameter bentonite plugs with or without additives, used in the tracer tests, the bacteria tests, and accessory mineral enrichment tests.

The choice of block compaction technique was based on experiences from previous SKB projects concerning block production (Johannesson 1995). A new uniaxial compaction device was constructed in order to make it possible to produce blocks with the accurate dimensions, density and composition. A slight axial conic form, and chamfered edges between mantle and end sides were used in order to facilitate the expulsion after compaction and to avoid subsequent stress induced cracks (Figure 3-5).

The bentonite material was compacted without pre-treatment. Water content was checked in each 25 kg sack in order to determine the exact amount of solid bentonite in each block batch. The governing figure for the production was the final density in the test hole after expansion by water uptake. A possible value for a KBS3 repository is 2000 kg/m^3 with an accepted divergence of ± 50 kg/cm^3 (SKB, SR 97). The accomplished calculations were made by use of a bentonite solid density of 2750 kg/m^3, a mean block radius of 139.3 mm and an inner radius of 56 mm, a borehole radius of 150 mm and copper tube radius of 54 mm.

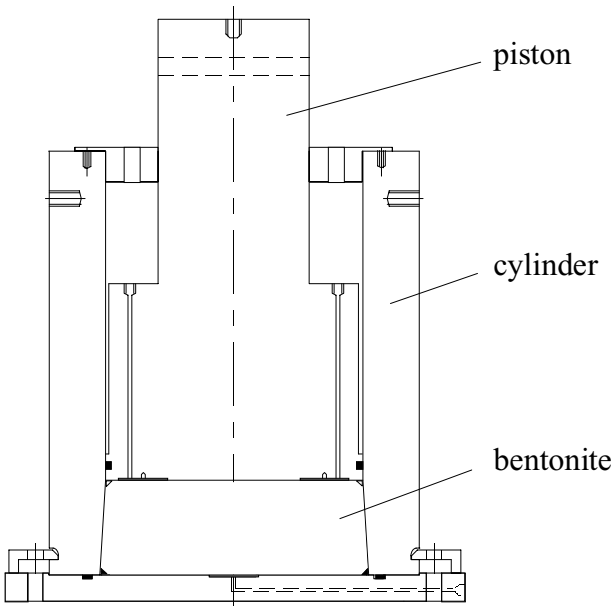

Figure 3-5 Explanatory sketch of the block production device. The conical form is exaggerated in the drawing. The mean minimum was 277 mm and mean maximum diameter was 281 mm.

Two extra blocks were made in the production series in order to be dissected and analysed with respect to homogeneity. For each produced block, approximately 250 g of the same material, i.e. from the same 25 kg sack, was marked and stored as reference material for background analyses. The following items describe the pressing technique sequence:

- Removal of the piston
- Pouring in a defined mass of bentonite, taking actual water content into account
- Reserve 250 g reference material in a closed plastic jar
- Replacement of the piston
- Reduction of air pressure in the system by use of a vacuum pump
- Placement of the compaction device in the hydraulic press
- Constant speed loading the press up to 100 MPa compaction pressure
- Increase of air pressure in the system
- Removal of the bottom plate
- Expulsion of the block
- Visual inspection of the produced block
- Measurement of mass and dimensions, notations
- Drilling the central hole (diameter 112 mm)
- Wrapping up the block in plastics
- Marking of block and reference material
- Storage in controlled conditions with respect to temperature and humidity

The 3 special blocks with additives in the A1 parcel were compacted in the same way as the standard blocks with the exception that a defined part of the bentonite mass was exchanged for the same mass of the various additives. The additives were 25% K/Na-feldspar, 10% KCl and 7.5% NaCl (all by weight). The purpose of adding potassium to the bentonite was to study possible transformation of the montmorillonite component

into illite. The amount of KCl was calculated to supply the bentonite with an amount of potassium, which correspond to a total conversion. The amount of NaCl was calculated to correspond to KCl with respect to the amount of cations.

The blocks predestined for gauges or plugs were made from standard blocks by drilling and carving out the necessary volume. The bentonite material is well suited for this technique and the produced unintentional gaps between the gauges and plugs on the one hand and the bentonite on the other are small and insignificant with respect to the final buffer density (Figure 3-6). Special blocks produced for the S1 parcel:

02 excavations for 2 thermocouples
05 20 mm cylindrical holes for tracer tests
08 excavations for 5 thermocouples, 2 total pressure gauges, 1 water pressure gauge, 1 relative humidity gauge
14 excavations for 5 thermocouples, 2 total pressure gauges, 1 water pressure gauge, 1 relative humidity gauge
17 20 mm cylindrical holes for bacteria tests
20 excavations for 5 thermocouples, 1 total pressure gauges, 1 relative humidity gauge
22 excavations for 4 copper plates
26 excavations for 3 thermocouples
29 20 mm cylindrical holes for bacteria doped plugs
30 excavation for 4 copper plates
32 excavations for 3 thermocouples
36 excavations for 1 thermocouples, 1 water pressure gauge

Special blocks produced for the A1 parcel:

02 excavations for 2 thermocouples
05 20 mm cylindrical holes for tracer tests
08 excavations for 5 thermocouples, 2 total pressure gauges, 1 water pressure gauge, 1 relative humidity gauge
10 excavations for 3×3 plugs of 5% of $CaCO_3$ and 3 plugs of 25% of $CaCO_3$
12 mixture of 25% of K-feldspar and bentonite to the same density as the standard block
14 excavations for 5 thermocouples, 2 total pressure gauges, 1 water pressure gauge, 1 relative humidity gauge
16 mixture of 7.5% of NaCl and bentonite to the same density as the standard block
18 mixture of 10% of KCl and bentonite to the standard block density
20 excavations for 5 thermocouples, 1 total pressure gauges, 1 relative humidity gauge
22 excavations for 2 copper plates, marked G and H
24 excavations for 3×3 plugs of 5% of $CaSO_4$ and 3 plugs of 25% of $CaSO_4$
26 excavations for 3 thermocouples
30 excavation for 2 copper plates, marked E and F
32 excavations for 3 thermocouples
34 excavations for 8 plugs of Aalborg White Portland cement (wct = 0.8)
36 excavations for 1 thermocouples, 1 water pressure gauge

In addition, the bottom blocks had excavations for the copper reinforcement.

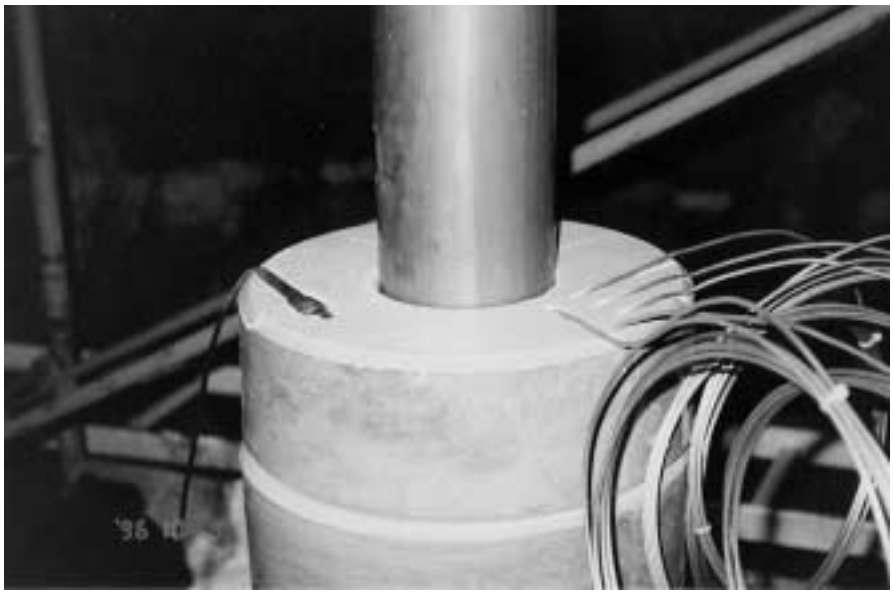

Figure 3-6 Gauges and thermocouples placed in excavations in block S108. The instruments were kept in place only by the subsequent blocks.

All blocks were given a specific denomination and placed at defined positions in the test parcels according to - block no S103 - referring to parcel S1 and third (03) block counted from bottom of the parcel.

The blocks were theoretically partitioned in 9 sections in order to get a system for orchestrating and sampling. The fist section ranging from the inner mantel surface and 1 cm outwards was termed section 0, and the following volume, i.e. between 1 and 2 cm from the inner mantel surface, was termed section 1, etc. The last section at the emplacement was consequently 8, and this section only had an extension outwards of 6 mm. After swelling, due to water uptake, section 8 represented the volume between 8 and 9 cm from the inner mantel surface, and a new clay section, i.e. no 9, with an extension of approximately 6 mm was formed. Furthermore, the point of the compass was used to describe the horizontal orientation.

3.4.5 Test plugs

All bentonite-containing plugs had a cylindrical form with a length and diameter of 20 mm. They were compacted in a laboratory compaction device working by the same principle as the block compaction device. The plugs were compacted to a density corresponding to the standard density of 2000 kg/cm^3 after full water saturation regardless of the additives. The compaction was accordingly controlled by the final sample volume and not by the maximum compaction pressure.

The plugs were placed in cylindrical holes, which were drilled from the mantle surface into the specified blocks halfway between, and parallel to, the end surfaces. The hole diameter was constantly around 21 mm, while the depth depended on the purpose of the test. The outer plugs were sprayed with a small amount of de-ionised water before they were inserted into the test holes in order to let the bentonite swell and thereby seal up the slots. The positions of the plugs were marked by millimetre thick titanium wires inserted into drilled holes, which were placed 20 mm above the centre of the plugs. Two

wires marked the northern position, and one wire marked the other 3 main directions of compass.

Two types of calcite containing plugs were produced for the A1 test parcel. One type containing 5% and the other containing 25% (by weight). The calcite material was a finely ground pure quality which was thoroughly mixed with the bentonite and compacted to the defined density. Cylindrical holes were drilled from the mantle surface into block A110 from the west, north and south side to a depth of 30 mm and from the south side to a depth of 70 mm. Three plugs with the lower calcite content were inserted into the longer hole, and one plug with the higher content was inserted into each of the shallow ones. All four holes were sealed with a slightly wetted half plug in the outer 10 mm.

Two types of gypsum containing plugs were produced for the A1 test parcel. One type containing 5% and the other containing 25% (by weight) of gypsum. The used $CaSO_4$ (0.5 hydrate) material was a finely ground pure quality which was thoroughly mixed with the bentonite and compacted to the defined density. Cylindrical holes were drilled from the mantle surface into block A124 from the west, north and south side to a depth of 30 mm and from the south side to a depth of 70 mm. Three plugs with the lower gypsum content were inserted into the longer hole, and one plug with the higher content was inserted into each of the shallow ones. All four holes were sealed with a slightly wetted half plug in the outer 10 mm.

8 plugs were cast to a cement water ratio (cwt) of 0.8 by use of an Aalborg white Portland cement and de-ionised water. The cement was allowed to harden in water for 14 days before the emplacement. Two cylindrical holes were drilled into block A134 from the north and from the south side to a depth of 80 mm. Four plugs were placed in each hole. Neither marks nor sealing were used.

Four identical tracer doped plugs were produced (Chapter 6). A few cubic millimetres of bentonite were ion-exchanged to contain 1 MBq of ^{57}Co and ^{134}Cs, respectively. The prepared material was placed in the centre of the bentonite plugs. Cylindrical holes were drilled from the north and south side into the mantle surface in block S105 and A105. The diameter of the holes was 21 mm and the depth was 80 mm, meaning that there was approximately 3 mm left to the inner radius of the cylinder ring. The initial total distance between the copper tube and the tracers were consequently approximately 15 mm. The tracer doped plugs were placed into the block during the submerging of the parcels.

32 bentonite plugs doped with bacteria were produced for use in the S1 parcel. The plugs were divided in two series; one containing 3 types of anaerobic bacteria and the other 5 types of aerobic bacteria (Chapter 7). The bentonite was prepared by spraying a nutrient solution, containing the actual viable bacteria, over the calculated amount of bentonite material. The mixture was thoroughly mixed and compacted to a semidry plug. The plugs were kept in closed test tubes (50 ml Falcon tubes) until just before the emplacement in the designated bentonite blocks at the test site. All handling of the plugs was made by use of sterile equipment in order to reduce the risk for contamination. Cylindrical holes were drilled from the four cardinal points into the mantle surface in block S117 and S129. The depth of the holes was 80 mm, implying that there was approximately 3 mm bentonite left to the inner radius of the cylinder ring. The bacteria

doped plugs were placed into the bentonite blocks approximately half an hour before the S1 parcel was submerged.

3.4.6 Copper samples

Two copper samples were placed in block S122, S130, A122 and A130, respectively (Chapter 8). Slots were drilled and sawed from the upper side of the blocks and the copper samples were placed in the blocks during the pile up of the bentonite column. The samples were cut by travelling-wire electric discharge machining by Outokumpu Poricopper Oy, Finland, which kindly placed the samples at our disposal.

3.5 Instrumentation

3.5.1 General

The basic aim for the field activity in the LOT tests was to expose the bentonite clay to conditions similar to those in a KBS-3 repository and to expose the clay to adverse physico-chemical conditions, with i.a. respect to temperature. A fundamental demand was therefore to measure the temperature in order to regulate the power, and to register the obtained temperature distribution in the parcels. An important objective with the LOT pilot series was to test equipment for use in the forthcoming long term tests and full scale buffer tests at Äspö. The above mentioned in combination with the relatively limited volume in the clay and the potential risk for artefacts due to the instrumentation led to the following compromise about instrumentation of the two parcels, respectively:

- 25 thermocouples,
- 4 total pressure gauges,
- 1 water pressure gauge,
- 3 water filters equipped with external gauges,
- 3 relative humidity sensors,

The gauges and sensors were placed in the parcels as shown in Figure 3-3 & 3-4 and were termed in accordance with the following example:

S1084P where

S1 describe the test character (S for standard) and the number of the test,
08 indicate block number counted from the bottom,
4 specifies the position in the block (according to section 3.4.3),
P specify the type of measuring equipment.

The following specification of measuring equipment was used:

E temperature in the pressure gauges ,
M relative humidity sensors,
P total pressure gauges,
T thermocouples,
W water pressure gauges.

3.5.2 Thermocouples

The thermocouples were delivered by Hereaus Electro-Nite AB, Lidingö. All were of type K according to IEC 584 standard. The measuring soldering spots were isolated by inconel alloy which also jackets the wires up to the tunnel from where a PVC insulation was used. The diameter of the jackets was 3 mm, the lengths were 2, 4 or 5 m, and the length of the PVC parts was 20 m.

The placing strategy was to concentrate the thermocouples in the clay volume around the heater in order to monitor the temperature gradient over the buffer in detail. Consequently, thermocouples were placed in position 0, 2, 4, 6, and 8 in the blocks 08, 14, and 20. Below the most interesting sections, two thermocouples were placed in position 0 and 8 in block 02. And above, three thermocouples were placed in position 0, 4 and 8 in blocks 26 and 32. All measuring soldering points were placed from the upper surface of the blocks, into pre-drilled holes, down to a depth of 35 mm. The jackets were easily formed and placed in the blocks as shown in Figure 3-6 in order to reduce the problem with the heat transport outwards in the jackets.

Calibration is generally not needed for thermocouples, however, a function control was made by connecting all thermocouples were connected to the actual test data collecting system and the measuring soldering spots were first placed in room temperature and subsequently in ice-water and the measured temperatures were registered.

3.5.3 Pressure gauges

The pressure gauges were delivered by Kulite Benelux BV and termed HKM-86-375MT-100BAR-SG. The housing was made of titanium and the gauges were connected to the data scan units by 20 m Teflon cables equipped with high pressure seals (10 MPa). The working pressure range was 0 to 10 MPa. A fifth wire in each transducer made it possible to register the temperature, which was used for automatic temperature compensation in the range of 0 to 120°C. One gauge, in each test parcel, was equipped with a titanium filter in front of the diaphragm in order to measure water pressure only. All pressure transducers were individually calibrated to check the delivery calibration data. Detailed description of the calibration is given in the installation report SKB PR HRL-97-30.

3.5.4 Moisture gauges

The relative humidity sensors were delivered by BFI-IBEXA Nordic AB and termed IH-3602-L. Cylindrical titanium housings were manufactured in order to physically protect the sensors. The moisture exchange between the sensors and the surrounding clay took place through round titanium filters placed at the end of the housing.

All moisture gauges were individually calibrated in order to check the delivery calibration data both with respect to relative humidity and to temperature dependence. The sensors were connected to the actual data collecting system, including all cables etc.. The gauges were placed in specially designed plastic boxes which were partly filled with different saturated salt solutions. A fan was used in each box to ensure that no moisture or temperature stratification took place within the boxes. Saturated

solutions of $(NH_4)_2SO_4$, KCl, $BaCl_2$ and KH_2PO_4 were used. The temperature was kept at 22°C and the equilibrium relative humidity 81.2, 84.8, 90.4 and 94%, respectively, were used for the calibration. The results were plotted and a linear function (RH=k×U+l) was determined for each transducer individually.

The $BaCl_2$ solution was also used for the temperature compensation calibration, since the humidity equilibrium is relatively stable in the examined temperature range. Temperatures close to 40, 50 and 60°C were used and a linear function, describing apparent dRH as a function of T, was determined for each sensor. Significant differences between the factory calibration and the Clay Technology laboratory calibration were noticed both with respect to relative humidity and to temperature. The combined effect for the actual test data results in a maximum difference of about 5% RH. Detailed data of the calibration is given in the installation report SKB PR HRL-97-30.

3.5.5 Data collection and registration system

All measuring sensors and gauges were connected to DATASCAN 7000 units, which in turn were connected to a Compac 166 MHz computer working under Windows NT. The software was named Orchestrator and was manufactured by Eurosoft Technology, UK. MSS AB, Åkersberga, delivered the software and DATASCAN units. The program had a range of output/input drivers and real time data acquisition which i.a. admitted the use of event-governed logging in addition to periodic logging and alarm functions. The standard logging interval was set to 1 hour during the entire test period.

4 Field operation

4.1 Preparation

4.1.1 Parcel assembly

The entire parcel systems were prepared and checked in laboratories in Lund, dismantled and loaded on to a lorry for transport to Äspö HRL. At the test site, the water in the test holes were pumped and the bottom part was filled with sand up to approximately 10 cm from the bottom. The deeper 86 mm central pilot holes were thereby also filled with sand. The copper tube was fixed at a bottom support and the predestined blocks were thread onto the tube from above one by one from a scaffold (Figure 4-1). The gauges and sensors were placed in the prepared cavities before the successive block was placed. The instruments were fixed in position only by overlying blocks without additional equipment. The cables were not fixed to the clay column in order to admit movements during the subsequent swelling of the bentonite. The various plugs were placed in position after all bentonite blocks were in position. The plugs were fixed and sealed by adding a small amount of water on the outer plug surface before they were pressed into position. The tracer test plugs were the lasts to be placed in order to reduce the exposure to radiation. The block joints in the bottom meter of the columns were smeared on with bentonite paste to prevent a fast water penetration through minor gaps. The entire mounting procedure of one parcel at the test site was achieved within one day, since the parcel was constructed as a ”building kit”.

4.1.2 Installation

The top of the copper tube was connected to the lift device of a crane lorry and the parcel was slightly heaved and the bottom support was removed. The test hole was again emptied on water and the parcel was carefully centred and slowly lowered into the test hole. The total submergence procedures took approximately 10 to 15 minutes and the only incident was minor tangle with cables in the S1 parcel, since these were pre-connected to the measuring system. The filter equipped tubes for water pressure measurement were placed after the submergence in the S1 test-hole and before in the A1 test-hole. The change was made since the cables partly hindered the placement in the former hole. Further, the tubes enabled pumping water during the emplacement, which was necessary because of the large water inflow in the A1 hole. In each hole the upper slot between the bentonite and the rock was caulked by use of mineral insulation (Rockwool) in order not to let sand penetrate downwards. An approximately 10 cm thick sand layer was placed on top of the clay column and the cables were brought together and placed within plastic tubes. The uppermost 10 cm of the test-hole and a square-formed concrete top plug were cast. After hardening, the plug was prevented from heaving, due to bentonite swelling and water pressure, by use of two steel beams, which in turn was fixed by 4 rock bolts (Figure 4-2). The S1 parcel was put in place Thursday 10th of October 10, 1996, and the A1 Saturday 16th of November 1996.

Figure 4-1 Mounting of the S1 parcel at test site.

Figure 4-2 Final appearance of the pilot test site after installation.

A few days after the emplacement of the A1 test parcel a clay gel oozed out through the plastic tubes on top of the concrete plug. The relatively large water inflow into the A1 test-hole, in combination with the course of initial bentonite swelling, were assumed to

be the reasons. The test hole was likely partly sealed by the swelling bentonite to make a water pressure build up possible, and the bentonite was still loose enough to be pressed out along the cables through the plastic tubes (also section 4.3.2). No action was taken since the flow was assumed to stop by the progressive bentonite swelling. The flow was successively reduced and fully stopped after a few additional days. The total volume loss was estimated to be less than 5 litres and the water ratio of the squeezed out clay gel was determined to be around 200%. The total loss of bentonite was consequently around 1.5 kg which is considered insignificant since the total initial block mass was 361 kg.

4.2 Heating phase

4.2.1 Temperature control

There are in principle two main options to control the temperature in this kind of tests, i.e. regulation of the heater power to a fixed value, or to regulate the power to give a defined temperature at a certain position. The former method best simulates the real conditions of spent fuel and the latter ensures a defined maximum temperature. Since the tests were not aimed to simulate initial repository conditions but to examine the effects of temperature related processes the temperature-based regulation was used from test start. A mean value of the three thermocouples 08T1, 14T1 and 20T1 in the respective tests were used to govern the power in such a way that the final mean temperature was kept at 90°C in the S1 parcel and at 130°C in the A1 parcel. At test start the target temperature was increased in relatively small steps (10 to 15°C) to further ensure that no over-heating took place. The heating of the S1 parcel started October 30, 1996, and the final increase to reach defined temperature was made November 20. The corresponding dates for the A1 parcel were December 4, 1996 and January 15, 1997. Some minor starting problems with the regulation system were noticed in the S1 parcel, which led to relatively large oscillation of the temperature before stabilising at the defined value (Figure 4-3).

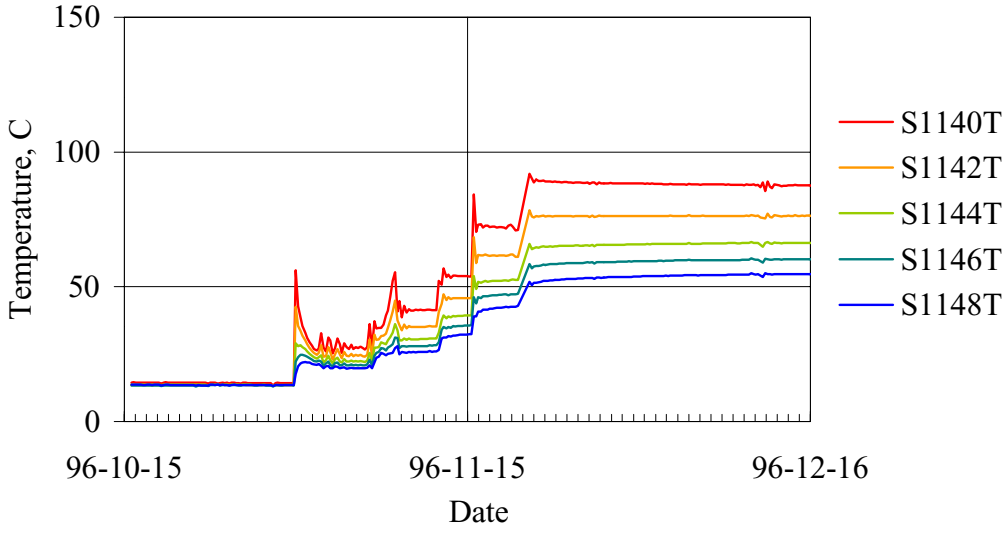

Figure 4-3 *Temperature recordings from block 14 in parcel S1 during the temperature increase period. The last figure shows the radial distance from the copper tube, where 0 represents the distance 0 to 1 cm, 2 represents 2 to 3 cm, etc.*

No further problem of significance was experienced during the test period. In mid March 1997 the regulation was changed to fixed power in order to get a safer system and to follow the temperature development under constant power conditions. Based on the previous recorded data, which corresponded well with scoping calculations, the power was determined to be 600 W in the S1 parcel, and 1000 W in the A1 parcel.

4.2.2 Measuring principles

A standard interval of 1 hour was used for all collection of data since the course of events was expected to be relatively slow. In addition, an event governed data collection was programmed for each type of measuring equipment. The triggering measuring event was exceeding or falling short of a fixed value, or a fixed interval related to the previous measured value. The configuration was made in such a way that all channels related to the test was read off if an event-triggered measurement was started by a single instrument.

The recording and real time handling of data may be divided in three levels of importance. The handling of data used for regulating the system was of course most important since a malfunction may have lead to a fast destruction of the system. Of second most importance were the data needed for the evaluation of the test conditions, and finally there is a group of data which is of general interest but which is not necessary for the accomplishment of the tests series. In consequence, several levels of alarm function were used in the monitoring system. Depending on the type of released alarm different measures were stipulated, ranging from simple notes to immediate actions from the safety guard organisation at the Simpevarp nuclear plant.

All recorded data were stored in the specific project computer and backup was regularly made on a separate hard disc. The standard recorded data concerning temperature, pressure and humidity were copied approximately once a month and sent to Clay Technology. The data were processed by means of MS EXCEL and are stored on CD-ROMs and in the SICADA database. All data are stored as raw data in the original form, and as “treated data”, in which:

- Time has been calculated from date
- Project gauge names have been introduced
- Appropriate gauge sequence has been introduced
- Zero-recordings have been sorted out

4.2.3 Results from heating period

Temperature

The recorded temperature data give an extensive picture of the temperature distribution during the course for both parcels. The results are in reasonable agreement with the scoping calculations with respect to necessary power and temperature distribution. During the period of temperature regulation, a typical reduction in the temperature gradient in the radial direction was noticed, and after the change to power regulation, an expected small increase in maximum temperature was noticed. The latter may be

explained as an effect of temperature increase in the surrounding rock, since equilibrium was not reached. Figure 4-4 shows the temperature distribution in the two parcels at April 30 1997, which approximately represents the condition at the change to power regulation.

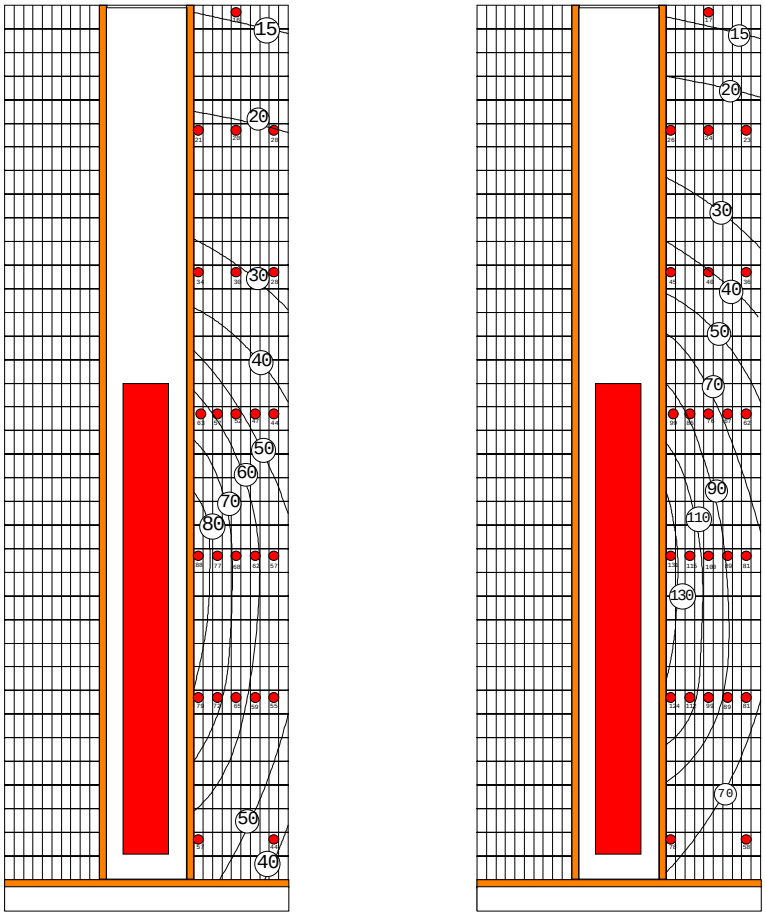

Figure 4-4 *Temperature distribution in parcel S1 (left) and A1 (right) April 30, which approximately represents mid test period. Horizontal scale is exaggerated.*

Figures 4-5 to 4-8 show the temperature development in the two parcels during the whole test period. The long-term temperature conditions in the tunnel may be tracked down in the S1 parcel, at least, to block 20, which imply 2 m down into the parcel. Notable is also a constant temperature increase in all positions in block 08 in the S1 parcel. The same tendency may in principle be found also in the A1 parcel.

One thermocouple in the S1 parcel and 3 placed in the A1 parcel stopped functioning during the test period. None of these were placed in the hottest positions at the respective levels. Damages, which were interpreted as corrosion, were found on some of these sensors after termination

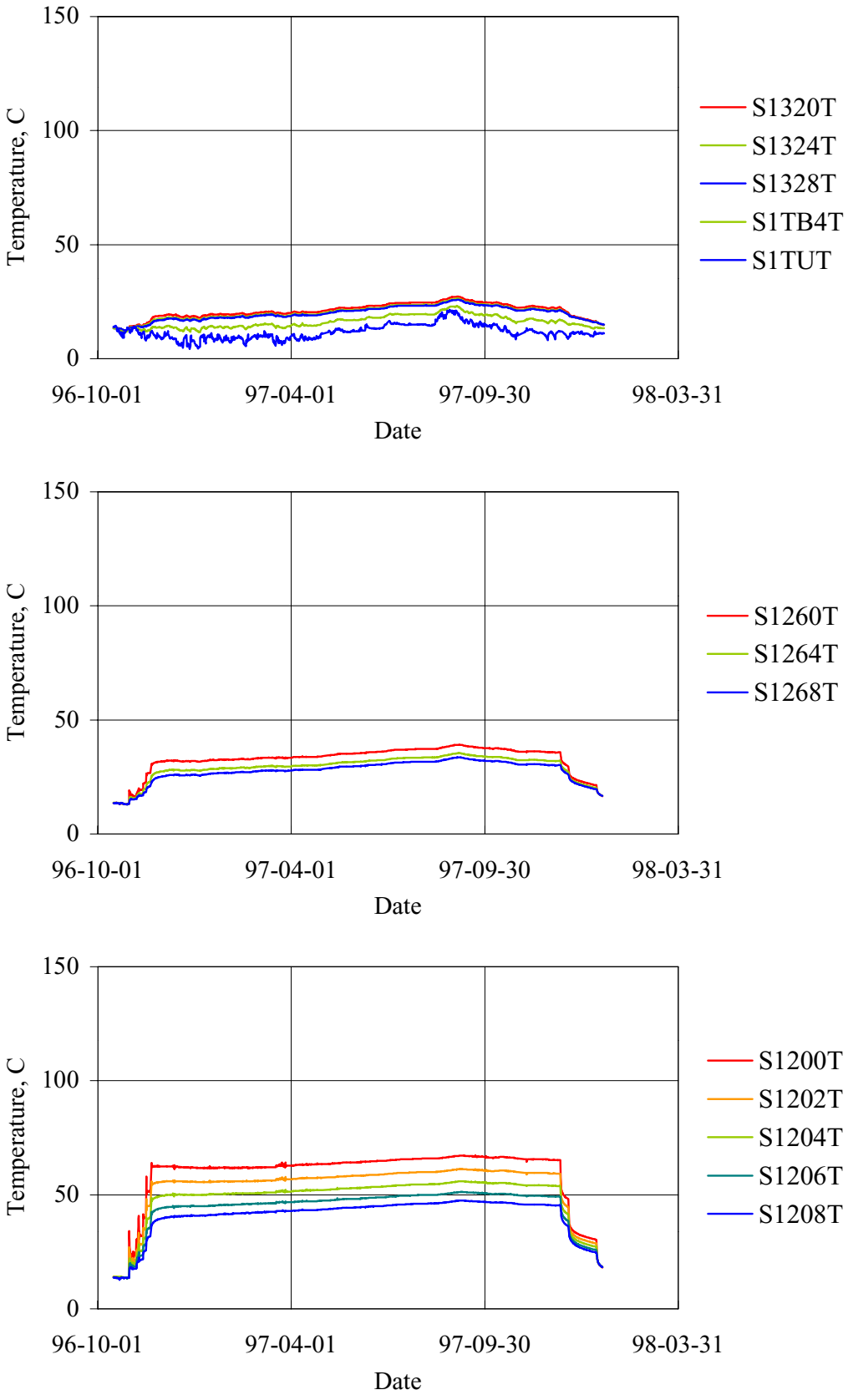

Figure 4-5 *Temperature recordings from the upper part of parcel S1. S1TB4T denotes the top block and TUT tunnel temperature. Last figure denotes distance in cm to central copper tube.*

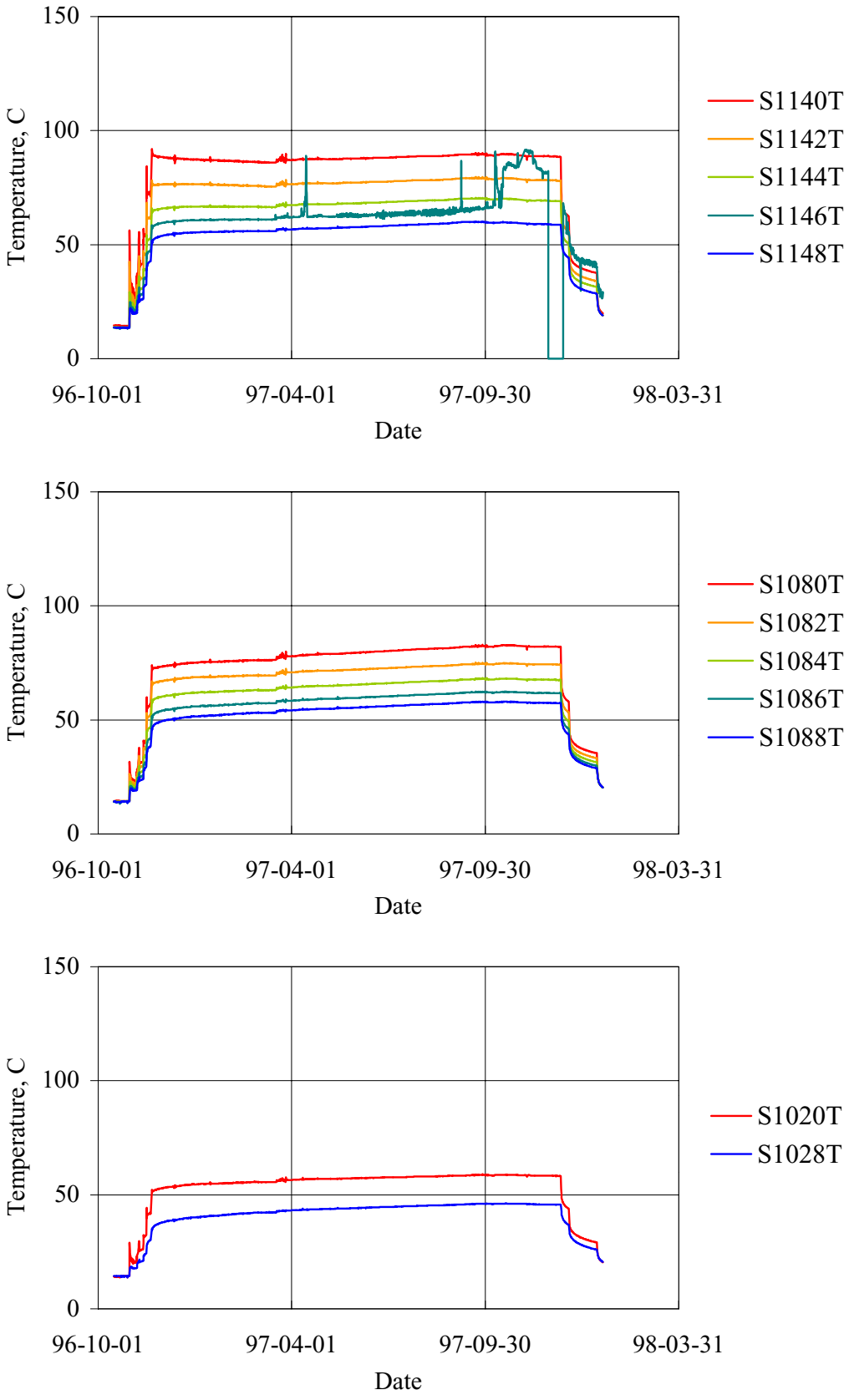

Figure 4-6 Temperature recordings from the lower part of parcel S1. Last figure denotes distance in cm to central copper tube.

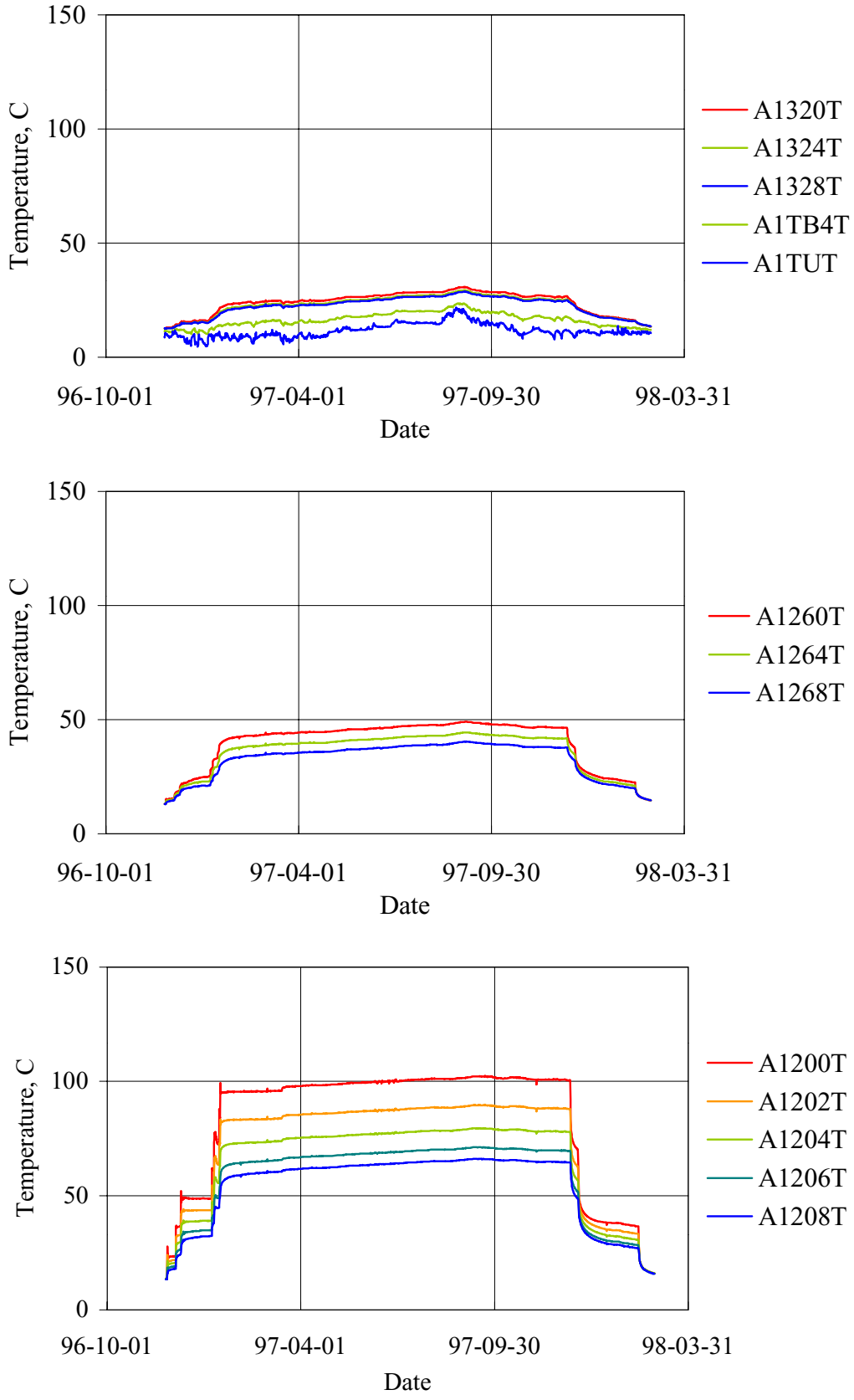

Figure 4-7 *Temperature recordings from the upper part of parcel A1. A1TB4T denotes the top block and TUT tunnel temperature. Last figure denotes distance in cm to central copper tube.*

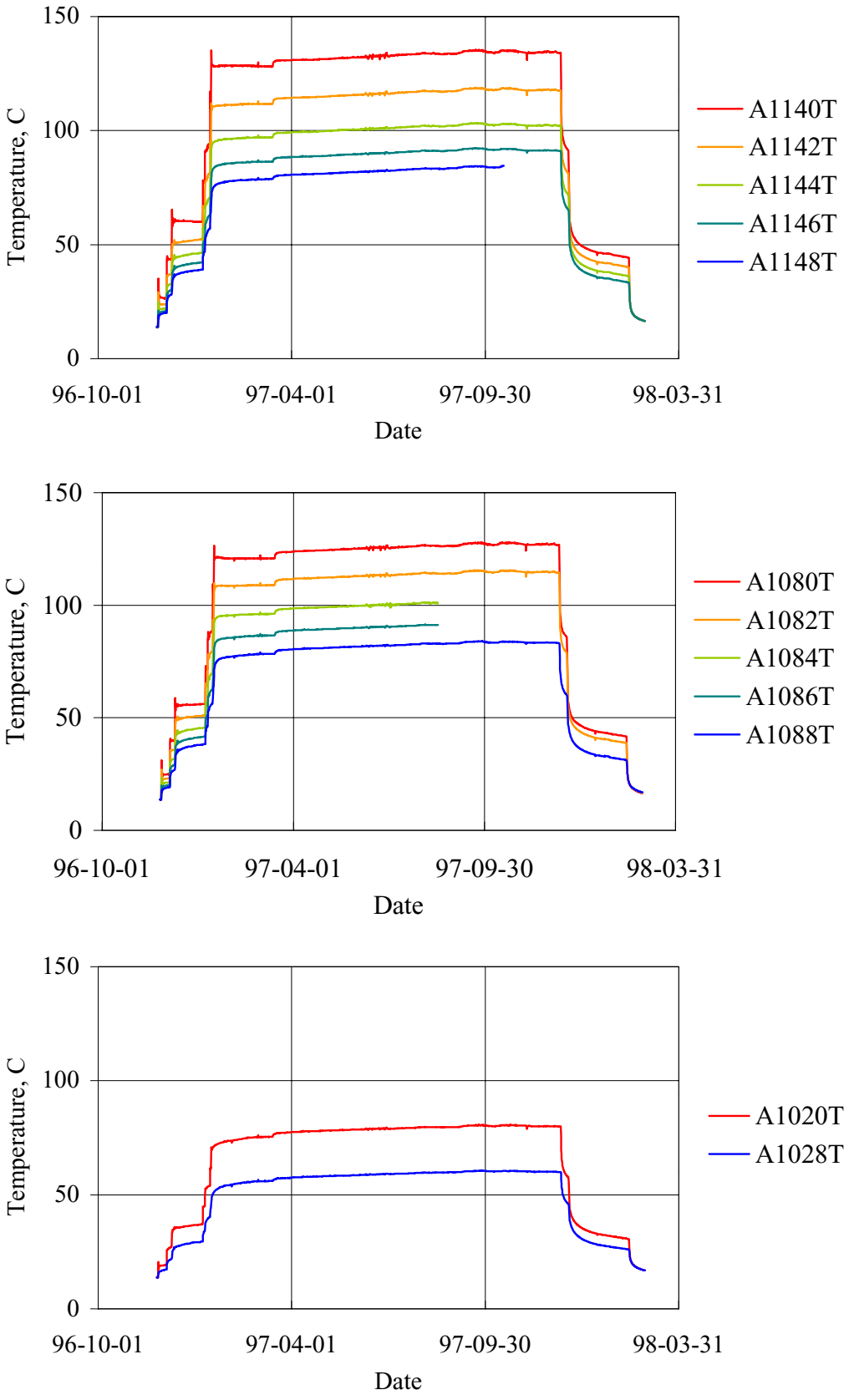

Figure 4-8 Temperature recordings from the lower part of parcel A1. Last figure denotes distance in cm to central copper tube.

Pressure

The pressure measurement by use of electronic gauges suffered from two grave problems. One was electric interference between the channels and the other was malfunction of individual gauges after varying time of operation. The recorded data are therefore of uncertain value and the presented results have to be used carefully. However, the following general description of the pressure in the S1 parcel is possible to discern.

All the gauges showed a jerky pressure increase during the first two weeks with a maximum pressure of around 3 MPa (Figure 4-9). A decrease was thereafter noticed down to around 2 MPa. A marked unrealistic increase took place when the connection of the A1 gauges was made. The unrealistic values were concluded to be an effect of electrical interference between sensors. Between the relatively distinct periods of unrealistic values the remaining S1 gauges (S1146P and S1204P) showed a slow increase from the 2 MPa up to almost stable values of 4.5 MPa in about 6 month time. No unrealistic values were recorded during the last part of the test and the pressure seems to have stabilised at around 4.5 MPa. The general trend, including the initial peak and the subsequent slow build up of pressure, is in accordance with previous laboratory experiments. The equilibrium value of around 4.5 MPa is further close to the expected 5 MPa.

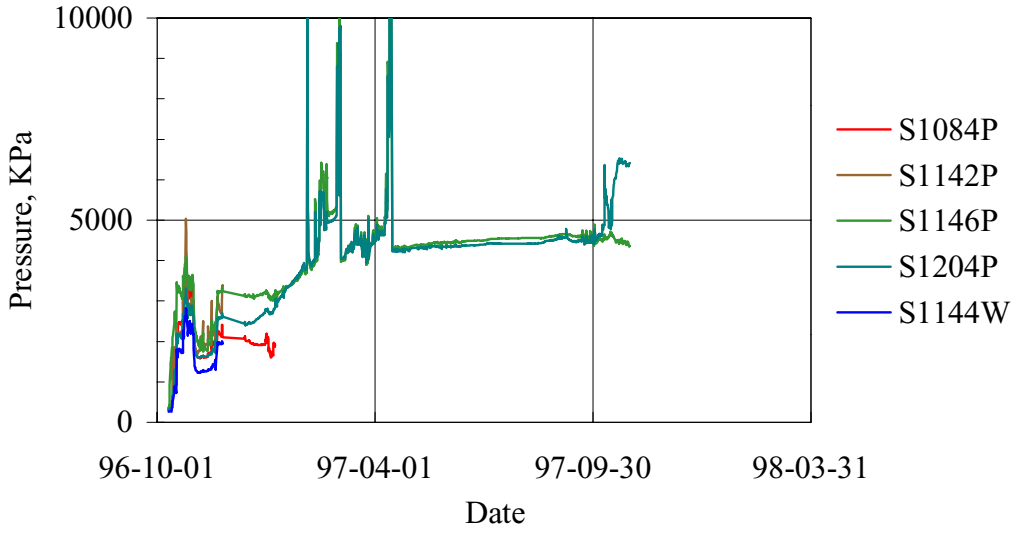

Figure 4-9 *Pressure recordings from the S1 parcel. The jerky behaviour is an artefact due to interference from malfunctioning sensors in the system.*

Moisture content

The possible information from humidity sensors is limited to the water saturation process. At full saturation the sensors are filled with liquid water, which disturb the signals and the sensors finally become unusable. In the actual tests, all the sensors in the S1 parcel seems to have been adequate during the entire wetting phase and the sensor collapses coincided very well with the measured relative humidity reaching 100%, but only partly in the A1 parcel. The results from the S1 parcel seem very probable, and are in accordance with a typical saturation process of bentonite, and the disturbance from the temperature gradient seems to have been moderate (Figure 4-10).

The conditions in the A1 parcel seem to have been more complicated (Figure 4-10). The initial peaks in sensor S1144M and S1204M in the S1 parcel are likely an effect of water intrusion into the sensor cavities, through the thin slots between the bentonite blocks, before the bentonite sealed off the water flow. In the lowest sensor (S1084M) this intrusion was prevented by the bentonite paste, which was smeared outside the column in order to prevent water intrusion into the radioactive doped plugs. After a few days the surrounding clay likely sucked up excess water, and the humidity adapted to a typical saturation curve.

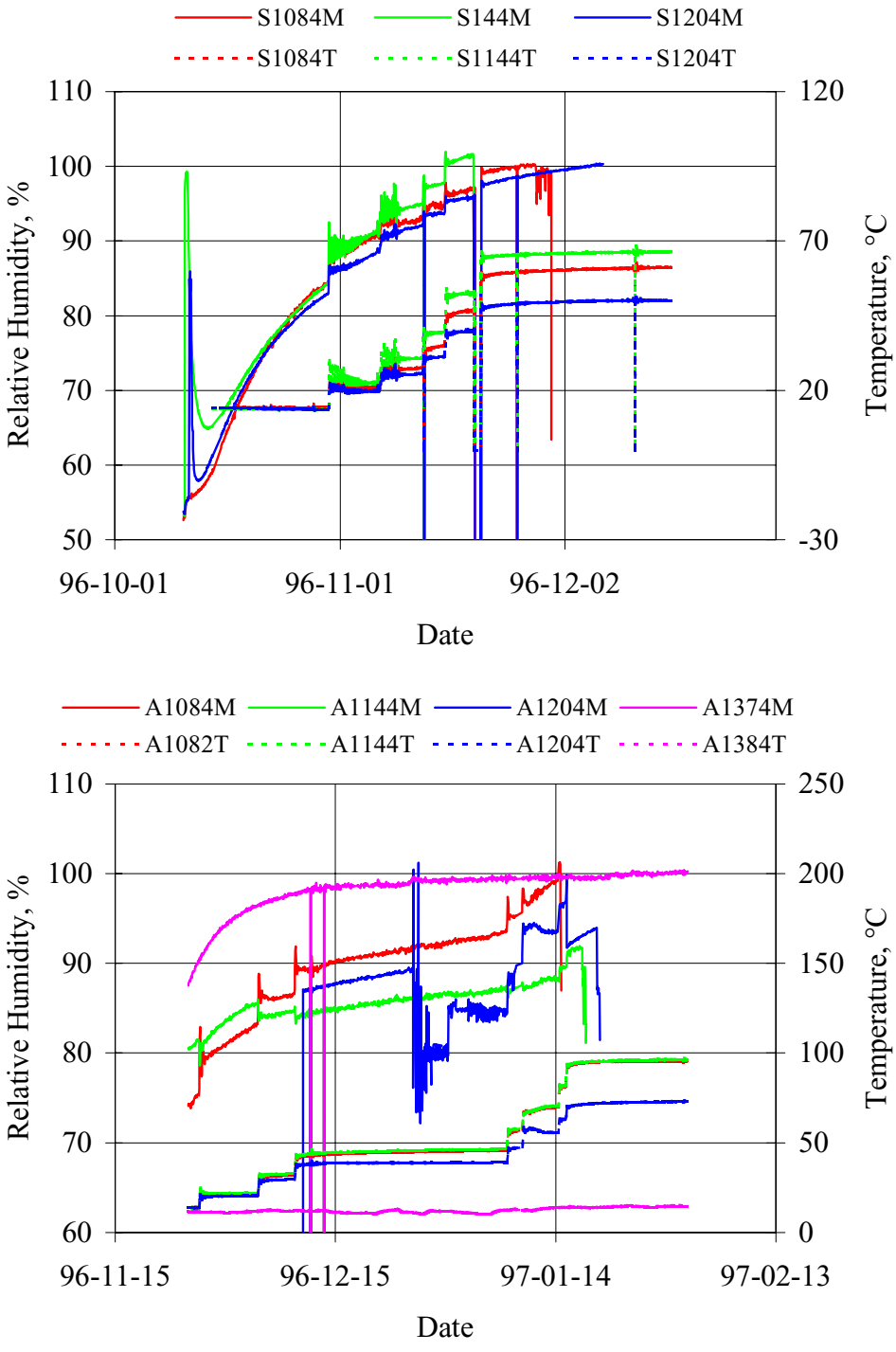

Figure 4-10 Recorded relative humidity in the S1 parcel (upper diagram) and in the A1 parcel (lower). In each diagram the lower curves refer to temperature (right axis).

4.3 Termination of field-tests

4.3.1 Uplift

The heater power was decreased in steps and finally reduced to zero in both parcels in order to facilitate the uplift and sampling. The first power reduction in the S1 parcel was made December 10th, 1997, and zero power was reached January 13th, 1998. The corresponding dates in the A1 parcel were December 10th, 1997 and February 12th, 1998.

The parcels were released by overlapping core drilling in the rock around the parcels at a distance, which left approximately 20 cm rock cover of the parcel. The standard borehole diameter was 125 mm and the overlap approximately 20 mm leading to a minimum opening of 70 mm. Two drilling machines were used in parallel, one for the 125 mm holes and the other for two 300 mm holes, which were used for final wire sawing in order to release the parcel in the bottom.

The drilling around the S1 parcel began on January 26th, 1998, and the lift-up took place on February 9th (Figure 4-11). The drilling around the A1 parcel began March 2nd, and the up-lift took place March 17th.

The sampling was started immediately after uplift of the parcels, respectively. The rock cover around the S1 parcel was removed in steps and a rough partition, approximately into the former blocks, was made at the test site. The blocks dedicated for bacteria analyses were promptly transported to an anaerobic box at Äspö. The bottom 80 cm of the parcels were cut off and transported to KTH for analyses of the tracer element distribution. The remaining released blocks were placed in airtight plastic bags, and transported to Clay Technology, Lund for analyses and storage, and further transport to Studsvik of the copper coupon containing blocks.

The following visual observations were made at test site:

- The contact between the bentonite and rock was completely sealed in the S1 parcel (Figure 4-12)
- The bottom meter in the S1 parcel was not fully water saturated
- The central part of the A1 parcel was missing
- The outer part of the remaining two parts of bentonite in the A1 parcel was soft due to free swelling (Figure 6-2)
- A white thin precipitation was found in the warmest section on both copper tubes (Figure 4-13)
- The innermost 1 to 2 mm of bentonite in the S1 parcel was affected by precipitation with the same gridiron pattern as on the copper tube (Figure 4-14)
- Sign of corrosion on a few thermocouple jackets (4-15)

The remaining clay material in the A1 parcel included all the tracer test material, and no release of radioactive material did consequently take place. The remaining material admitted planned tests and analyses regarding single effects of high temperature, but not the tests and analyses concerning the combined effects with the different additives.

Figure 4-11 Uplift of the S1 parcel after termination.

Figure 4-12 The first rock part has been removed from parcel S1 and the bentonite is partly exposed in the centre on the left side.

Figure 4-13 White precipitation on the copper tube in the S1 parcel. Note also the darker mm-thick precipitation affected layer just below the copper tube. Photograph by Kjell Svärdström, KTH, Stockholm.

Figure 4-14 Inner mantel surface of the bentonite, which was in contact with the copper tube in parcel S1. The small holes in the centre are due to sampling for tracer analyses. Photograph by Kjell Svärdström, KTH, Stockholm.

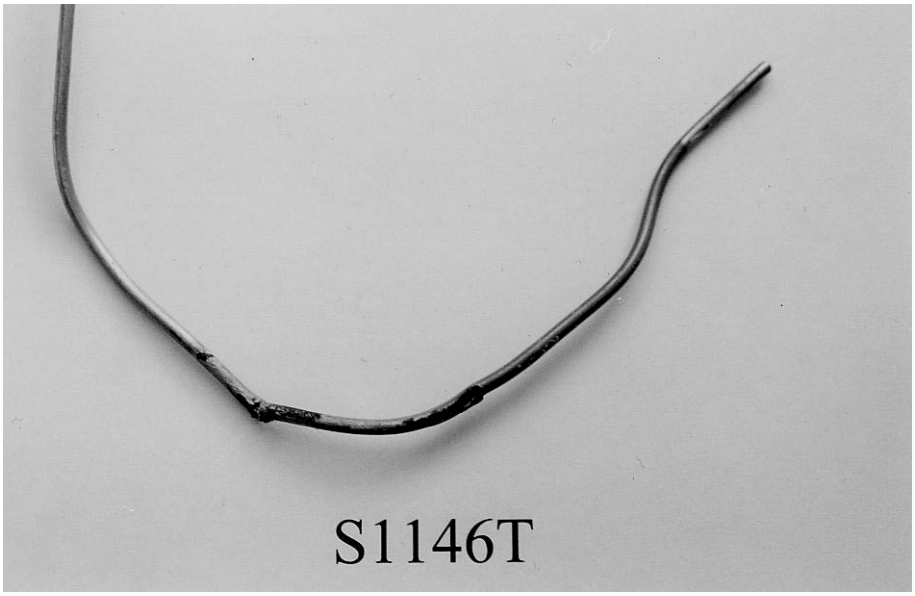

Figure 4-15 Corrosion on thermocouple in parcel S1, mid position in block 14.

4.3.2 Comments on loss of material in the A1 parcel

General

In principle, the time span during which the parcels were placed in the rock may be divided into the following phases with respect to potential loss of material:

- Emplacement/swelling,
- Heating,
- Slot drilling,
- Between drilling and uplift.

Emplacement/swelling phase

The emplacement phase may in general be a critical part in a KBS3-type of construction with respect to loss of bentonite. The slot between the bentonite blocks and rock has to be sealed by swollen bentonite before the function of the buffer system is obtained with respect to low hydraulic conductivity and mechanical stability.

There are two principle scenarios possible with respect to groundwater inflow; at a low inflow rate the groundwater will follow the walls of the test-hole to the bottom, and cause a slow bentonite swelling in the lower part. The slot will thereby be filled from below by bentonite with a relatively high density. At a high inflow rate the groundwater will fill the slot fast enough to leave the bentonite relatively unaffected, initially. The bentonite thereafter starts to swell into the groundwater parallel to water uptake into the bentonite. The dispersion into the slot thereby creates bentonite slurry with successively increasing viscosity. Bentonite material will in this case be transported out from the test hole if a groundwater flow is possible. The maximum groundwater pressure determines

the viscosity necessary to stop the transport. A critical condition is if the transport of bentonite by groundwater out from the hole is large enough to balance the swelling from the compacted bentonite. If so, the viscosity does not increase, which leads to a constant flow and washout of bentonite from the test-hole. As described in section 4.1.2 an outflow actually took place in the A1 parcel, but stopped spontaneously after a few days.

Heating phase

The flow and mechanical properties of the water-saturated bentonite were expected to be largely developed at the start of the heating phase in the LOT tests. The water flow in the test holes was thereby dramatically reduced, and the disposition to erosion minimised. The natural fractures, which intersect the test-holes, were assumed to be to small to lead to any significant erosion at the bentonite interface during the short test time.

Theoretically, bentonite loss due to erosion into fractures instead of to the tunnel floor could continue throughout the entire heating period. However, the measured data from the two parcels show very similar results. Especially, the 13 thermocouples originally placed in 3 levels (5+5+3 units) in the part, which was lost all showed constant and expected values both in radial and longitudinal directions during the heating period. Also the temperature course during the reduction of power strongly indicates that the bentonite in the A1 parcel were intact when the drilling operation was started (Figure 4-16).

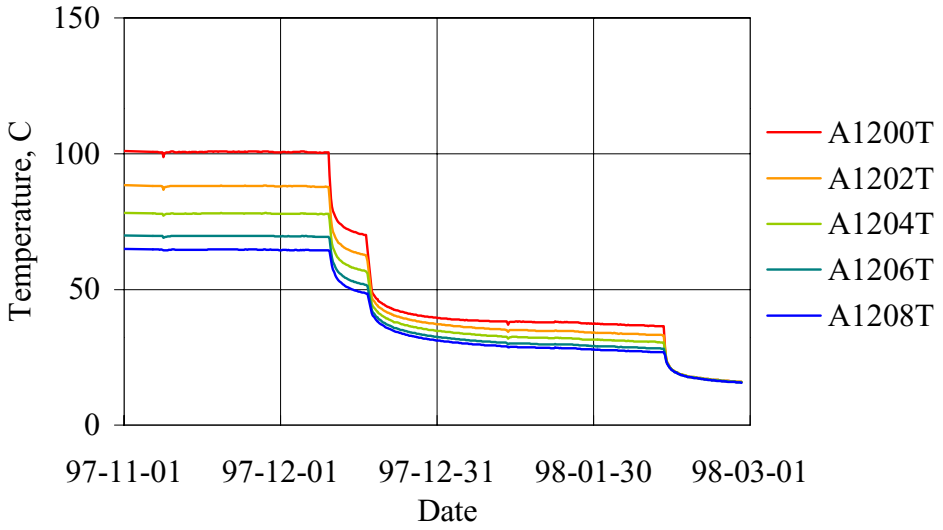

Figure 4-16 *Temperature evolution in one of the eroded blocks (no. 20) during the three power reduction steps. High temperatures to the left represent the heating test conditions, and the values to the right show the conditions at drilling start. Uppermost curve shows the conditions close to the central tube, and the lowest the outermost part close to the rock.*

Drilling phase

An open contact between the drilling water and the bentonite would have led to bentonite swelling, and to erosion if there was a sufficient flow in the bentonite-water contact zone. The natural fractures in the test-hole were assumed to be to small to lead to any significant erosion during the short drilling time. However, larger induced fractures or openings in the rock between the drilling holes and the bentonite may have led to relatively fast erosion. The maximum swelling in salt environment is generally significantly smaller compared to non-salt conditions, which leads to a faster loss of mechanical stability in the clay-water interface, which in turn leads to a fast transport of water into the bentonite. The bentonite blocks mixed with powdered salt were consequently especially sensitive to this kind of swelling/erosion scenario.

The drilling staff reported various problems during the drilling phase of which cracked cores and splinter led to fear for direct contact between the drilling fluid and the bentonite. Repeated inspections did not reveal significant contacts. However, minor contacts e.g. by longitudinal fractures or small rock parts falling out from the clay covering part were difficult to detect deep down in the slot. The final sawing in the bottom, after the slot drilling was completed, led to breakage of the rock column and large rock parts were strongly displaced.

Between drilling and uplift

The bentonite swelling pressure acts initially on the rock wall of the test holes. The mechanical tension strength of the 20 cm rock cover is limited and the risk for swelling induced damage of the rock increases with the progress of the slot drilling, and a maximum risk when the slot is completed. Possible damage by bentonite swelling pressure is restricted to initial longitudinal fractures if the access to water is restricted. On the other hand, if there is a free water supply the bentonite swelling will continue, the rock will be displaced and the bentonite will swell into the slot. The worst possible scenario is repeated filling and emptying by intermittent pumping of the system, which may lead not only to swollen bentonite but also mechanical erosion. The general aim was therefore to keep the slot continuously pumped also after the drilling operation.

The time period between drilling/sawing operation and the uplift was 5 days. This relatively short term, minor water flow and the distinct upper clay water contact indicate that the material loss did not take place during this period.

Probable scenario

Based on the above it seems most likely that the loss of material in the A1 parcel took place during the drilling operation.

Specific problems were reported at the following occasions:

March 2: Splinter at drilling start and down to 1 m in the first 300 and 125 mm holes. This has probably not caused the loss of material since significant openings at this level likely should have been noticed, and because the water level was lower most of the drilling time.

March 5: One 125 mm hole was inclined and the drilling was stopped at a depth of 1.4 m. An unsuccessful attempt was made to correct the hole from 1.15 m.
March 7: Crushed rock in the second 300 mm hole at a depth of 2.8 m.
March 8: Major problems caused by crushed rock in the second 300 mm hole at a depth of 3.5 m and in 125 mm hole. This cannot be the cause of the material loss since the level 3.5 m was below the lost part of bentonite and the rock cylinder ring was found to be intact at this level at the lift-up.
March 8: longitudinal fracture detected.

The lower water-clay interface coincided quite well with the level 2.8 m where crushed rock was found. Speculatively, this may have been the original contact between the flowing water and the bentonite. The induced swelling may have created the longitudinal fracture which gave access to the salt containing blocks at level 2.4 to 2.1 m below the tunnel floor. Approximately 25 m of 125 mm core and 1 m 300 mm core were drilled after this event.

Bentonite is easily pumped at an estimated water ratio of 1000% for fresh water conditions, which were used as drilling fluid. The minimum amount of water to flush away the lost bentonite is thereby approximately 2000 litres. A considerable smaller amount is needed if the bentonite is exposed to salt solutions, which partly must have been the case since the salt containing blocks were affected.

The amount of water used for cooling of the borer and transport of drilling material was in the order of 10 litres/minute. The limiting factor is consequently the disintegration time of the bentonite and not the available amount of water.

Consequently, the loss of material in the A1 parcel most likely took place during the drilling operation, but there is no obvious detailed scenario based on the available documentation, or from personal working at the site during the drilling operation (drilling staff (Borrbolaget/Såg och Betong) , LOT co-ordinator (Äspö), characterising geologist (SGU), water sampling chemist (KTH).

5 Bentonite tests and analyses

5.1 Test philosophy

Reference material and material from defined positions in parcel material were tested and analysed. The results were compared with respect to changes in physical properties, mineralogy and microstructure.

The following physical properties were determined (test technique within brackets):

- Water ratio (oven drying)
- Density (weighing in paraffin oil)
- Hydraulic conductivity, (oedometer flow test)
- Swelling pressure, (oedometer swelling test)
- Tensile strength (beam test)
- Shear strength (triaxial test)

The following mineralogical properties were examined (methods within brackets):

- Element distribution in the bulk and clay fraction material (ICP-AEM)
- Cation exchange capacity (CEC, Chapman method, Cu-trien method)
- Mineralogical composition in bulk and clay (XRD, SEM-EDX)
- Microstructure of accessory minerals (SEM-EDX)

Since absolute quantitative data are difficult to direct convert into several of the above properties, the aim has been to reveal possible systematic discrepancies between material from different positions in the parcels and the reference material.

5.2 Test material

The rough partition of the clay at the test site enabled a relatively fast and precise sampling of the bentonite and the various additives was fairly easy localised.

The bottom part was cut off for transport in one piece to KTH for analyses of the tracer element distribution. The cut was made in block number 10 by use of chisels, in order to get through the bentonite, and by an angle grinder in order to cut the copper tube. It was noticed that the bentonite in the S1 parcel was not fully saturated in the cut-zone.

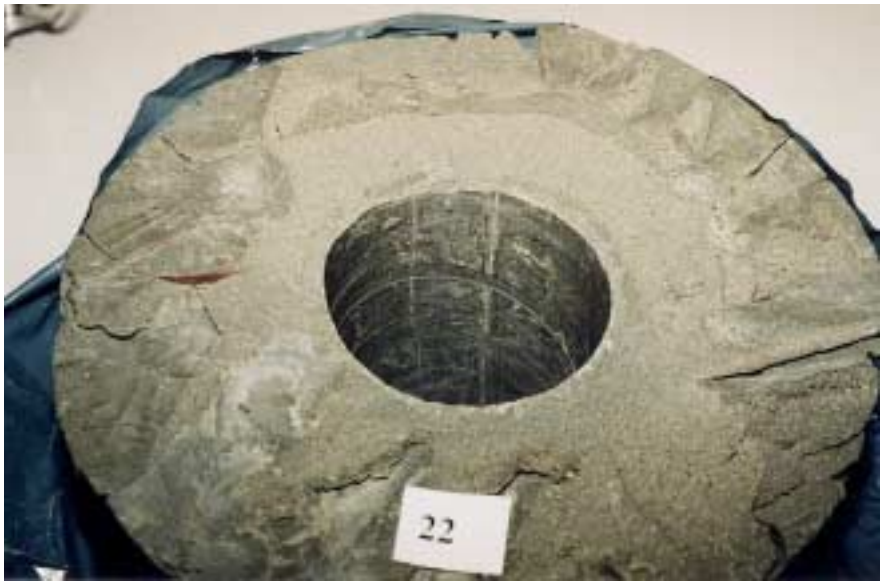

Figure 5-1 Block 22 from parcel S1 after removal. Note the copper coupon in the centre on the left side.

The test parcels were divided immediately after uptake into parts, as similar to the original blocks as possible (Figure 5-1), by use of chisels and putty knifes. The blocks were carefully placed in plastics in order to prevent drying. The denomination of a single parcel in the SICADA database were made according to the following example: PXBLOTS1, where

P	point
X	experiment
B	bentonite type of experiment
LOT	Äspö test series
S1	parcel type and number

The reference material was related to the imaginary point PXBLOTR1 (R1 for reference batch no 1). Reference material from a specific block was termed according to ex.

RS109 where

R	reference material,
S1	parcel type and number,
09	block number (counted from the bottom of the parcel).

After transport to Clay Technology's laboratory, selected blocks were divided by use of an electric band saw in order to produce test material according to Figure 5-2. The partition was made within a few days in order to reduce redistribution of elements in the material. The sawn samples were made large enough to supply several planned tests from a specific position. In other words, material with the same specimen denomination was used for several different kinds of tests and analyses. In the southeast direction the A-level was used for the general water ratio scan, and the B and C-levels for element,

X-ray and cation exchange capacity analyses. The denomination of a specific point (centre of a volume) was according to the following example:

08ASE3 where

08	block number (counted from the bottom of the parcel),
A	vertical level in the block,
SE	direction of compass in the test hole,
3	radial distance in centimetre from the inner mantel surface to the centre of the specimen.

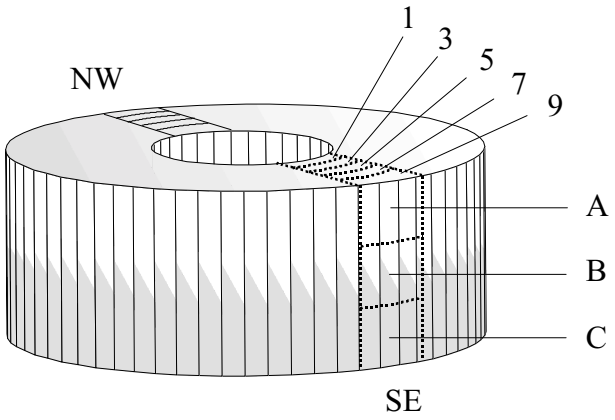

Figure 5-2 Schematic block partition. SE and NW denote the directions of compass in the test-hole, figures denote the centre of the specimens expressed in centimetres measured from the block inner mantel surface, and A, B and C denotes the analysed three vertical position in the blocks.

The lowest part of the parcels (block 1 to 7) containing the radioactive tracer material was not analysed according to the general test scheme. Some general information was though produced by KTH parallel to the tracer analyses.

5.3 Water ratio determination

5.3.1 Test principle

The water ratio (w) was determined for a large number of positions in the S1 test parcel in order to give a general picture of the water distribution in the parcel. All blocks designated with even numbers, starting with block no. 8, were analysed at the A level in the south-east (SE) and north-west (NW) directions, since this principle gave the least interference with gauges and other tests (bacteria and copper). The test series was termed LWR-A (LOT, Water Ratio, series A).

Table 5-1 Specification of the standard points for water ratio determination in the LWR-A test series. Figures show measured values in percent.

block	level	SE1	SE3	SE5	SE7	SE9	NW1	NW3	NW5	NW7	NW9
08	A	10.7	10.2	23.8	24.9	27.2					
11	A	25.7	26.4	27.7	30.5	32.9	24.9	25.5	26.1	27.0	29.5
12	A	27.6	28.1	29.2	31.3	34.4	25.8	26.2	27.4	27.8	31.0
14	A	28.2	28.0	28.3	28.9	31.6	28.9	29.0	29.4	30.4	33.8
15	A	28.7	28.4	28.6	29.1	31.9	29.6	29.8	30.6	32.9	35.8
16	A	29.3	29.9	32.1	35.1	37.8	27.7	27.5	30.6	28.1	31.1
18	A	27.9	27.6	27.7	28.1	29.7	28.9	28.8	29.4	34.0	31.4
20	A	27.7	27.7	27.8	28.1	30.2	30.3	30.6	32.0	35.0	38.0
22	A	28.1	28.1	28.5	29.4	33.2	29.9	29.7	30.5	32.8	36.0
24	A	28.1	28.0	28.5	29.5	32.9	29.0	29.0	29.6	31.6	36.6
26	A	27.8	27.9	27.8	28.3	30.4	34.9	29.6	30.5	33.0	36.2
28	A	28.0	27.9	28.1	28.4	30.5	28.8	29.3	30.0	31.7	35.1
30	A	27.7	27.6	27.7	27.8	29.2	30.8	31.0	32.4	35.0	37.7
32	A	28.6	28.6	28.8	29.0	32.7	30.0	30.3	31.4	33.9	37.4
34	A	30.1	30.3	31.0	32.7	36.6	29.7	30.3	31.5	34.5	37.7
36	A	30.4	30.9	32.1	33.9	37.6	31.0	30.6	31.3	32.5	35.7
min		10.7	10.2	23.8	24.9	27.2	24.9	25.5	26.1	27.0	29.5
max		30.4	30.9	32.1	35.1	37.8	34.9	31.0	32.4	35.0	38.0
mean		27.2	27.2	28.6	29.7	32.4	29.3	29.1	30.2	32.0	34.9

The total standard number of water ratio determinations in each block was 10 (5 radial samples and 2 directions). In addition, block number 14 and 30 were analysed at 3 levels (A, B and C) in the north direction in order to find possible vertical anomalies. The number of specimens in each of these two blocks was consequently 25. The two blocks were chosen in order to represent a high and a low temperature position.

Block number 10 in the S1 parcel could not be analysed since it was sacrificed during the separation operation of the lower tracer prepared part. Instead, block number 11 was analysed, which turned out to be of special interest since it represented the limit between fully saturated clay and the lower dryer zone. In addition to the SE/NW direction it was therefore analysed in 5 positions and 3 levels on the north (N) and south (S) side (additional 30 positions). The vertical test series and additional tests in sample 11 were termed LWR-B.

Table 5-2 Specification of the additional points for water ratio determination in the LWR-B test series. Figures show measured values in percent. Figures in italics have been corrected.

block	level	S1	S3	S5	S7	S9	N1	N3	N5	N7	N9
11	A	25.8	26.5	28.1	30.8	32.9	25.3	*25.8*	26.2	27.1	29.8
11	B	25.8	26.7	27.9	30.7	32.9	25.0	25.5	26.1	26.9	29.3
11	C	*26.5*	27.7	29.2	32.1	34.1	24.7	25.2	25.7	26.6	29.0
14	A						29.1	29.2	29.7	30.6	33.5
14	B						29.4	29.4	30.0	31.1	34.2
14	C						29.5	29.6	30.6	31.7	34.9
30	A						26.9	27.6	27.8	28.1	29.7
30	B						27.7	27.6	27.8	28.1	30.3
30	C						27.6	27.7	27.8	28.1	30.0
min		25.8	26.5	27.9	30.7	32.9	24.7	25.2	25.7	26.6	29
max		26.5	27.7	29.2	32.1	34.1	29.5	29.6	30.6	31.7	34.9
mean		26.0	27.0	28.4	31.2	33.3	27.2	30.4	28.0	28.7	31.2

Since the A1 parcel was exposed to liquid water without mechanical support prior to the lift-up, the water ratio is of no use to describe the parcel conditions during the heating test period. Therefore, analyses were made only in conjunction with tests and analyses, which require water ratio data for the evaluation.

5.3.2 Equipment, test procedure and evaluation

No specific preparation of the test material was made. Quick handling between sawing after oven-drying etc. and weighing was necessary in order to minimise the interaction between the specimens and air with respect to humidity.

Immediately after partitioning the specimen was placed in aluminium baking tin and the bulk mass (m_b) was determined by use of a standard laboratory balance (mg resolution). The specimen was placed in a ventilated oven for 24 h at a temperature of 105°C. The solid (dry) mass (m_s) was determined immediately after take out.

The sample bulk mass and the sample solid mass were measured. The water mass (m_w) was considered to be:

$$m_w = m_b - m_s \,, \qquad 5\text{-}1$$

and the water ratio (w) was determined from:

$$w = \frac{m_w}{m_s} \,. \qquad 5\text{-}2$$

The raw and calculated data were stored in an Excel file and transferred to the SICADA database. The individual specimens in one parcel were denominated according to the general description ex. 08ASE3WR (WR for water ratio test).

5.3.3 Results

The original water ratio in the blocks was close to 10%. At full water saturation the water ratio was calculated to be 27% at the intended density of 2000 kg/m^3. The dimensions and mass of the produced bentonite blocks were very close to the intended, and were calculated to result in a water ratio of 28% for the whole intended test volume. However, the test hole dimensions varied between the intended 300 mm and 310 mm, which increase the mean maximum block water ratio to 33%. The actual test results are shown in Table 5-1 and 5-2 and in Figure 5-3. The discrepancies between theoretical and measured results in a specific point may be explained by the following conditions:

- Minor inhomogeneity in final buffer density
- Loss of solid material
- Reduced supply of water

The fact that the copper tube was fixed in the upper part by the top concrete slab may lead to the preservation of a minor heterogeneity due to divergence from perfect centring of the tube. The loss of solid material during the test was expected to be insignificant. The supply of water into the test holes was in general very good both with respect to flow and pressure. The restrictions for water uptake were consequently bentonite permeability and distribution of the water inlet points. For the case of free supply of pure water at the rock surface, the permeability restriction was expected to lead to full saturation well before termination. In the lower part of the S1 parcel the distribution of the water inlet points, consequently, seem to have been governing the saturation rate.

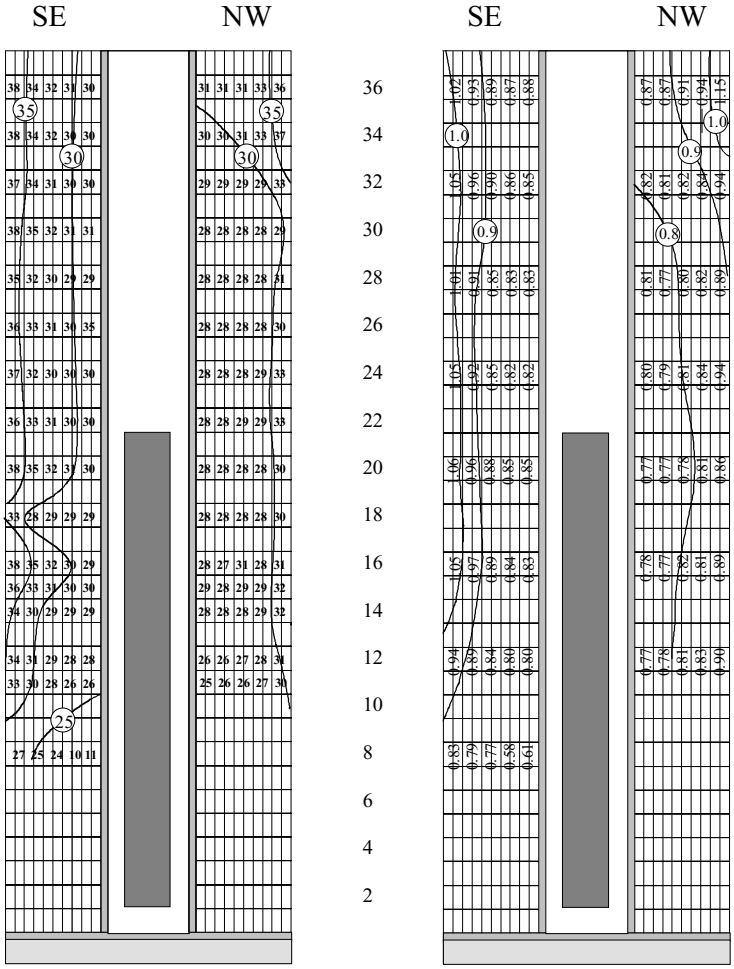

Figure 5-3 The water ratio (left) and void ratio (right) distribution in parcel S1. SE and NW indicate the original direction of compass and central figures show block number.

5.4 Bulk density determination

5.4.1 Test principle

The bulk density (ρ_b) was determined for every 4th block starting with block 8 (8, 12, 16 etc.). The blocks were split to give 5 specimens in radial direction in the southeast (SE) and northwest (NW) direction, respectively. The total standard number of bulk density determinations in each block was consequently 10. The test series was termed LDY-A (LOT, Density, series A).

Table 5-3 Specification of the standard water ratio determination points and results in the LDY-A series. Figures show measured density in kg/m^3.

block	level	SE1	SE3	SE5	SE7	SE9	NW1	NW3	NW5	NW7	NW9
S108	A	1910	1941	1940	1934	1935					
S112	A	1971	1979	1955	1928	1923	1976	1967	1960	1943	1913
S116	A	1967	1958	1943	1910	1868	1990	1995	1993	1970	1925
S120	A	2000	2000	1994	1970	1947	1960	1962	1947	1911	1859
S124	A	1981	1983	1972	1957	1905	1971	1967	1949	1900	1850
S128	A	1972	2008	1977	1957	1921	1954	1963	1950	1919	1873
S132	A	1964	1977	1972	1953	1897	1957	1949	1927	1900	1861
S136	A	1926	1946	1944	1931	1891	1948	1945	1914	1894	1755
min		1910	1941	1940	1910	1868	1948	1945	1914	1894	1755
max		2000	2008	1994	1970	1947	1990	1995	1993	1970	1925
mean		1961	1974	1962	1943	1911	1965	1964	1949	1920	1862

5.4.2 Equipment, test procedure and evaluation

The equipment consisted of the following parts:

- Thin thread with low absorption capacity,
- Laboratory balance (mg resolution),
- Laboratory glass beaker,
- Paraffin oil (density = 863 kg/m^3),
- Laboratory lifting table.

The test blocks were split in the radial direction by use of a band saw and promptly wrapped into plastics. The specimens were placed in a loop made by a thin thread, hanged under the balance and weighed. The specimens were thereafter submerged into the paraffin oil and the balance value was again noted.

The bulk mass weighed in air (m_b) and in paraffin oil (m_{bp}) were used to calculate the volume (V) of the sample according to:

$$V = (m_b - m_{bp}) \cdot \rho_p \ , \qquad 5\text{-}3$$

where ρ_p is the paraffin oil density. The bulk density was calculated according to:

$$\rho = \frac{m}{V} \ , \qquad 5\text{-}4$$

5.4.3 Results

In accordance with the water ratio discussion the density at full water saturation was intended to be 2000 kg/m^3. The produced bentonite blocks were calculated to give a density of 1990 kg/m^3 at full saturation in the theoretical 300 mm test hole. The

measured test hole dimension variation between 300 mm and 310 mm and the minimum block density thereby decreases to 1920 kg/m^3.

The measured density values are shown in Table 5.3 and Table 5.4, and can be summarized in the following way:

- Trend with decreasing densities from tube to rock,
- Trend with lower densities in the upper part,
- Difference between the two examined sides of the blocks,
- No density variations at different levels in one direction in a block,

All results are in agreement with expectations due to the conditions, i.e. initially open slot, larger upper diameter of the test holes and fixation of the copper tube.

5.5 Oedometer tests

5.5.1 Test principle

The general principle was to determine the correlation between density at full saturation, and swelling pressure and hydraulic conductivity, respectively, and to compare the results from exposed parcel material with reference material. The following 4 test series were included in the test:

- LOE-A: reference material, air-dry preparation, deionised water, 5 samples,
- LOE-B: reference material, air-dry preparation, Äspö-groundwater, 5 samples,
- LOE-C: parcel material, air-dry preparation, Äspö-groundwater, 10 samples,
- LOE-D: parcel material, naturally saturated, Äspö-groundwater, 10 samples.

The specimens in test series LOE-A and LOE-B were produced from the reference air-dry bentonite granular material (RLOT1). In test series LOE-C the test material from the parcels was air-dried and re-compacted, and in the LOE-D series the specimens were trimmed from parcel material as undisturbed as possible. The reason for the re-compaction preparation techniques was to measure at the correct density, since the trimming technique leads to an inevitable small swelling. The trimming technique, on the other hand, was used to ensure that small e.g. precipitation effects were not lost by the re-compaction preparation technique.

Table 5-4 Test scheme for the LOE-A test series.

test	preparation	material	solution	density kg/m^3
LOE01	air-dry	RLOT1	deionized	1850
LOE02	air-dry	RLOT1	deionized	1900
LOE03	air-dry	RLOT1	deionized	1950
LOE04	air-dry	RLOT1	deionized	2000
LOE05	air-dry	RLOT1	deionized	2050

Table 5-5 Test scheme for the LOE-B test series.

test	preparation	material	solution	density kg/m3
LOE06	air-dry	RLOT1	LOT1-rgw	1850
LOE07	air-dry	RLOT1	LOT1-rgw	1900
LOE08	air-dry	RLOT1	LOT1-rgw	1950
LOE09	air-dry	RLOT1	LOT1-rgw	2000
LOE10	air-dry	RLOT1	LOT1-rgw	2050

Table 5-6 Test scheme for the LOE-C test series.

test	preparation	material	solution	density kg/m^3
LOE11	air-dry	S108BSW1	LOT1-rgw	1950
LOE12	air-dry	S108BSW8	LOT1-rgw	1950
LOE13	air-dry	S114BSW1	LOT1-rgw	1950
LOE14	air-dry	S114BSW8	LOT1-rgw	1950
LOE15	air-dry	S132BSW1	LOT1-rgw	1950
LOE16	air-dry	S132BSW8	LOT1-rgw	1950
LOE17	air-dry	A108BSW1	LOT1-rgw	1950
LOE18	air-dry	A108BSW8	LOT1-rgw	1950
LOE19	air-dry	A136BSW1	LOT1-rgw	1950
LOE20	air-dry	A136BSW8	LOT1-rgw	1950

Table 5-7 Test scheme for the LOE-D test series.

test	preparation	material	solution	density kg/m^3
LOE21	trimmed	S108BSW1	LOT1-rgw	parcel
LOE22	trimmed	S108BSW8	LOT1-rgw	parcel
LOE23	trimmed	S114BSW1	LOT1-rgw	parcel
LOE24	trimmed	S114BSW8	LOT1-rgw	parcel
LOE25	trimmed	S132BSW1	LOT1-rgw	parcel
LOE26	trimmed	S132BSW8	LOT1-rgw	parcel
LOE27	trimmed	A108BSW1	LOT1-rgw	parcel
LOE28	trimmed	A108BSW8	LOT1-rgw	parcel
LOE29	trimmed	A136BSW1	LOT1-rgw	parcel
LOE30	trimmed	A136BSW8	LOT1-rgw	parcel

5.5.2 Equipment

Five specially designed swelling pressure oedometer cells were used (Figure 5-4). The samples were confined by cylinder rings with a diameter of 20 mm and filters at the top and bottom, all made of acid proof stainless steel .The test volume was sealed by o-rings placed between the bottom plate and the cylinder ring, and between the piston and the cylinder ring. At test start the height of the test volume was fixed to 20 mm by the flange on the moveable piston. The transducer placed between the piston and the upper lid measured the axial force from the sample. The displacement of the piston due to transducer deformation is 100 μm at maximum force, corresponding to 0.5% of the sample height, which was considered insignificant.

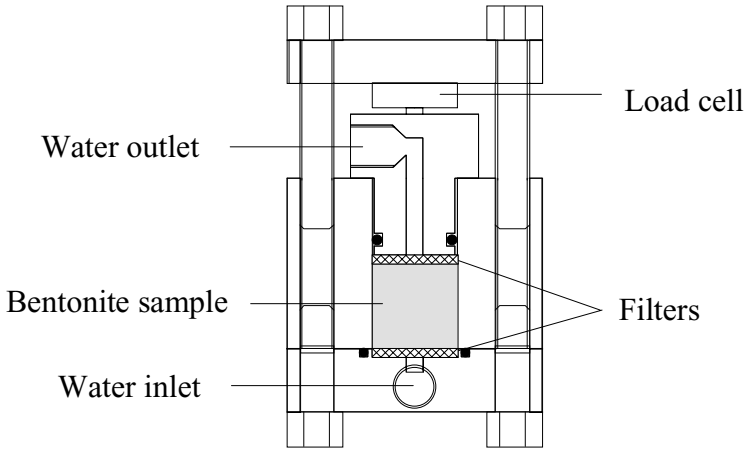

Figure 5-4 Schematic drawing of the swelling pressure oedometer, which was used for determination of swelling pressure and hydraulic conductivity.

5.5.3 Test technique

Reference samples in test series LOE-A and LOE-B were prepared from reference material stored from the block production. The material was placed in the oedometer, slightly over-compacted, and the flange-equipped piston finely defined the volume.

In the LOE-C test series, the material was sawn, by use of a band saw, from the blocks in the S1 and A1 parcels, air-dried, gently ground and compacted in the same way as the reference samples. The compaction corresponded to a saturated density of 1950 kg/m^3.

In the LOE-D test series, the specimens were sawn and trimmed to fit the sample holder, the mass of the specimens was determined and the specimens were placed in the fixed volume of the oedometers. The aim was to get a final density as close as possible to the previous density in the parcel.

The test solution simulating Äspö reference groundwater (LOT1-rgw) was based on analysis of water sampled in the bottom filter of parcel A1 during the heating period (Table 5-8).

Table 5-8 Main elements in the water analysis of the LOT1-rgw solution sampled in the bottom filter placed below the A1 parcel.

	Valence	g/mole	mg/litre	mmole/litre	meq/litre
Ca	2	40	2840	71.0	142.0
K	1	39.1	12	0.3	0.3
Mg	2	24.3	44	1.8	3.6
Na	1	23	2770	120.4	120.4
Cations			5666		266.4
Cl	-1	35.5	8600	242.3	-242.3
SO4	-2	96	1000	10.4	-20.8
Anions			9600		-263.1

Air was evacuated from the test volume by use of a vacuum pump (approximately 2 kPa absolute pressure) and the test solution was allowed to enter the specimen from both filters. A minor water over-pressure (10 kPa) was applied and the water uptake was indirectly supervised by the registration of the force transducer. Stable force conditions was reached within 1 week, and the water pressure in the bottom inlet was increased to maximum 50% of the measured swelling pressure in order to start percolation. The volume of the percolated water solution was registered daily by visual observations of the water/air interface meniscus. At constant flow the water pressure was reduced to zero and the tests were terminated when the recorded axial force had stabilised. The two stable force conditions, i.e. before and after percolation, were used to evaluate the swelling pressure.

5.5.4 Evaluation

The swelling pressure P_s (Pa) was calculated from the measured force at zero water pressure according to:

$$P_s = \frac{F}{A} \qquad 5\text{-}5$$

where F is the axial force (N) and A is the sample area acting on the piston (m^2). The accuracy of the measured values is governed by the force transducer, which was calibrated against a dead weight before and after each test.

The hydraulic conductivity k (m/s) was evaluated from the percolated water volume according to Darcy´s law:

$$k = \frac{V \cdot l}{A \cdot h \cdot t} \qquad 5\text{-}6$$

where V is the percolated volume (m^3), l is the sample length (m), A is the sample area (m^2), h is the water pressure difference over the sample expressed as water column (m) and t is the time (s).

It is of vital importance for the evaluation to correlate the results to the final sample density. The intended density was fairly well reached in the reference tests due to the relatively constant grain density of the MX-80 material. However, in the exposed specimens there was a significant density variation due to the previous saturated block density and to trimming. The density and water ratio were therefore determined after each test by the following technique:

- The sample weight (m_{tot}) was determined (mg resolution),
- The sample was axially split in two approximately equal parts,
- The weight (m_{part}) of each part was determined,
- One piece was submerged into liquid paraffin and the weight was determined, the volume was calculated according to description in section 5.4.2,
- The other piece was exposed to 105°C for 24 hours and the solid mass (m_s) was determined.

The density of the entire water saturated sample ρ_m (kg/m^3) was calculated from item 1 and the defined sample holder volume according to:

$$\rho_m = \frac{m_{tot}}{V_{holder}} \qquad 5\text{-}7$$

The density of one sample half was calculated from item 3 and 4.

$$\rho_m = \frac{m_{part}}{V_{part}} \qquad 5\text{-}8$$

The water ratio w (%) was calculated from item 3 and 5 according to eq. 5-2. The samples were considered as fully water saturated due to the test conditions. Differences between calculated density by eq. 5-7 and 5-8 on the one hand, and from water ratio on the other (eq. 5-9), thereby will reveal changes in grain density, if any.

$$\rho_m = \frac{1 + w_m}{w_m + \frac{1}{\rho_s}} \qquad 5\text{-}9$$

The raw and calculated data are stored in Excel files and transferred to the SICADA database. The individual specimens were denominated according to the general scheme, ex. 08BSW2OE (OE for oedometer test).

5.5.5 Results

General

The general hypothesis was that material exposed to repository conditions was expected to have the same swelling pressure and hydraulic conductivity as the reference material saturated and tested with the artificial Äspö groundwater solution.

Further, the results from the reference test series both for de-ionised water and for LOT1-rgw solution were expected to correspond to the relatively large number of data available in literature, e.g. in the Valuclay database (Figure 5-5 and 5-6).

The difference due to different test solutions in the LOE test series was expected to be small and significant only for low densities. The effect of the LOT1-rgw solution at the saturated density 1800 kg/m^3 was expected to be a reduction to around 50% with respect to swelling pressure and an increase by around a factor 3 with respect to hydraulic conductivity according to previous laboratory data (SKB AR 92-35). Theoretical treatment of the effects on swelling pressure of salt solutions is given in SKB TR 97-31.

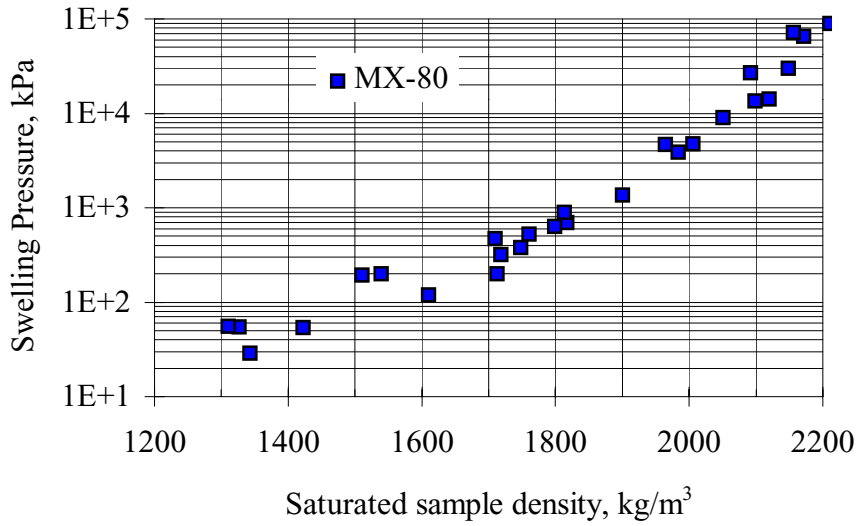

Figure 5-5 *Swelling pressure data from previous laboratory tests on MX-80 material. From SKB Valuclay database.*

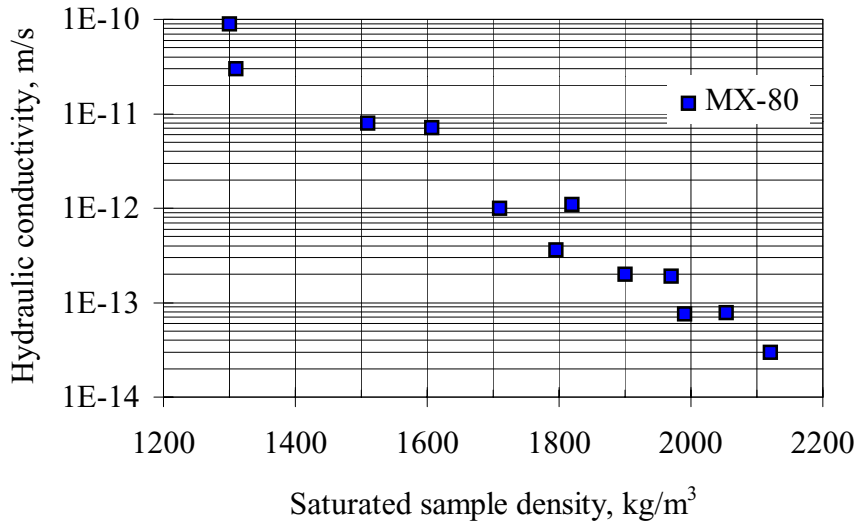

Figure 5-6 *Hydraulic conductivity data from previous laboratory tests on MX-80 material saturated by deionised water. From SKB Valuclay database.*

Swelling pressure

Figure 5-7 shows examples of swelling pressure build-up during water saturation. The total pressure increase after approximately one week is a response to the applied water pressure increase caused by the flow measurement. The water pressure is again reduced to zero after 26 days and stable pressure values are again reached after a few days. The final stable values are used in the subsequent presentation of swelling pressure.

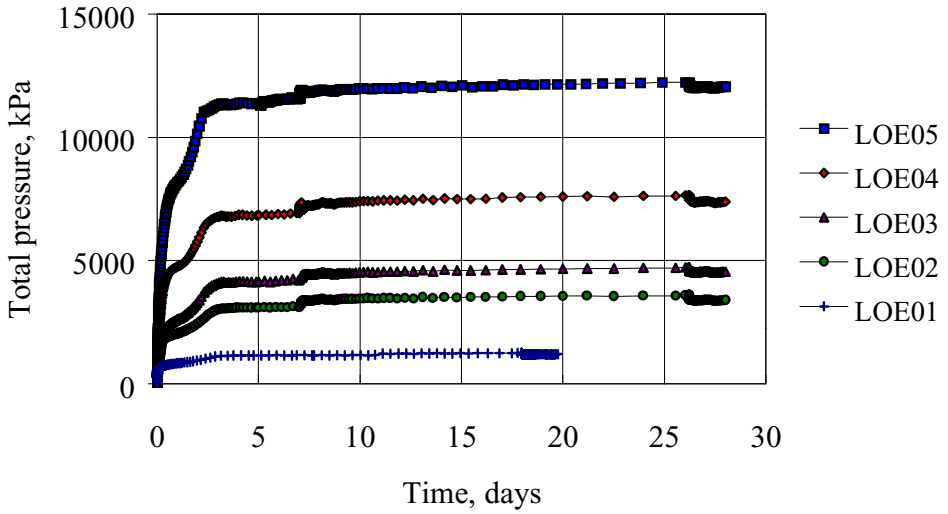

Figure 5-7 *The total pressure build-up as a function of time at water uptake in the LOE-A test series, i.e. the reference material saturated with deionised water.*

Compared to previous data, the LOE test series data turned out to have considerable less scatter despite the small size equipment, likely because the LOT tests material was from one material batch, and because the test conditions were better standardised (Figure 5-8).

No significant difference in swelling pressure due to the different test solutions is possible to detect between the reference samples. However, around 2 MPa higher values were measured compared to previous tests at the highest densities. At the saturated density 1800 kg/m^3 the measured pressures were close to old values, and for the lowest density (1600 kg/m^3) the pressure was lower than previously measured values. The difference is well in agreement with the expected effect of salt containing test solution on low-density material.

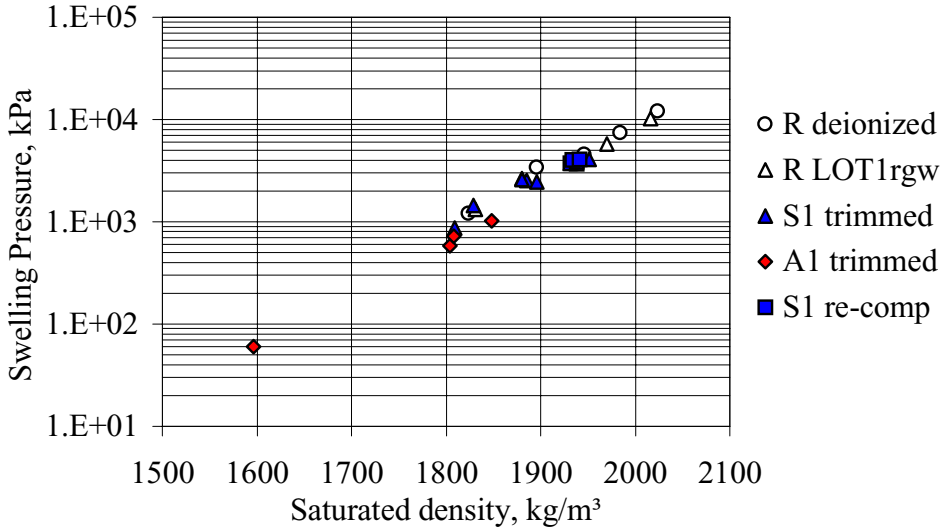

Figure 5-8 *Measured swelling pressure in all tested samples versus saturated clay density.*

Hydraulic conductivity

Stable flows were normally reached after a few days indicating that the samples were fully saturated (Figure 5-9). The percolated volume was calculated based on around 10 days of relatively stable flow. Compilation of results calculated according to Darcy's law (eq. 5-6) is shown in Figure 5-10. The hydraulic conductivity was lower compared to previous results at high density, about the same at medium density, and higher at low density, which is in accordance with the swelling pressure results.

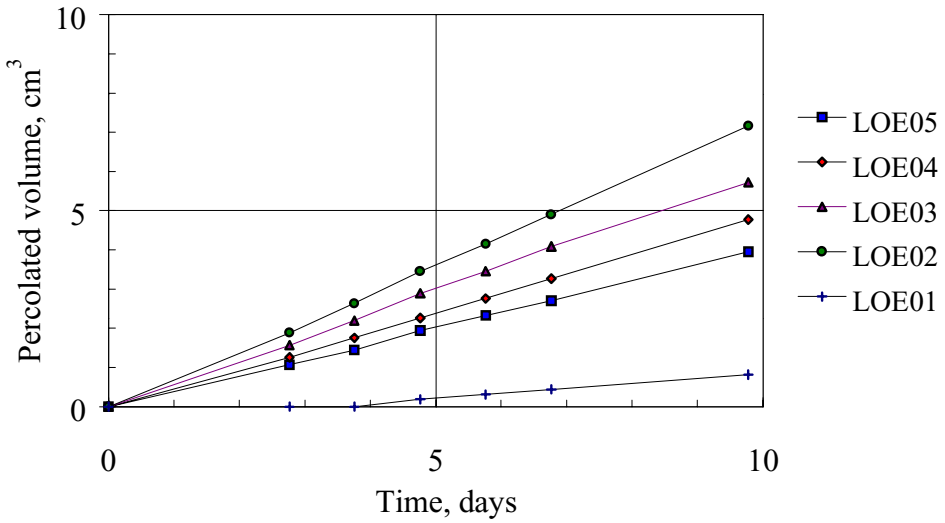

Figure 5-9 *Percolated water volume versus time during the flow measurement in the LOE-A series.*

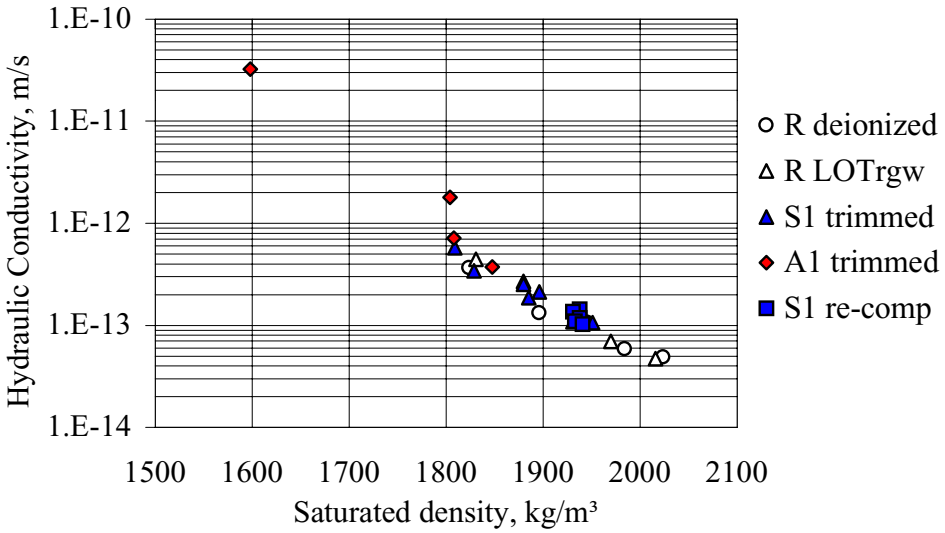

Figure 5-10 *Evaluated hydraulic conductivity in all tested samples versus saturated clay density.*

5.6 Beam tests

5.6.1 Test principle

The balk test technique do not give detailed information concerning rheological properties of the material but was used in order to detect relative rheological changes between different positions in the test parcels and reference material. A detailed description concerning technique and evaluation is given in SKB TR 95-19. The technique is simple and it enables a relatively large number of tests in order to scan the parcels. Possible discrepancies compared to reference material could thereby be detected and further examined by use of other methods, suitably by triaxial test technique. The tensile strength and strain were determined by beam tests in the following four test series:

- LBM-A: reference material, air-dry preparation, deionised water, 5 samples,
- LBM-B: reference material, air-dry preparation, LOT-solution, 5 samples,
- LBM-C: S1 parcel material, LOT-solution, 15 samples,
- LBM-D: A1 parcel material, LOT-solution, 4 samples.

Table 5-9 Test scheme for the LBM-A test series.

test	prep.	material	solution	density kg/m^3
LBM01	air-dry	RLOT1	deionized	1850
LBM02	air-dry	RLOT1	deionized	1900
LBM03	air-dry	RLOT1	deionized	1950
LBM04	air-dry	RLOT1	deionized	2000
LBM05	air-dry	RLOT1	deionized	2050

Table 5-10 Test scheme for the LBM-B test series.

test.	prep.	material	solution	density kg/m^3
LBM06	air-dry	RLOT1	LOT1-rgw	1850
LBM07	air-dry	RLOT1	LOT1-rgw	1900
LBM08	air-dry	RLOT1	LOT1-rgw	1950
LBM09	air-dry	RLOT1	LOT1-rgw	2000
LBM10	air-dry	RLOT1	LOT1-rgw	2050

Table 5-11 Test scheme for the LBM-C test series.

test	prep.	material	solution	density kg/m^3
LBM11	sawn	S108BSW1	LOT1-rgw	parcel
LBM12	sawn	S108BSW4	LOT1-rgw	parcel
LBM13	sawn	S108BSW7	LOT1-rgw	parcel
LBM14	sawn	S114BSW1	LOT1-rgw	parcel
LBM15	sawn	S114BSW4	LOT1-rgw	parcel
LBM16	sawn	S114BSW7	LOT1-rgw	parcel
LBM17	sawn	S120BSW1	LOT1-rgw	parcel
LBM18	sawn	S120BSW4	LOT1-rgw	parcel
LBM19	sawn	S120BSW7	LOT1-rgw	parcel
LBM20	sawn	S124BSW1	LOT1-rgw	parcel
LBM21	sawn	S124BSW4	LOT1-rgw	parcel
LBM22	sawn	S124BSW7	LOT1-rgw	parcel
LBM23	sawn	S132BSW1	LOT1-rgw	parcel
LBM24	sawn	S132BSW4	LOT1-rgw	parcel
LBM25	sawn	S132BSW7	LOT1-rgw	parcel

Table 5-12 Test scheme for the LBM-D test series.

test	prep.	material	solution	density kg/m^3
LBM26	sawn	A108BSW1	LOT1-rgw	parcel
LBM27	sawn	A108BSW4	LOT1-rgw	parcel
LBM28	sawn	A136BSW1	LOT1-rgw	parcel
LBM29	sawn	A136BSW4	LOT1-rgw	parcel

A standard beam test device, principally shown in Figure 5-11 and a hydraulic press was used to load the samples. A force and a strain transducer, fixed on to the press, measured the load and displacement, respectively. The transducers were calibrated before and after the tests by use of dead weight and a mechanical length calibration device.

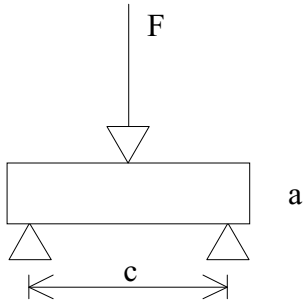

Figure 5-11 Schematic drawing of the beam test device.

Parcel material was sawn to form cuboids with the dimensions slightly less than 40×20×10 mm^3 (length, width, height). The specimens were placed in a specially designed saturation device with the above dimensions. Air-dry reference material was compacted to the intended density and placed into the saturation device. Air was evacuated from the system by use of a vacuum pump (approximately 2 kPa) and the test solution was allowed to enter the specimen from filters at both sides. The expected saturation time for the air-dry reference samples was a few days. Since there was no

monitoring of the saturation, the minimum standard time was 1 week after which the samples were removed and wrapped in plastic awaiting testing.

Each specimen was weighed just before they were placed in the press. The press loaded the specimen at a constant speed of 0.1 mm/min, and the load and deformation at the centre of the specimen were recorded every second. The broken specimens were examined with respect to water ratio according to section 5.3.

5.6.2 Evaluation

The vertical central force (F) was used to determine the tensile stress according to:

$$\sigma_t = \frac{6 \cdot F \cdot c}{4 \cdot b \cdot a^2}\ , \qquad 5\text{-}10$$

where a is the sample height, b the sample width, and c is the specimen length (Figure 5-12). The tensile stress at failure (σ_{tf}) (tensile strength) was used to calculate an approximate value of the shear strength (τ_f) according to:

$$\tau_f = \frac{\sigma_{tf}}{2} \qquad 5\text{-}11$$

A compilation of results is shown in Figure 5-13.
The maximum tensile strain (ε_f) was calculated from:

$$\varepsilon_f = \frac{a \cdot D \cdot 6}{c^2} \qquad 5\text{-}12$$

where D is the maximum displacement at the centre of the specimen (Figure 5-14).

The maximum tensile stress (at failure) is partly a function of the density of the specimens and the density was therefore calculated after the beam tests by the technique described in section 5.4.

The raw and calculated data concerning deformation and force versus time have been stored in an excel file together with the calculated water ratio, density, tensile strength and shear stress, and transferred to the SICADA database. The individual specimens were denominated according to the general scheme, e.g. 08BSW2BM (BM for balk test).

5.6.3 Results

No significant cementation effects were expected in the parcel material compared with reference material, i.e. no increase in tensile strength or decrease in strain at failure. A minor trend in the opposite direction can be seen in the recorded data, i.e. the parcel material has become slightly “softer” or more “plastic”. This general trend has been found in previous laboratory tests as an effect of heating. One exception is sample LBM12 (mid position in block 8), which has a higher tensile strength compared to

reference material. The mineralogical analyses of block S108 show minor but significant chemical anomalies e.g. reduced silica-aluminium ratio, which may be the cause of the rheological changes. The mineralogical changes were most pronounced in the innermost part of the block and the corresponding specimen does not show higher tensile strength. The measured density of the central specimen was low and an alternative, and more likely, explanation may be that this value is simply wrong since the absolute tensile strength value is close to those in the other parcel specimens.

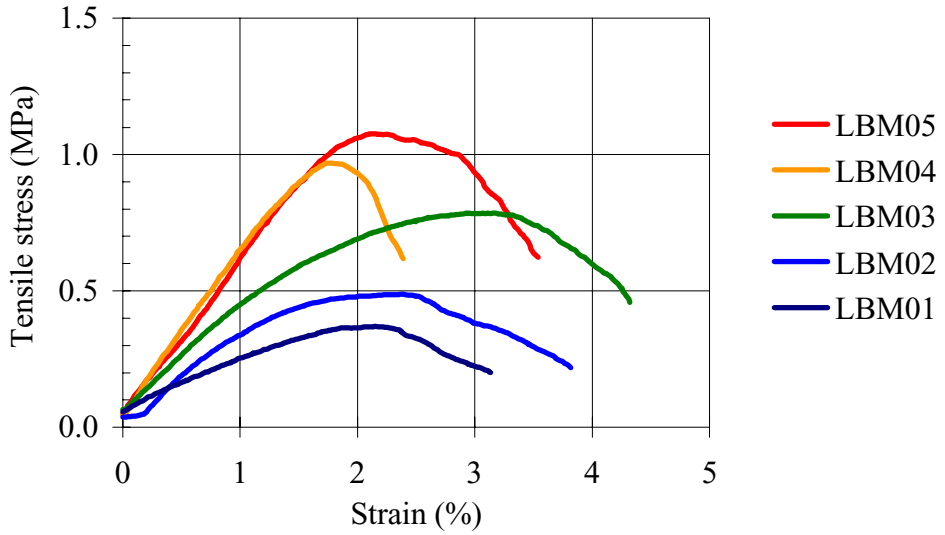

Figure 5-12 Recorded tensile stress versus strain for the reference samples saturated with deionised water.

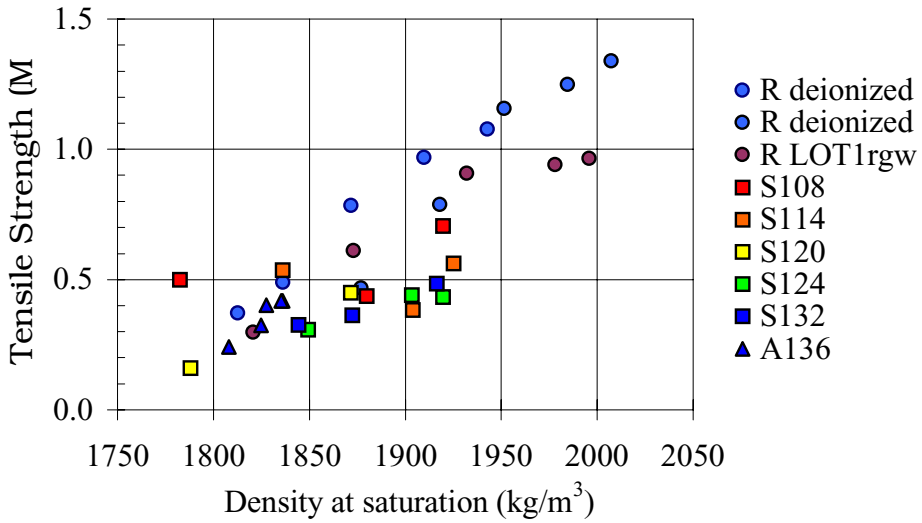

Figure 5-13 Compilation of calculated tensile strength versus density for all samples in the test.

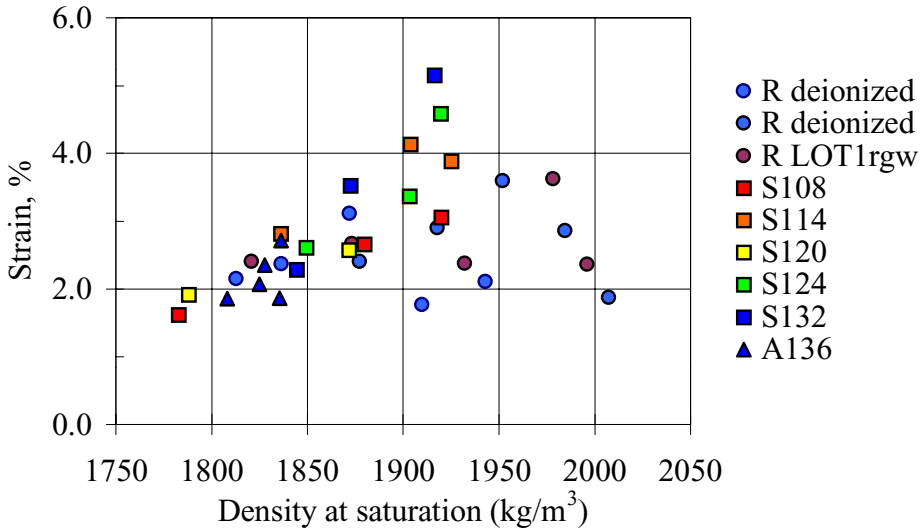

Figure 5-14 Compilation of calculated tensile strain at failure versus density for all samples in the test.

5.7 Triaxial tests

5.7.1 Test principle

The stress-strain-strength properties are preferably evaluated from triaxial tests. A detailed description concerning technique and evaluation is given in SKB TR 95-20. The technique requires relatively large test specimens and is resource consuming, and since no major discrepancies between the reference material and parcel material were found in the balk test series, only the originally planned 4 triaxial tests were carried out.

One test was run on reference material (R1) in order to get reference data for the LOT-solution. Three tests were run on parcel material, representing low temperature and maximum temperature conditions in the two S1 parcels and low temperature conditions in the A1 parcel. The parcel specimens were sawn from the innermost part of the block cylinder ring (position 0 to 4 in the radial direction). The test series was termed LTL-A.

Table 5-13 Test scheme for the LTL-A test series.

test	prep.	material	solution	density
				kg/m^3
LTL1	air-dry	reference	LOT1rgw	1950
LTL2	air-dry	S132BSW2	LOT1grw	parcel
LTL3	sawn	S114BSW2	LOT1rgw	parcel
LTL4	sawn	A136BSW2	LOT1grw	parcel

The test specimens were pre-saturated in a new-constructed cylindrical saturation device equipped with a cylindrical filter to achieve radial saturation. A piston in the cylinder mantel surface allowed for measurement of the swelling pressure parallel to the saturation. The cylinder ring was slightly conical, which made it possible to extrude the filter including the specimen. Finally, the filter was divisible which made it possible to remove the specimens without the use of axial force.

Two types of triaxial cells were used; one standard type for the low-density specimen and one high pressure cell for the remaining 3 specimens. The cells were equipped with standard strain gauges, force transducers and pore-pressure transducers according to Figure 5-15.

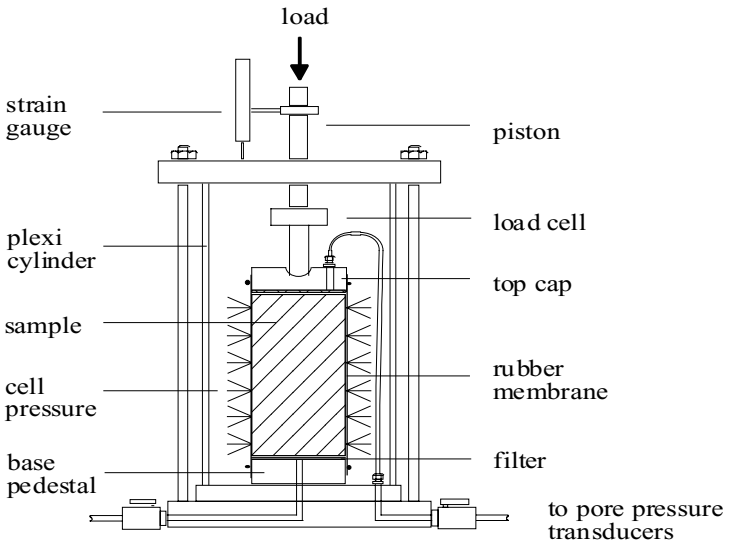

Figure 5-15 Schematic cross section view of the standard triaxial cell. The high-pressure cell was sturdier and had a stiff steel cylinder replacing the Plexiglas cylinder.

Cylindrical specimens were prepared from the parcel material by sawing rough cylinders, which were trimmed to a diameter of 35 mm and a height of 70 mm. The reference sample was prepared in a compaction device from air-dry powder to the same dimensions. The specimens were saturated for 4 weeks. After standard mounting with a rubber membrane a cell pressure (σ_3), corresponding to the measured swelling pressure during saturation, was applied in the cell. The valves to the pedestal and top-cap were kept closed during the equilibration period, which lasted for about one week, in order to measure the pore pressure (u).

The cells were placed in a hydraulic press and sheared at a rate of 7.5 mm/week (~10% strain/week). The sample was undrained also during the course of shearing. After failure the water ratio and density of the specimens were determined according to section 5.3 and 5.4.

5.7.2 Evaluation

The cell pressure (σ_3), pore pressure (u), displacement (Δl), and axial force (F) were measured. The deviator stress was calculated from:

$$q = \frac{F}{A} \quad , \qquad 5\text{-}13$$

where A is the specimen cross-section area (the contact area between load piston and topcap was considered insignificant).

The vertical effective stress (σ'_1) was calculated from

$$\sigma'_1 = \frac{F}{A} + \sigma_3 \ , \qquad 5\text{-}14$$

The average effective stress (p') was calculated from:

$$p' = \frac{1}{3} \cdot (\sigma'_1 + 2\sigma_3 - 3u) \qquad 5\text{-}15$$

The strain was calculated from

$$\varepsilon = \frac{\Delta l}{l} \ , \qquad 5\text{-}16$$

where l is the original length of the sample and Δl is the change in length.

The measured cell pressure, pore pressure, displacement, and axial force versus time have been stored together with the calculated stress, strain, water ratio and density data in an Excel file and transferred to the SICADA database. The individual specimens were denominated according to general scheme ex. 14BSE2TL (TL for triaxial test).

5.7.3 Results

No significant discrepancies were expected between the reference and parcel material with respect to shear strength and shear course and the results shown in Figure 5-16 fall close to the line curve-fitted to previous results from MX-80 material saturated with deionised water. The tendency towards higher deviator stress may be due to the effect of the salt groundwater solution.

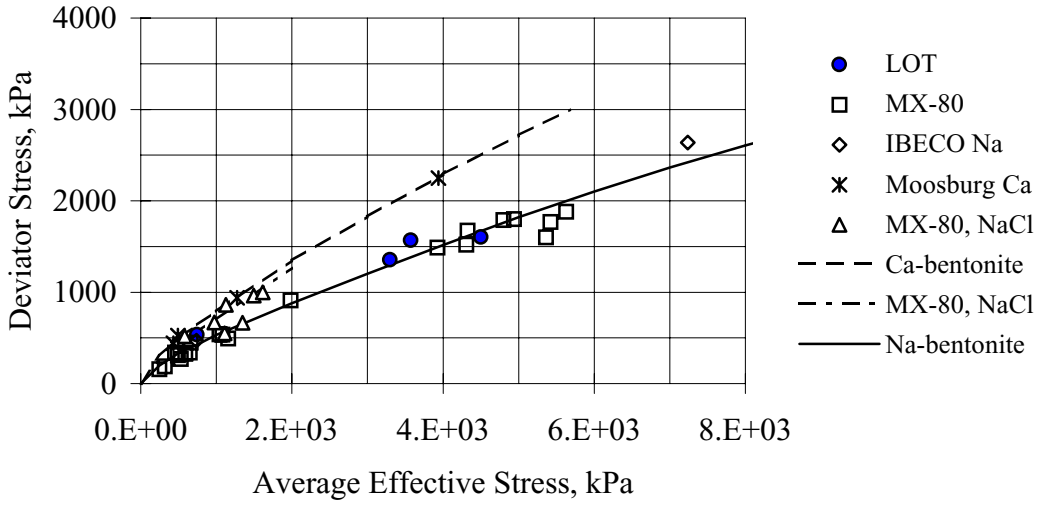

Figure 5-16 Compilation of maximum deviator stress versus effective average stress for different bentonite materials saturated with different solutions. Lines indicate tendencies based on curve fitting.

5.8 Element analysis

5.8.1 Test principle

Reference material and parcel material from the two parcels were analysed by a standard ICP/AES technique at SGAB, Luleå. The reference material was saved during the block production, and the parcel material was sampled radial from 5 defined blocks in the S1 and A1 parcels, respectively (section 5.2). Both the bulk buffer material and the clay fraction were analysed for all positions. The test series concerning reference bulk material was termed LEA-A, the reference clay fraction test series was termed LEA-B, the parcel bulk material series was termed LEA-C, and the parcel clay fraction series was termed LEA-D.

Table 5-14 Test scheme for the LEA-A series.

specimen	preparation	material	origin
LEA1	original	RS109	R1
LEA2	original	RS115	R1
LEA3	original	RS121	R1
LEA4	original	RS127	R1
LEA5	original	RS133	R1
LEA6	original	RA109	R1
LEA7	original	RA115	R1
LEA8	original	RA121	R1
LEA9	original	RA127	R1
LEA10	original	RA133	R1

Table 5-15 Test scheme for the LEA-B series.

specimen	preparation	material	origin
LEA11	< 2 µm	RS109	R1
LEA12	< 2 µm	RS115	R1
LEA13	< 2 µm	RS121	R1
LEA14	< 2 µm	RS127	R1
LEA15	< 2 µm	RS133	R1
LEA16	< 2 µm	RA109	R1
LEA17	< 2 µm	RA115	R1
LEA18	< 2 µm	RA121	R1
LEA19	< 2 µm	RA127	R1
LEA20	< 2 µm	RA133	R1

Table 5-16 Test scheme for the LEA-C series.

test	prep.	material	origin
LEA21	air-dry	S108BSE1	parcel
LEA22	air-dry	S108BSE3	parcel
LEA23	air-dry	S108BSE5	parcel
LEA24	air-dry	S108BSE7	parcel
LEA25	air-dry	S108BSE9	parcel
LEA26	air-dry	S114BSE1	parcel
LEA27	air-dry	S114BSE3	parcel
LEA28	air-dry	S114BSE5	parcel
LEA29	air-dry	S114BSE7	parcel
LEA30	air-dry	S114BSE9	parcel
LEA31	air-dry	S132BSE1	parcel
LEA32	air-dry	S132BSE3	parcel
LEA33	air-dry	S132BSE5	parcel
LEA34	air-dry	S132BSE7	parcel
LEA35	air-dry	S132BSE9	parcel
LEA36	air-dry	A108BSE1	parcel
LEA37	air-dry	A108BSE3	parcel
LEA38	air-dry	A108BSE5	parcel
LEA39	air-dry	A108BSE7	parcel
LEA40	air-dry	A108BSE9	parcel
LEA41	air-dry	A136BES1	parcel
LEA42	air-dry	A136BSE3	parcel
LEA43	air-dry	A136BSE5	parcel
LEA44	air-dry	A136BSE7	parcel
LEA45	air-dry	A136BSE9	parcel

Table 5-17 Test scheme for the LEA-D series.

test	prep.	material	origin
LEA46	< 2 µm	S108BSE1	parcel
LEA47	< 2 µm	S108BSE3	parcel
LEA48	< 2 µm	S108BSE5	parcel
LEA49	< 2 µm	S108BSE7	parcel
LEA50	< 2 µm	S108BSE9	parcel
LEA51	< 2 µm	S114BSE1	parcel
LEA52	< 2 µm	S114BSE3	parcel
LEA53	< 2 µm	S114BSE5	parcel
LEA54	< 2 µm	S114BSE7	parcel
LEA55	< 2 µm	S114BSE9	parcel
LEA56	< 2 µm	S132BSE1	parcel
LEA57	< 2 µm	S132BSE3	parcel
LEA58	< 2 µm	S132BSE5	parcel
LEA59	< 2 µm	S132BSE7	parcel
LEA60	< 2 µm	S132BSE9	parcel
LEA61	< 2 µm	A108BSE1	parcel
LEA62	< 2 µm	A108BSE3	parcel
LEA63	< 2 µm	A108BSE5	parcel
LEA64	< 2 µm	A108BSE7	parcel
LEA65	< 2 µm	A108BSE9	parcel
LEA66	< 2 µm	A136BES1	parcel
LEA67	< 2 µm	A136BSE3	parcel
LEA68	< 2 µm	A136BSE5	parcel
LEA69	< 2 µm	A136BSE7	parcel
LEA70	< 2 µm	A136BSE9	parcel

5.8.2 Sample preparation

No treatment was made of the bulk reference material (LEA-A series). The parcel bulk material (LEA-C series) was air-dried and gently crushed prior to the analyses.

The clay fraction (mean particle diameter < 2µm) from the reference (LEA-B series) and parcel (LEA-D series) material was separated by use of Stoke´s law according to the following technique:

- Approximately 10 g of the bulk material was dispersed in 1L of pure water by use of mechanical stirring and ultrasonic sound treatment.
- The dispersion was left to rest for 10 min. in order to let the coarsest fraction settle.
- The supernatant was equally distributed into 4 centrifuge bottles (250 ml) by weighing.
- The dispersion was centrifuged during a time period calculated by:

$$t = \frac{6.3 \cdot 10^{-9} \cdot \eta \cdot \log \frac{R_1}{R_2}}{N^2 \cdot D^2 \cdot \left(\rho_k - \rho_w\right)}, \qquad 5\text{-}17$$

where t is the time (s), η is the solution viscosity (g/cms), R_1 is the radius of rotation to the upper surface of the sediment (cm), R_2 is the radius of rotation to the solution surface, sedimentation distance (cm), N is the speed of rotation (r/min.), D particle diameter (cm i.e. 2×10^{-4} cm), g is the gravitational acceleration (cm/s^2), ρ_k is the particle density (g/cm^3) and ρ_w is the density of the solution (g/cm^3).

- The supernatants were carefully decanted off into one glass beaker.
- The suspension was concentrated by evaporation at 60°C in a ventilated oven.
- The dry material was gently ground.

The analysing laboratory (SGAB, Luleå) used standard treatment according to their G2 type analysis, both for the unsorted material and for the clay fraction. The specimens were melted in a mixture of lithium carbonate and dibortrioxide, dissolved in nitric acid and analysed by use of ICP-AES techniques.

5.8.3 Data flow and evaluation

The main elements in the G2 analyse are given in the form of oxides together with a LOI (Loss Off Ignition) value as percent of the total mass after drying. The analysed main elements were Si, Al, Ca, Fe, K, Mg, Mn, Na, P and Ti. The LOI value represents volatile substances, which were lost during the analyses, such as remaining water, carbon dioxide etc. In order to avoid misunderstandings it may be pointed out that elements present in the specimens are consequently shown in the analyses as oxides, e.g. SiO_2, which do not mean that Si existed in this form in the sample. Calculation of "true" Si content in the samples includes assumptions concerning light elements, such as hydrogen and oxygen, which may introduce errors. The standard way to present ICP-AES analyses results as oxides are therefore used in the following section. However, in order to make direct comparison possible between specific main elements in the various samples, the values were corrected with respect to the LOI according to:

$$P = \frac{P_{meas}}{\sum_{Si}^{Ti} P_{meas}} \cdot 100 \qquad 5\text{-}18$$

Where P indicates the presented percent value, P_{meas} represents the measured value relative to the total mass of the specimen, and summation concerns all main elements. In other words, the following diagrams show the content of an element relative to all main elements and not to the total mass of the specimen. The advantage of this technique is that a possible increase in non-analysed elements does not indicate a decrease in the presented elements. Possible presence of not analysed elements are indicated in the diagrams showing the loss of ignition (Figure 5-17), and the sum of loss of ignition and main elements (Figure 5-18)

Analysed trace elements are Ba, Be, Co, Cr, Cu, La, Mo, Nb, Ni, Sc, Sn, Sr, V, W, Y, Yb, Zn, and Zr, and content is given in ppm.

The results were delivered in Excel files from SGAB and were placed in a matrix with content values correlated to the specific parcel positions according to the general scheme. The individual specimens were denominated according to general scheme ex.

08BSW2EAB (EA for element analyses, B for bulk material, alt. C for clay i.e. > 2μm fraction).

5.8.4 Results

The following compiled presentation of results shows the element content or sum of elements versus radial position in analysed block. The results from reference samples are presented as crosses to the right in each diagram (x = 9.5), since they are not related to any specific position in the blocks. In all diagrams there are 10 reference values although they often overlap.

In addition to the main elements, the specimens may contain volatile substances (at 1000°C), trace elements, and finally elements, which are not covered by the analyses, e.g. chlorine. The contents of volatile substances, e.g. organic material, carbonates or water, are shown in Figure 5-17 as loss of ignition (LOI). There is no general trend in the LOI values and the deviations in three specimens may be due to random water content.

The sum of main elements and loss of ignition shown in Figure 5-18 is 100% ±1.5% in all analyses, and no significant difference between parcel material and reference material was found in the total material, indicating that no significant amount of not analysed elements were present. Since there is no physical meaning of values above 100% the results indicate the precision of the analyses. However, it should be noticed that there is a systematic tendency towards lower values in the clay fraction material from block S108 and the inner part of block S114, representing the warm and not fully saturated part of parcel S1.

The total amount of trace elements in the samples were around 0.1 to 0.16 % in the total material, and 0.05 to 0.10 % in the clay fraction. No significant trends were found in these data except for copper (se below).

The following changes compared to reference results were found:

- Minor silica content reduction in the warm part of parcel S1 (Figure 5-19),
- A corresponding minor increase in aluminium and magnesium content (Figure 5-20 and 5-21),
- Minor general increase in sodium, potassium and calcium content (Figure 5-23 to 5-25),
- Ion exchange from sodium to calcium (Figure 5-23 and 5-25),
- Minor increase in copper content close to the central copper tube (Figure 5-27) at all temperatures.
- Tendency of general sulphur decrease, and profile with higher values in the inner part (Figure 5-28),

The two first items indicate changes in the clay structure, but since the changes are small and in the range of the accuracy of the analyses no sure conclusions can be drawn.

The ion-exchange from sodium to calcium was not obvious in the analyses of the total material since both ion-types showed an increase, but after dispersion in water in

conjunction with the preparation of the clay fraction the effect is obvious. Normally, also unexposed material shows this tendency due to dissolution of mainly calcite, but in the swollen part of parcel A1 it is obvious that the effect of groundwater is significant.

The maximum copper content close to the central copper tube was around 100 ppm in the total material and dropped to a mean value of around 25 ppm at a distance of 3 cm from the tube. The copper content was only slightly lower in the clay fraction, indicating that the copper was incorporated in the montmorillonite structure likely as exchangeable ions or as central ions in the octahedral layer.

The following non-changes are considered important:

- No redistribution or absolute changes in iron content (Figure 5-22),
- No redistribution or absolute content changes in stable non-clay elements e.g. titanium (Figure 5-26),

The stable values for iron and titanium are considered important since they show that the measured changes are not relative effects. Iron representing medium content elements, which may be compared to e.g. magnesium, and titanium representing low content elements comparable to e.g. potassium. The decrease in sulphur content shows that no significant enrichment of sulphate minerals e.g. gypsum has taken place in the major part of the bentonite.

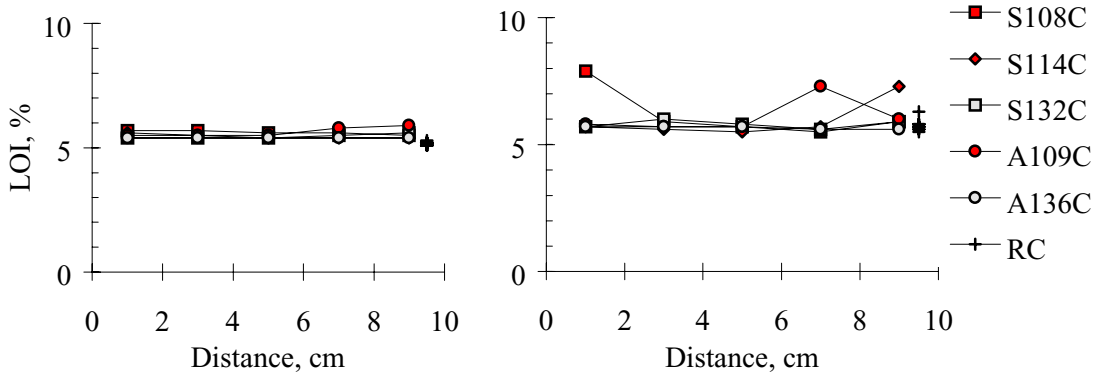

Figure 5-17 Compilation of ICP/AES results from total material (left) and clay fraction (right) showing loss of ignition (LOI) versus radial distance from the central copper tube. 10 reference results to the right (x=9.5).

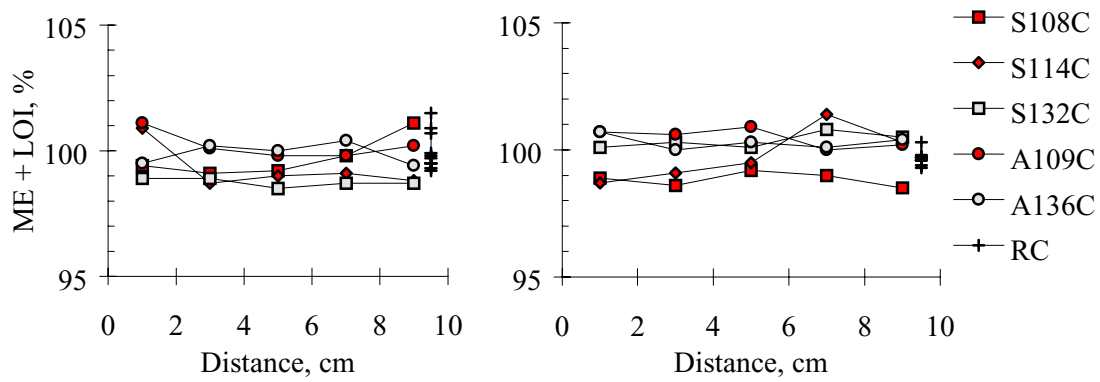

Figure 5-18 *Compilation of ICP/AES results from total material (left) and clay fraction (right) showing the sum of main elements and loss of ignition versus radial distance from the central copper tube. 10 reference results to the right (x=9.5).*

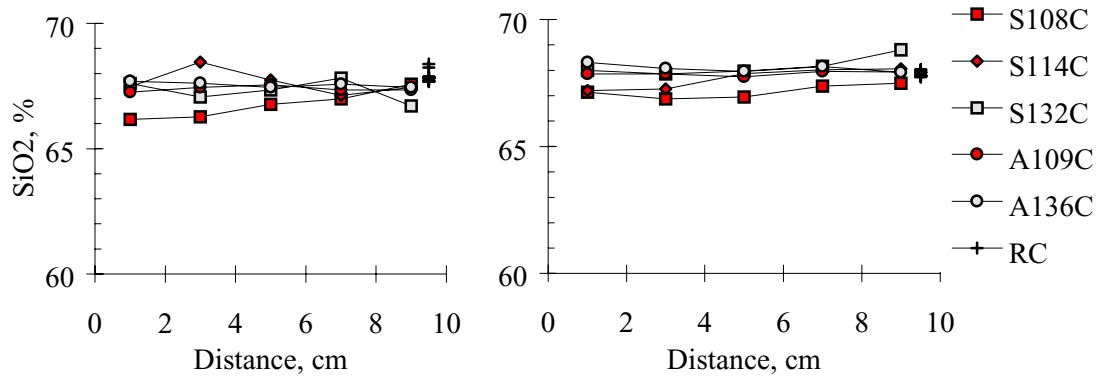

Figure 5-19 *Compilation of ICP/AES results from total material (left) and clay fraction (right) showing SiO_2 content of main elements versus radial distance from the central copper tube. 10 reference results to the right (x=9.5).*

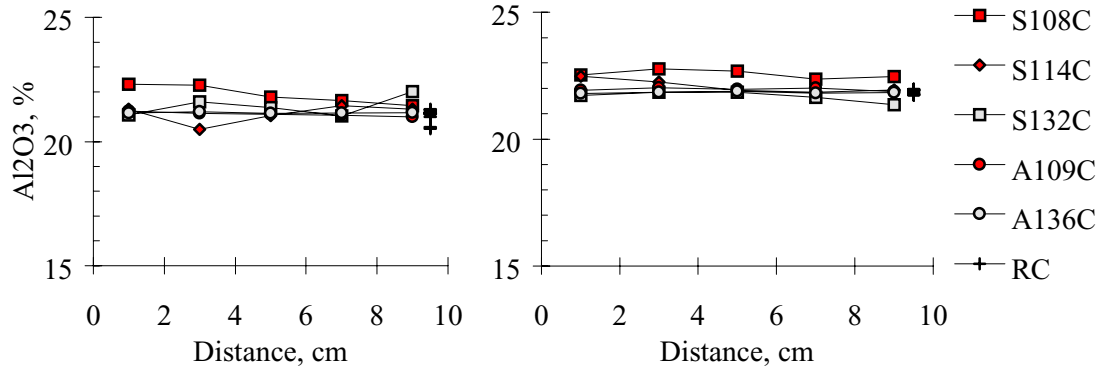

Figure 5-20 *Compilation of ICP/AES results from total material (left) and the clay fraction (right) showing Al_2O_3 content of main elements versus radial distance from the central copper tube. 10 reference results to the right (x=9.5).*

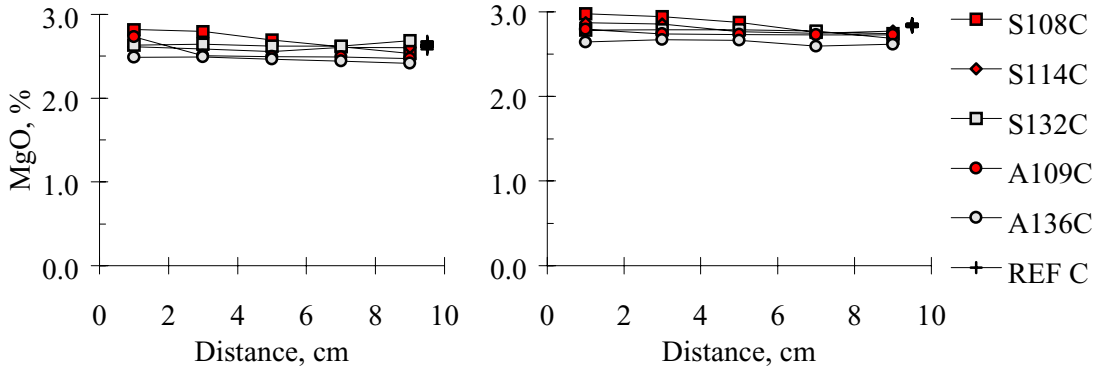

Figure 5-21 Compilation of ICP/AES results from total material (left) and clay fraction (right) showing MgO content of main elements versus radial distance from the central copper tube. Ten reference results to the right (x=9.5).

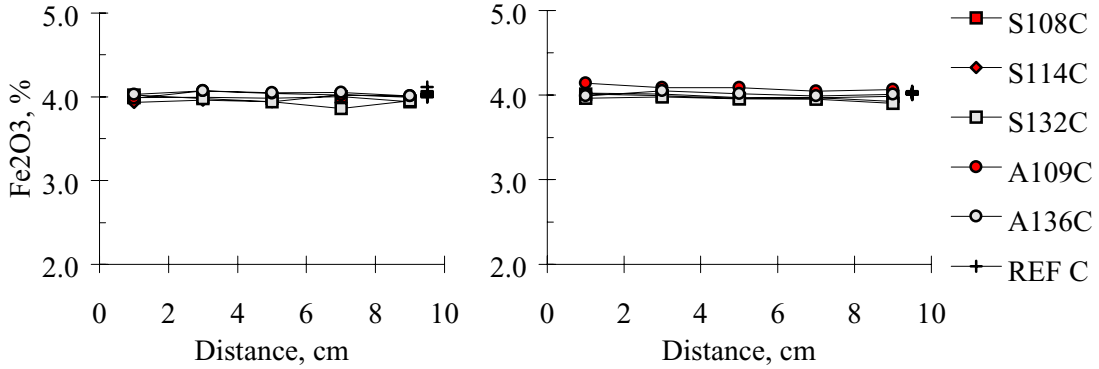

Figure 5-22 Compilation of ICP/AES results from total material (left) and clay fraction (right) showing Fe_2O_3 content of main elements versus radial distance from the central copper tube. Ten reference results to the right (x=9.5).

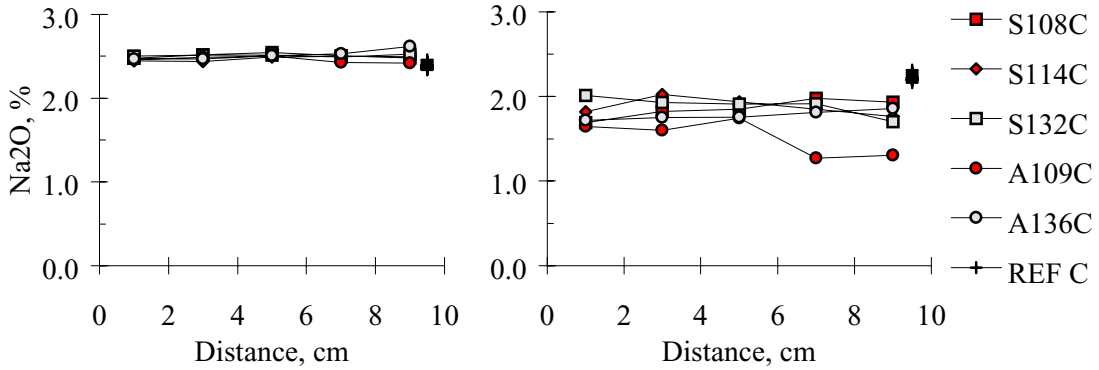

Figure 5-23 Compilation of ICP/AES results from total material (left) and clay fraction (right) showing Na_2O content of main elements versus radial distance from the central copper tube. Ten reference results to the right (x=9.5).

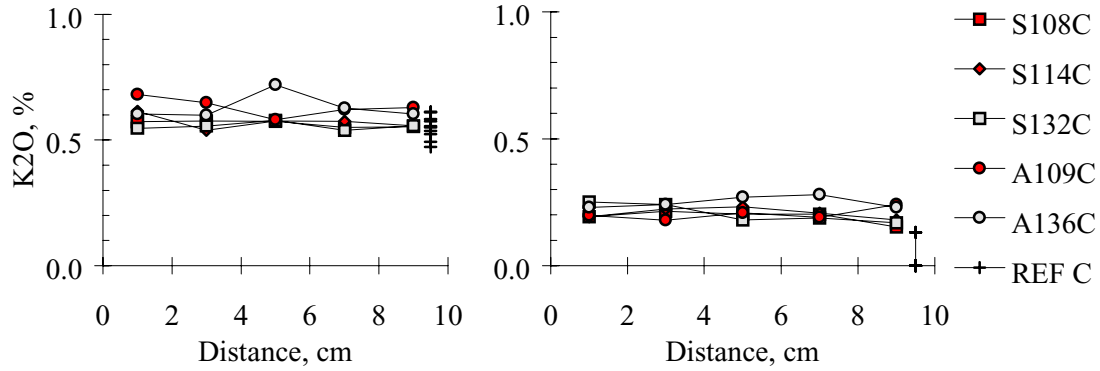

Figure 5-24 Compilation of ICP/AES results from total material (left) and clay fraction (right) showing K_2O content of main elements versus radial distance from the central copper tube. Ten reference results to the right (x=9.5).

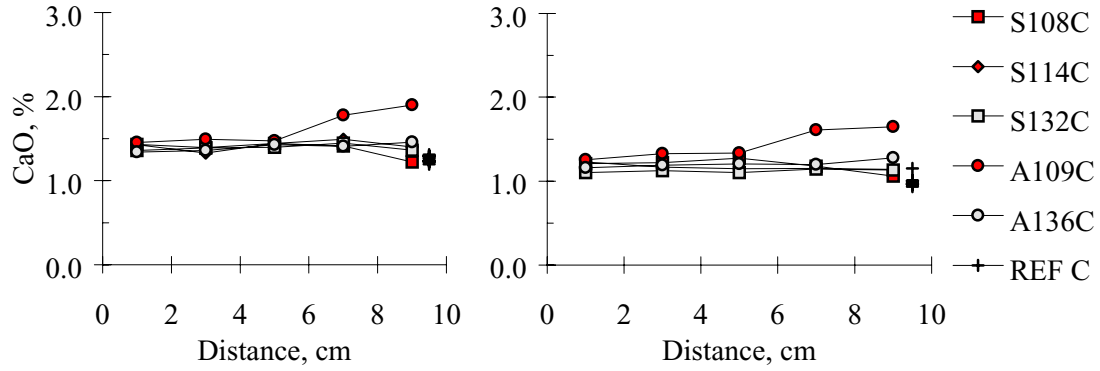

Figure 5-25 Compilation of ICP/AES results from total material (left) and clay fraction (right) showing CaO content of main elements versus radial distance from the central copper tube. Ten reference results to the right (x=9.5).

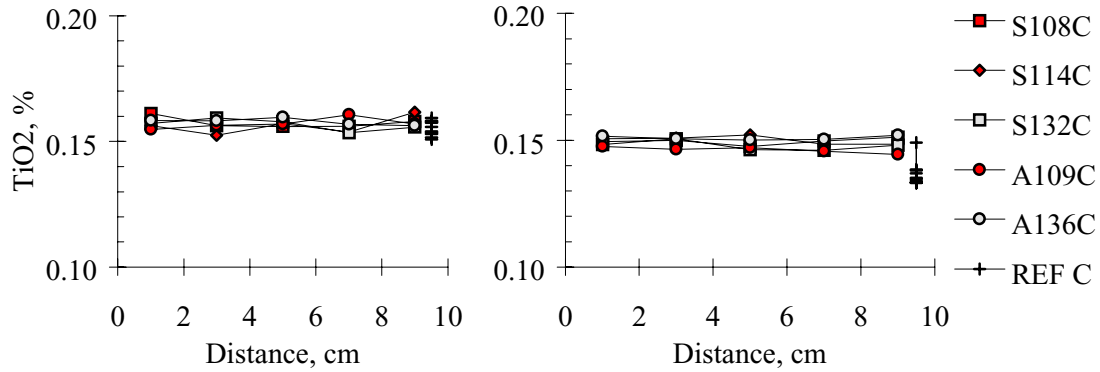

Figure 5-26 Compilation of ICP/AES results from total material (left) and clay fraction (right) showing TiO_2 content of main elements versus radial distance from the central copper tube. Ten reference results to the right (x=9.5).

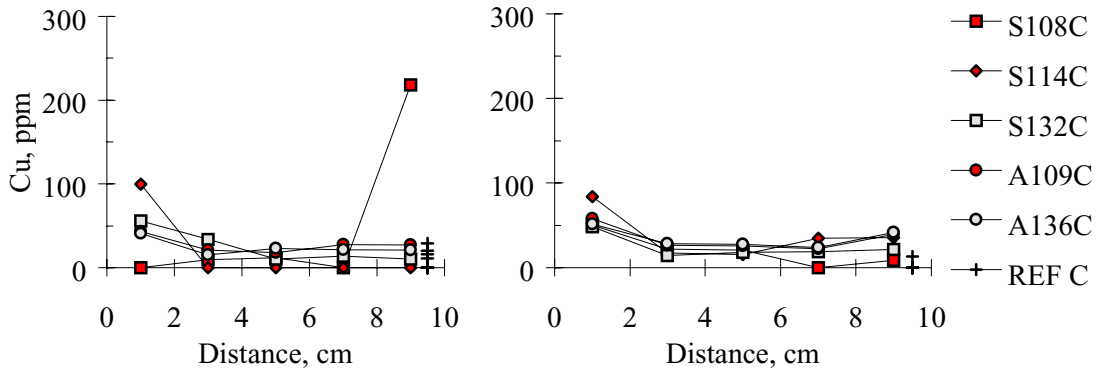

Figure 5-27 Compilation of ICP/AES results from the clay fraction showing Cu content versus radial distance from the central copper tube. Only one reference sample was above the detection limit of 6 ppm.

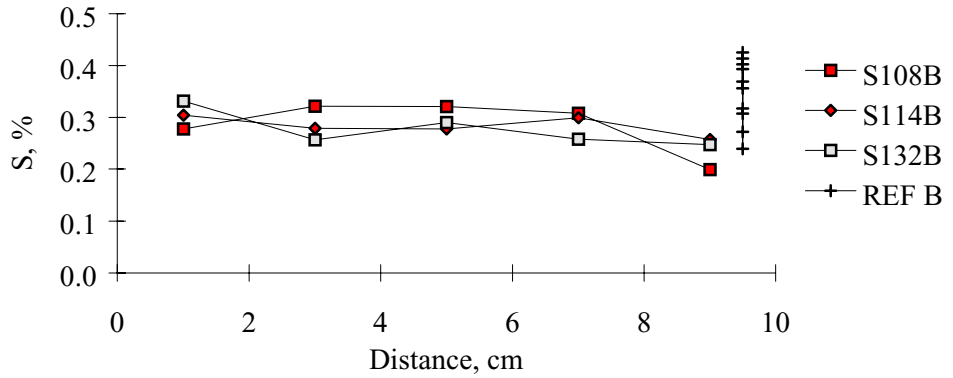

Figure 5-28 Compilation of ICP/AES results from total material showing S content of main elements versus radial distance from the central copper tube. Ten reference results to the right (x=9.5).

5.9 Cation exchange capacity analysis (CEC)

5.9.1 Test principle

The ion exchange property of a clay mineral is related to the abundance and nature of the lattice charge and can be expressed by the cation exchange capacity (CEC). A standard technique to determine the CEC is to exchange original ions by ammonium ions and analyse original replaced ions and introduced ammonium ions. The original ions in bentonite may include also ions from easily dissolving minerals or from groundwater. The sum of these ions will henceforth be referred to as extractable cations (EC). Differences between extractable and exchangeable ions may be indicative for processes in the test material, and both were therefore analysed by a method described by Chapman (Chapman 1961).

The precision in the ammonium analyses in this work with respect to CEC was low, however, and the results from reference material were not in agreement with literature

data. An additional method, based on exchange with copper(II) triethylenetetramine, was therefore used as a complement (Meier 1999) in order to determine the CEC.

The same sample selection principle as for the element analyses was used, i.e. material from the same references and parcels positions were analysed. However, all CEC analyses were made on non-fractionated material in order to include also larger grains, which may affect the CEC, e.g. zeolites. The test series was termed LCE-A for the reference material and LCE-C for the parcel material (analogue to the bulk element analyse test series). The LCE-A series comprises in total 10 samples and the LCE-C series 25 samples.

5.9.2 Test procedure

No pre-treatment was made of the reference material (LCE-A series). The parcel bulk material (LCE-C series) was air-dried and gently crushed prior to the analyses.

The principle technique for the ammonium acetate method is given by the following items.

- The mass of a specimen was determined (mg resolution)
- Water ratio was determined for a parallel specimen according to section 5.3.
- Approximately 1 g of material from each specimen was saturated with NH_4^+, by repeated (3 times) washings with 1 M ammonium acetate solution. pH was kept at 7 during the procedure by adding NH_4OH or HCl.
- The supernatants were analysed with respect to extractable ions by ICP/AES..
- The ammonium saturated clay specimens were washed 3 times with propanol in order to eliminate excess ammonium acetate.
- The specimens were ion-exchanged to sodium state by repeated (3 times) washings in acidified 2 M NaCl solution.
- The supernatants from the washings were finally analysed with respect to the ammonium concentrations by the Kjeldahl method, from which the CEC values were calculated.

The principle technique for the copper-trien method is given by the following items.

- Water ratio was determined for a parallel specimen according to section 5.3.
- 600 mg of the specimen was placed in 195 g deionised water in a centrifuge bottle and dispersed by means of ultrasonic treatment for 15 minutes,
- 39 g of 0.01 M Cu(II)-trien solution was added and mixed by means of vibrating table for 5 minutes,
- The solution was centrifuged at 4000 rpm for 11 minutes,
- The photometer was calibrated by reference solutions with the concentration 0.001667 M, 0.001 M and 0.0001 M Cu(II)-trien solution,
- The absorbency of 620 nm light of the supernatant was determined and the amount of Cu(II)-trien taken up by the clay was evaluated,
- The CEC value was calculated from the Cu(II) uptake.

The extractable ions were analysed by use of ICP/AES according to the SGAB V1 analyse, ammonium concentrations by Svedac micro-Kjeldahl method, and the copper-trien concentration by photometry at Clay Technology. The cation exchange capacity (equivalents/kg clay) was calculated from the ammonium ion concentration and from the copper-trien concentration according to the reference. The results from the reference material obtained by the copper-trien method were in accordance with literature data and the presented CEC data are therefore based on this technique. All results are, however, stored in the SICADA database.

The ICP/AES analyses of extractable ions include Ca, Fe, K, Na, Mg, P, S, and Si with mg/l resolution and Al, As, B, Ba, Cd, Co, Cr, Cu, Li, Mn, Mo, Ni, Pb, Sr, V, and Zn with µg resolution.

Results were delivered in Excel files from SGAB and from Clay Technology in a matrix with concentration values and calculated CEC values correlated to the specific parcel positions according to the general scheme, and were transferred to the SICADA database. The individual specimens were denominated according to general scheme ex. 08BSW2CE (CE for cation exchange capacity).

5.9.3 Results

The reference material was expected to have CEC values around 0.8 equivalents per kg dry clay, and no significant change was expected in the parcel material. A general minor increase of extracted cations in the parcel material compared to reference material was expected as a result of the groundwater uptake.

The CEC analyses made by the ammonium exchange method of reference material showed generally high values, and analyses of parcel material showed large scatter. The Kjeldahl analyse technique produce additional ammonium ions from organic material, which may be the cause of the high reference values since the organic content in the original bentonite is not negligible. The large scatter in the results from parcel material has not been possible to correlate to any other variable in the system despite extensive effort, and no satisfactory explanation is at hand. Further investigations are planned ahead of the forthcoming parcel analyses in order find the cause of the scatter.

The accuracy of the ICP/AES-analyses is generally high and expected minor changes from reference material to parcel material have been observed. A compilation of the ICP/AES analyses combined with Cu (II) trien analyses is shown in Figure 5-29 to 5-33. The copper (II) trien analyses of CEC showed results in agreement with literature data, and the scatter in results from parcel material was small. No systematic trends were found (Figure 5-29 to 5-33 and Table 5-17).

The most interesting findings with regard to bentonite may be summarised in the following items:

- General net cation uptake, (increase of EC),
- Indication of ion-exchange between Na and Ca in the most swollen parts (esp. block A109,)
- Minor redistribution of magnesium in blocks A109, A136 and S108,

- No significant change in potassium content
- No changes in cation exchange capacity.

In general there are good compatibility between the observed CEC and water analyses on the one hand and results from element analyses of solids and X-ray diffraction analyses, on the other, and no obvious incompatibility has been observed.

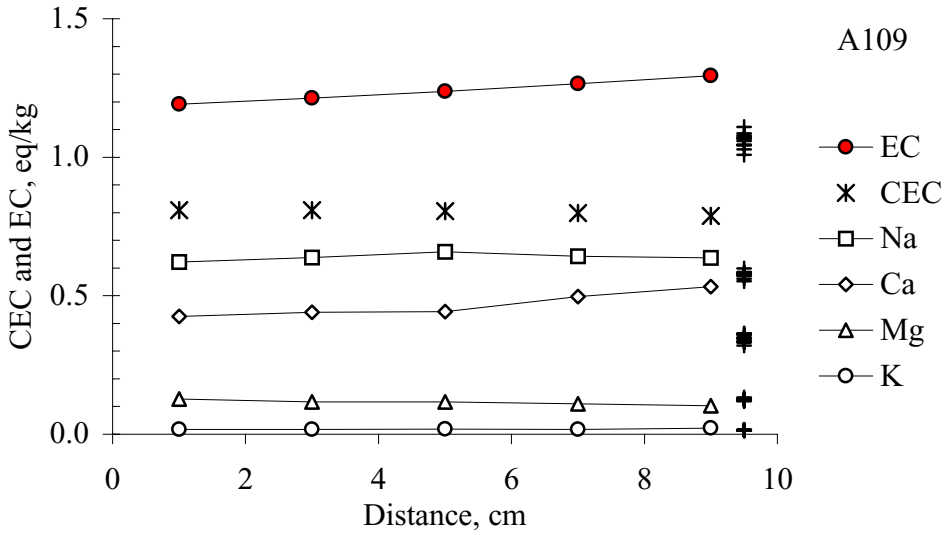

Figure 5-29 *Compilation of ICP/AES results concerning extracted cations (EC) and cation exchange capacity (CEC) versus radial distance from the central copper tube in block 09 in parcel A1. EC represents the sum of equivalents from Na, Ca, Mg, and K ions. Ten reference results to the right (x=9.5) for EC, Na, Ca, Mg, and K, respectively.*

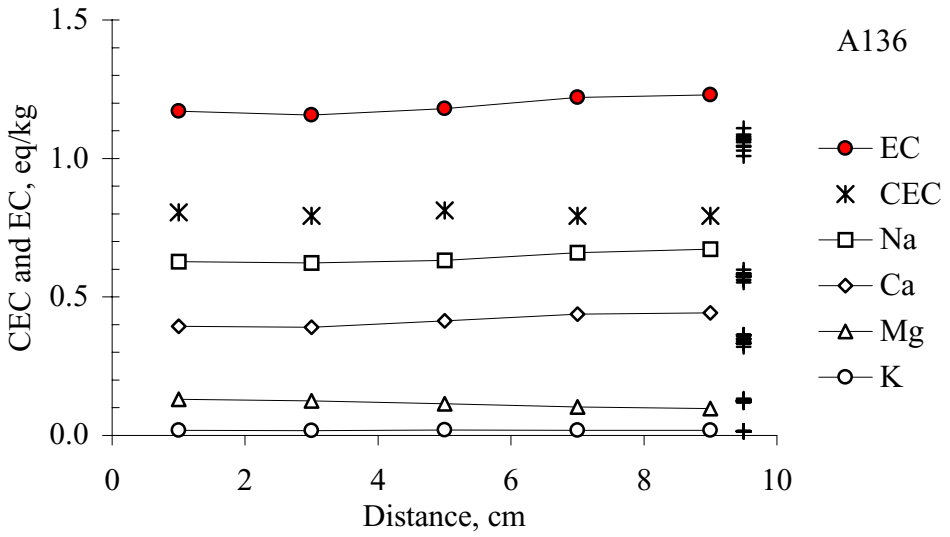

Figure 5-30 *Compilation of ICP/AES results concerning extracted cations (EC) and cation exchange capacity (CEC) versus radial distance from the central copper tube in block 36 in parcel A1. EC represents the sum of equivalents from Na, Ca, Mg, and K ions. Ten reference results to the right (x=9.5) for EC, Na, Ca, Mg, and K, respectively.*

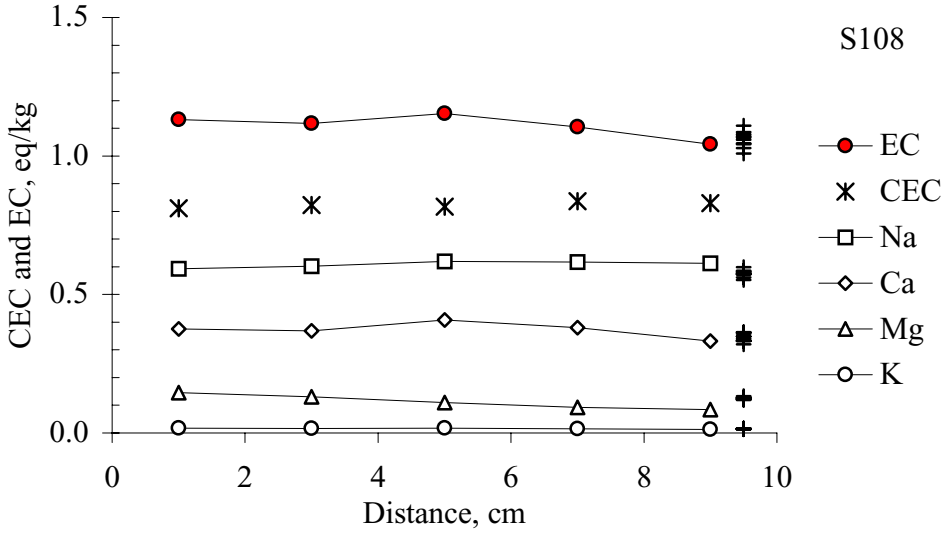

Figure 5-31 *Compilation of ICP/AES results concerning extracted cations (EC) and cation exchange capacity (CEC) versus radial distance from the central copper tube in block 08 in parcel S1. EC represents the sum of equivalents from Na, Ca, Mg, and K ions. Ten reference results to the right (x=9.5) for EC, Na, Ca, Mg, and K, respectively.*

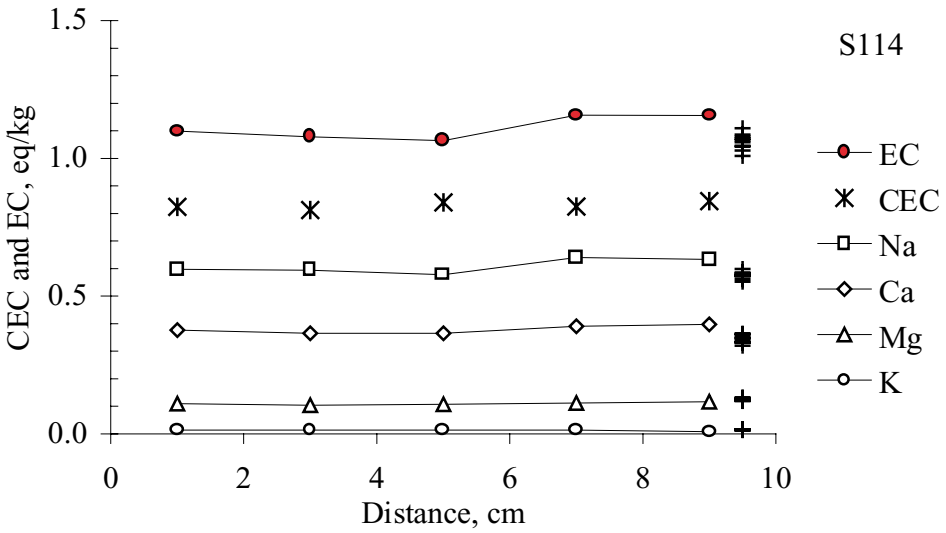

Figure 5-32 *Compilation of ICP/AES results concerning extracted cations (EC) and cation exchange capacity (CEC) versus radial distance from the central copper tube in block 14 in parcel S1. EC represents the sum of equivalents from Na, Ca, Mg, and K ions. Ten reference results to the right (x=9.5) for EC, Na, Ca, Mg, and K, respectively.*

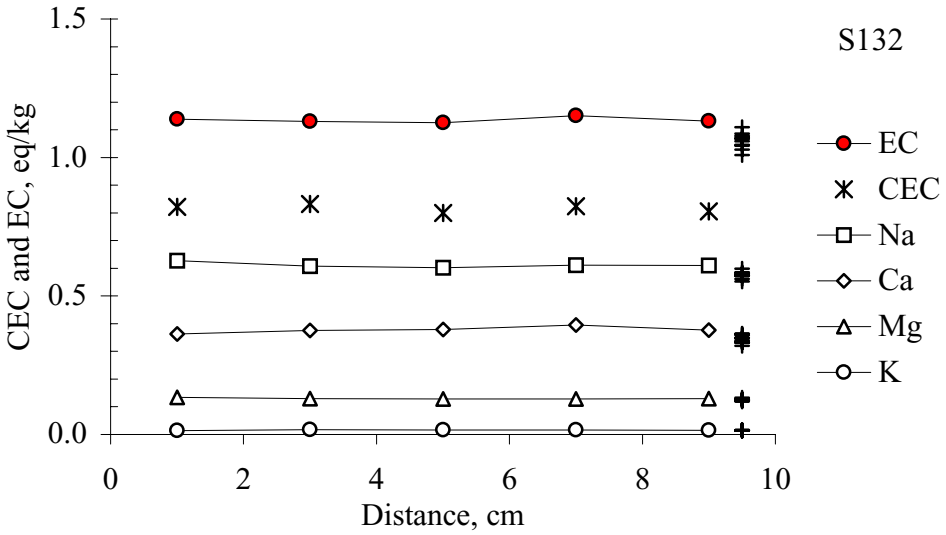

Figure 5-33 *Compilation of ICP/AES results concerning extracted cations (EC) and cation exchange capacity (CEC) versus radial distance from the central copper tube in block 32 in parcel S1. EC represents the sum of equivalents from Na, Ca, Mg, and K ions. Ten reference results to the right (x=9.5) for EC, Na, Ca, Mg, and K, respectively.*

Table 5-18 Results from CEC analyses made by Cu(II) trien technique of parcel material. Figures show the measured results in eq/kg. Reported literature values from Meier (1999) are in the range of 0.76 to 0.85.

Distance from Cu-tube, cm	A109B	A136B	S111B	S114B	S132B
1	0.81	0.81	0.81	0.82	0.82
3	0.81	0.79	0.82	0.81	0.83
5	0.81	0.81	0.82	0.84	0.80
7	0.80	0.79	0.84	0.83	0.82
9	0.79	0.79	0.83	0.84	0.81
min	0.79	0.79	0.81	0.81	0.80
max	0.81	0.81	0.84	0.84	0.83
mean	0.80	0.80	0.82	0.83	0.82

5.10 X-ray diffraction analysis (XRD)

5.10.1 Test principle

The same sample selection principle as for the element analyses was used, i.e. material from the same reference material and parcels positions were analysed.

The test series concerning reference bulk material was termed LXR-A (10 samples), the reference clay fraction test series was termed LXR-B (10 samples), the parcel bulk material series was termed LXR-C (25 samples), and the parcel clay fraction series was termed LXR-D (25 samples). Four additional samples from especially interesting positions were analysed.

The bulk test series mainly aimed at identifying the accessory minerals in the samples and cation exchange, while the clay fraction series aims at studying possible clay mineralogical changes. Two different preparation techniques were therefore used, one in order to produce specimens with unsorted and unoriented material, and the other in order to produce specimens with oriented material from the clay fraction. The former technique gives complete ”three-dimensional fingerprints" from all types of minerals, which are needed for a general identification. The latter technique enhances basal reflections from minerals with a ”two-dimensional” structure, which facilitate the identification of possible changes in the clay mineral, i.e. principally the montmorillonite.

The results are stored as intensity values versus 2θ values in the SICADA database. The individual specimens were denominated according to general scheme ex. 08BSW2EXRP (XR for XRD analyse, P for packed material, alt. O for oriented, and E for oriented and ethylene glycol treated material).

The interpretation has been made mainly by use of data from Crystal Structures of Clay Minerals (Brindley, 1984).

XRD technique is a precise and powerful tool with respect to the detection of e.g. illite neoformation. However, quantification by use of XRD is complicated and may be facilitated by computer code analyses (commercially available codes), and results have to be supported by element analyses and CEC determinations. The detection limit is

difficult to specify since it depends on the form of illite that is produced, i.e. the particle size and if the illite is a pure phase or if it is in the form of mixed layer structures.

No significant changes were found in the parcel material compared to reference material, and no interpretation was therefore made with respect to decomposition of superimposed peaks by use of computer analyse codes (e.g. DECOMPXR) or simulation codes (e.g. NEWMOD).

5.10.2 Sample preparation and test procedure

No pre-treatment was made of the bulk reference material (LXR-A series). The parcel bulk material (LXR-C series) was air-dried and finely ground in a mortar. The material from both series was carefully packed into an aluminium cavity mount, in order to avoid orientation.

The clay fraction material (LXR-C and LXR-D series) was dispersed in pure water and the suspension was placed in a vacuum filtration equipment in which the clay material was settled on a ceramic tile. The thereby oriented specimens were transferred to glass XRD sample holders and dried at ambient relative humidity and temperature.

A Siemens D500 diffractometer with Cu Kα radiation was used for the analyses. The scan resolution was 100 counts/degree. The oriented specimens (LXR-B and LXR-D series) were scanned in the 2θ interval 3-40°, and after saturation with ethylene glycol (EG) the 2θ interval 3-15° was scanned again in order to analyse the swelling characteristics. The packed, unsorted and unoriented specimens (LXR-A and LXR-C series) was scanned in the 2θ interval 3-65°.

5.10.3 Results

Reference material

The uppermost curve in Figures 5-34 to 5-36 shows the diffraction mean intensity from the 10 un-oriented reference specimens (LXR-A series). A peak indicates the presence of an atom layer distance in the material, and each mineral have a characteristic combination of distances. The vertical bars in Figure 5-44 indicate expected clay-related peak positions, where hk refers to internal montmorillonite lattice planes, 00l refers to basal distance reflection (001 to the left 002 etc), and illite indicates a compilation of illite related peaks. Many of the illite related peaks coincide for natural reasons with montmorillonite peaks, and at ~27° with quartz. The most informative peak with respect to pure illite is the basal plane related one at 8.8°. There is a tiny indication of the presence of illite in the original LOT MX-80 material. Indicative for the type of smectite is the hk (060) peak at 62° showing that the material is a di-octahedral smectite, and a shift towards lower values would indicate transformation into a more tri-octahedral character. The most informative peak with respect to montmorillonite alteration is the 001 peak at ~7°. A possible shift in position or in shape may be related to processes both in interlayer cation exchange and in clay mineral composition, and would call for further investigation.

The vertical bars in Figure 5-35 show the expected positions of peaks related to quartz, cristobalite and feldspars, which are the most common accessory minerals in the MX-80 bentonite. There is a large number of distinct quartz related peaks, which are very indicative, and the identification of quartz is consequently simple and precise. Cristobalite on the other hand has a low degree of crystallinity, which results in less defined peaks. The main peak interferes with albite, and secondary peaks with quartz and gypsum, which makes the identification less accurate. In the clay fraction all feldspar was removed but the main peak for cristobalite was still present, which strongly indicate the presence of cristobalite in the clay fraction (Figure 5-37). Feldspars give a number of distinct peaks but since there are intermediate forms it is sometimes difficult to determine the type. The crystals are relatively large, which make the variation in peak area accidental to a large extent. The dominating type in the reference material is however albite (Na feldspar).

Figure 5-36 shows peaks related to the less common accessory minerals gypsum, anhydrite and calcite, which may participate in precipitation reactions. A low content of gypsum and calcite is generally present.

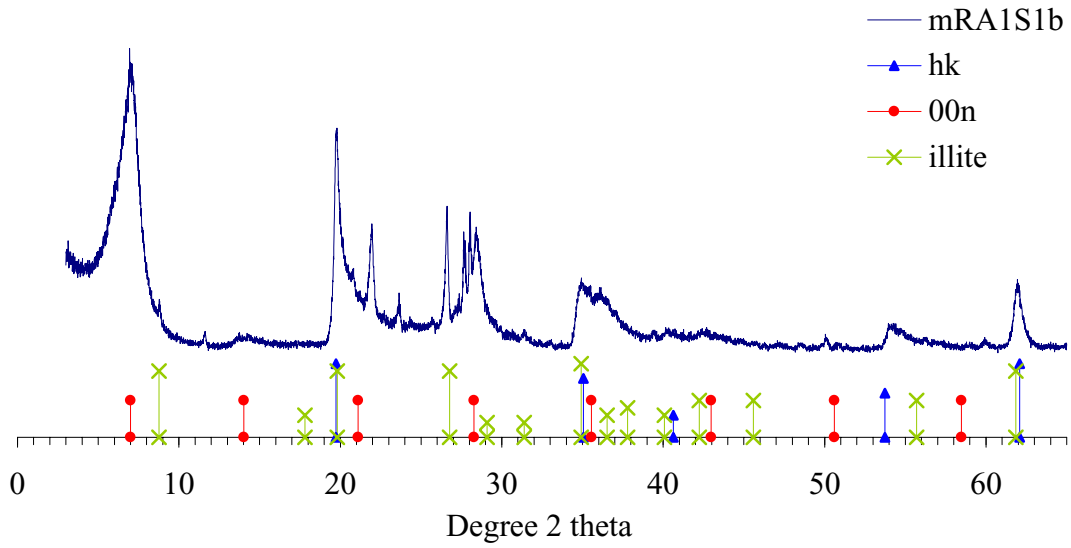

Figure 5-34 *The curve shows the mean intensity of diffraction patterns from the 10 reference samples. Vertical bars show the expected positions of clay related peaks.*

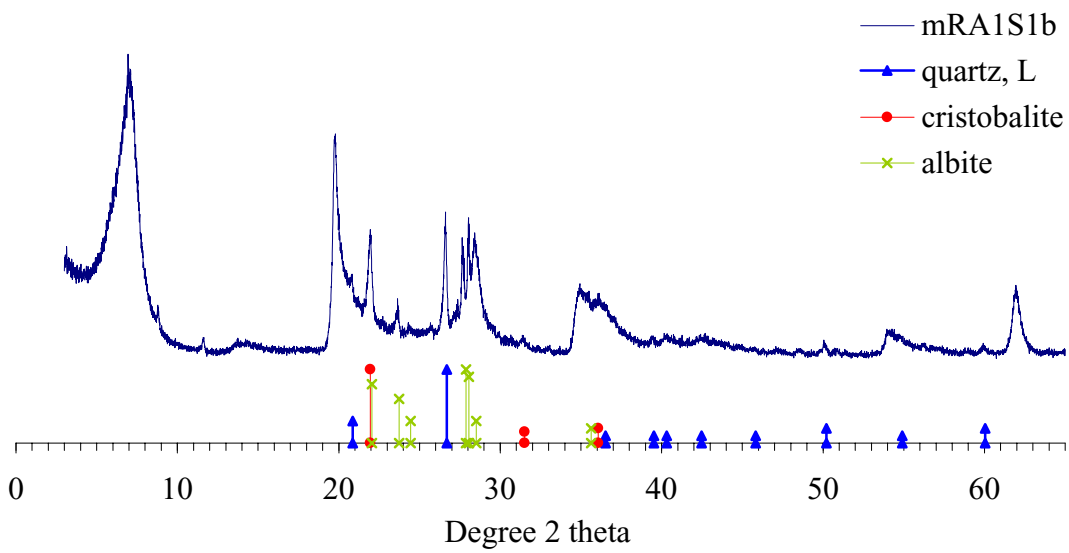

Figure 5-35 *The curve shows the mean intensity of diffraction patterns from the 10 reference samples. Vertical bars show the expected positions of silica and feldspar related peaks.*

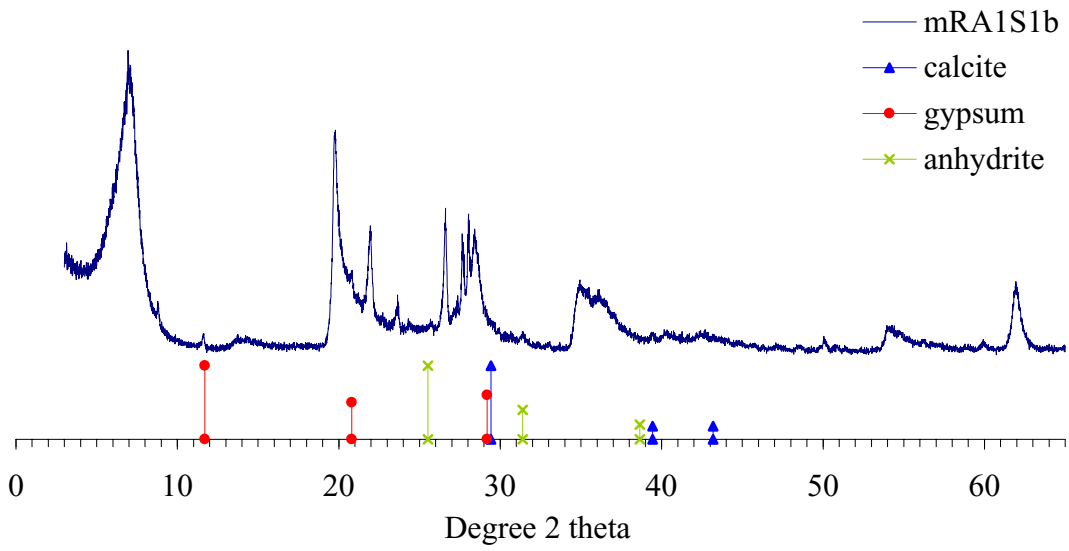

Figure 5-36 *The curve shows the mean intensity of diffraction patterns from the 10 reference samples. Vertical bars show the expected positions of peaks related to some sulphate and carbonate accessory minerals.*

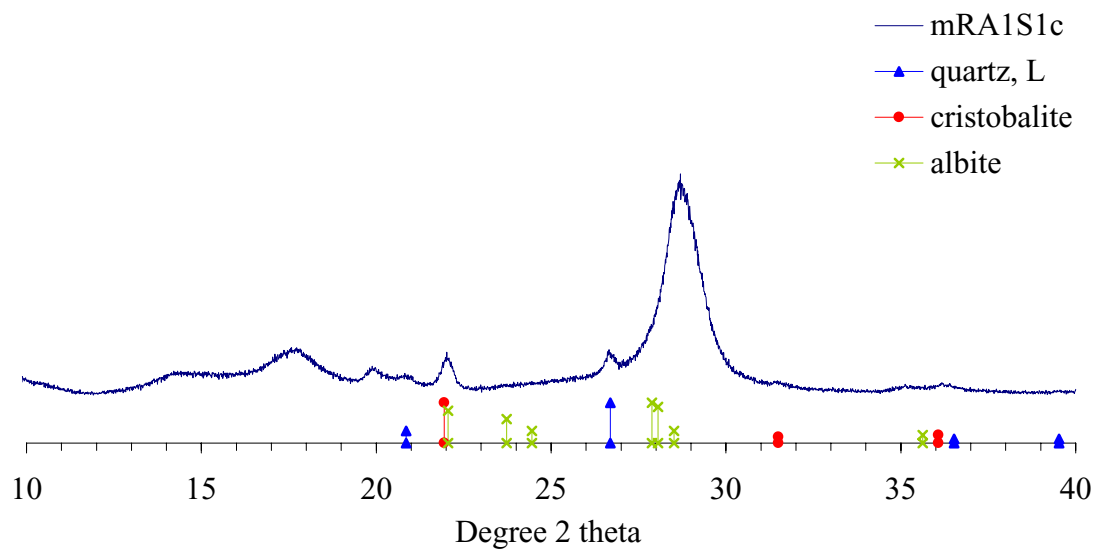

Figure 5-37 *The curve shows the mean intensity of diffraction patterns from the clay fraction of the 10 reference samples. Vertical bars show the expected positions of some silica and feldspar related peaks.*

Figure 5-38 shows individual results from 5 of the un-oriented reference samples and the mean results from all 10 reference samples (mRA1S1b) in order to illustrate the variations. The material was in general homogeneous, but small deviations in the material were present especially concerning feldspar, and 10 Å minerals (illite or muscovite).

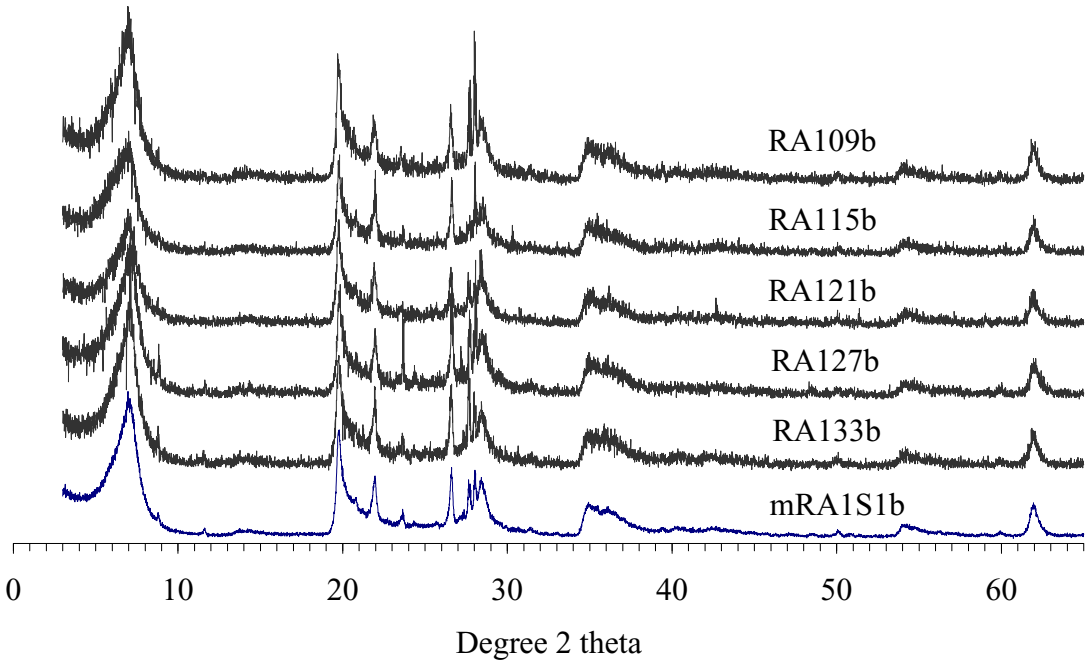

Figure 5-38 *The upper 5 curves show the diffraction patterns from the 5 reference samples from the A1 parcel. Lowest curve shows mean results from all 10 reference samples.*

The results from XRD analyses of reference material may be summarised in the following items:

- Montmorillonite basal distance close to 12.5 Å,
- Montmorillonite basal distance up to14.5 Å after dispersion,
- Montmorillonite basal distance between 17 to 17.5 Å after EG treatment
- Small variations in peaks related to quartz, cristobalite, gypsum and calcite,
- Larger variation in feldspar related peaks,
- Clay fraction (d < 2 μm) contains montmorillonite, cristobalite and quartz,

Parcel material

The one-year tests were not expected to give any changes with respect to clay lattice, and the results from series LXR-C did not show any significant trends. Therefore, standard investigations of the clay fraction and swelling properties have been made, but no further investigations with respect to the 001 peak. Figure 5-39 shows a compilation of results from block 09 in the A1 parcel as an example of results from a high temperature zone. Reference mean data are shown for comparison. Figure 5-40 and 5-41 show the corresponding results from the clay fraction, without and with ethylene glycol treatment, respectively.

Minor increase of calcium in exchange position was expected as a result of the introduced groundwater. A total conversion from Na-state to Ca-state would change the main montmorillonite peak in the untreated specimens from around 7.1° to 5.9°, 2 theta, corresponding to a basal spacing of 12.4 Å and 15 Å, respectively. Typical values for both cations after treatment with EG are 5.2° 2 theta, corresponding to a spacing of around 17 Å. A tendency of a shift in main peak position toward higher 2-theta value was also noticed in several of the exposed specimens compared to the reference material. There is no obvious gradient from rock towards the central parts of the parcels, which indicate that the source for calcium is original minerals and the saturating groundwater.

No clear indication of precipitation was found in the specimens from the general test program. However, the bentonite inner surface in both the A1 and the S1 parcels close to the warm parts of the copper tube was also analysed (Figure 4-14). Figure 5-52 shows the diffraction pattern from the innermost 0-3 mm material in block S103, the reference mean pattern and the difference between the two. An increase in gypsum content and larger basal spacing were obvious results. An increase in calcite content is further indicated.

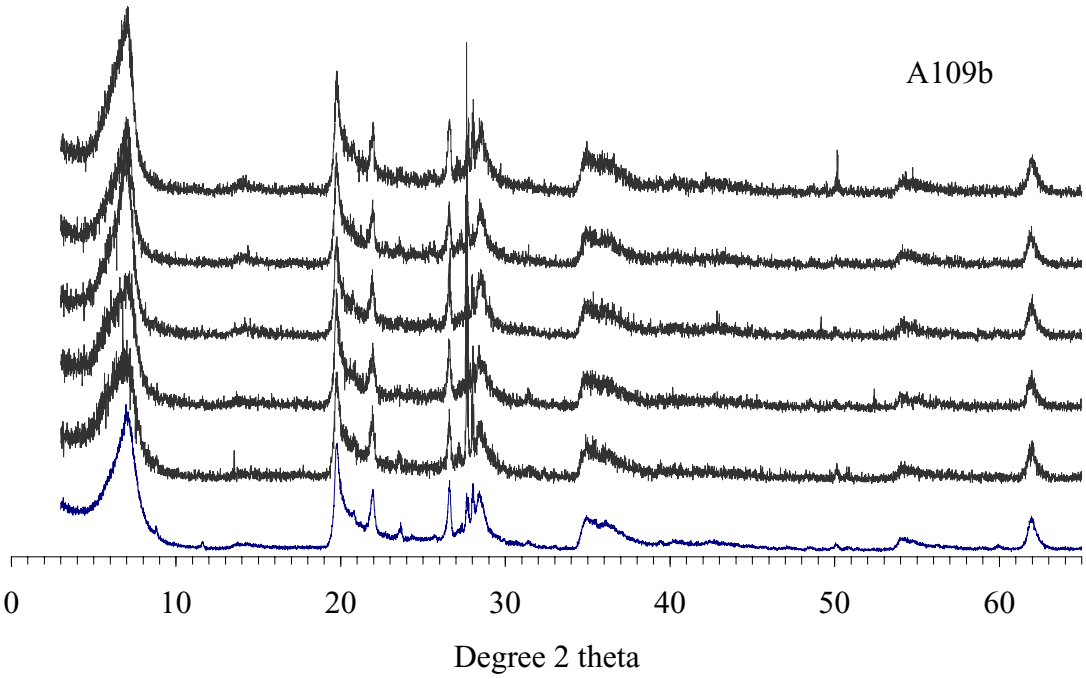

Figure 5-39 *XRD results from unsorted material from five positions in block A109. Uppermost curve represents material from innermost position (A1091), and second curve represents second position outwards in the block, etc. Lowest curve shows the mean results from the 10 reference samples (mRA1S1b).*

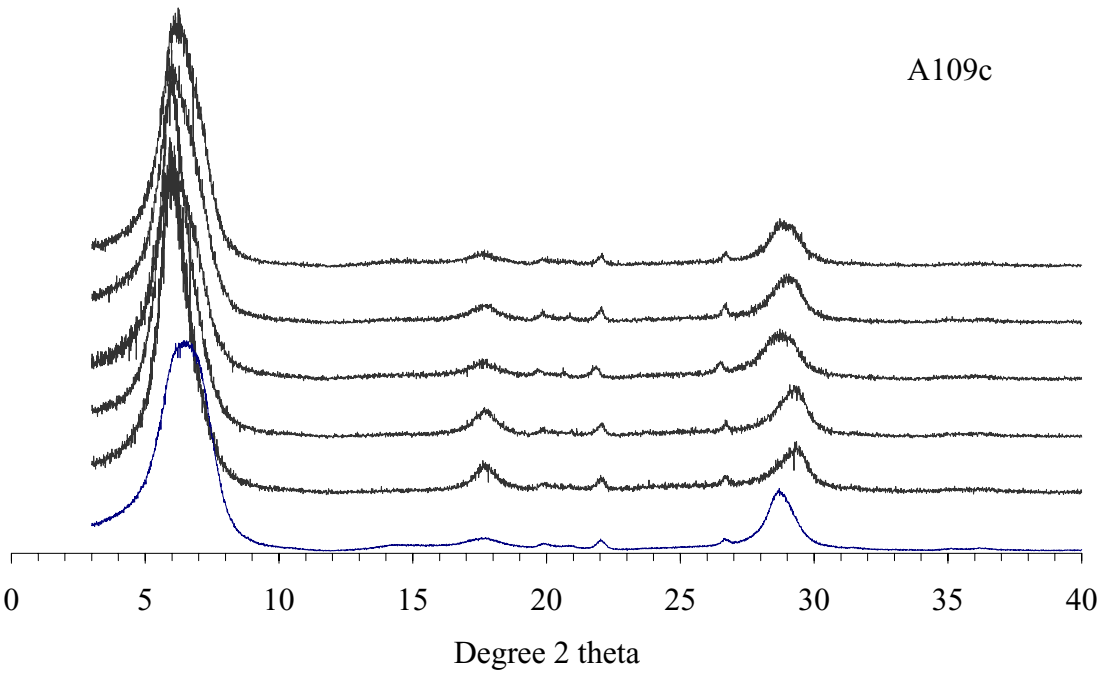

Figure 5-40 *XRD results from clay fraction material from five positions in block A109. Uppermost curve represents material from innermost position (A1091), and second curve represents second position outwards in the block, etc. Lowest curve shows the mean results from the 10 reference samples (mRA1S1c).*

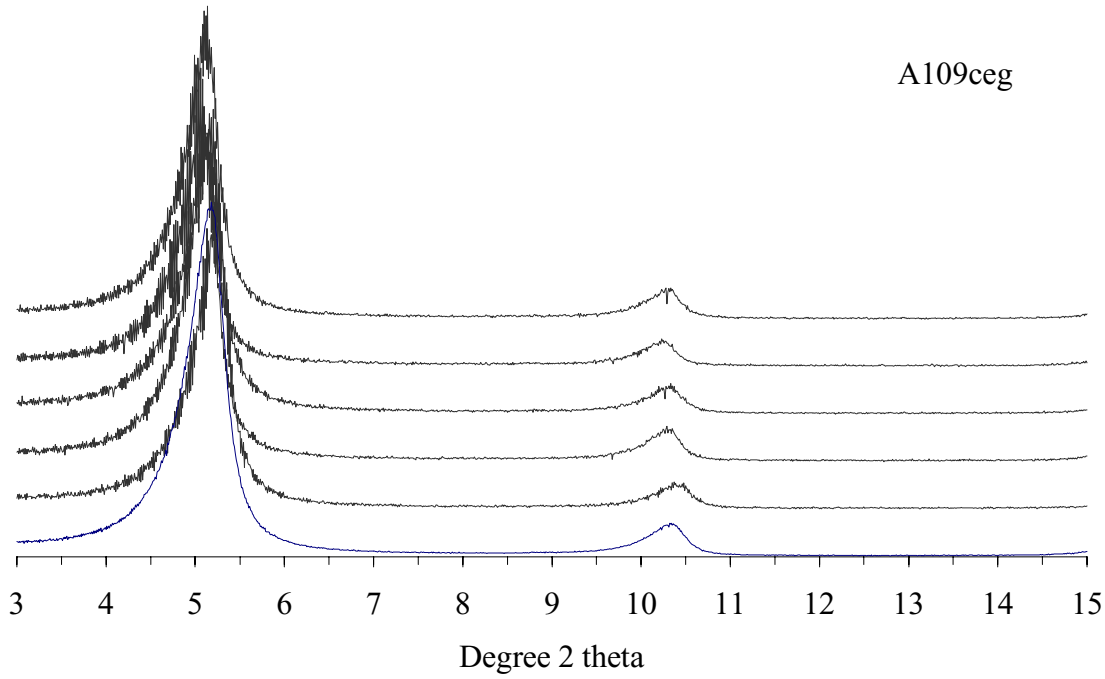

Figure 5-41 *XRD results from clay fraction material treated with ethylene glycol from five positions in block A109. Uppermost curve represents material from innermost position (A1091), and second curve represents second position outwards in the block, etc. Lowest curve shows the mean results from the 10 reference samples (mRA1S1ceg).*

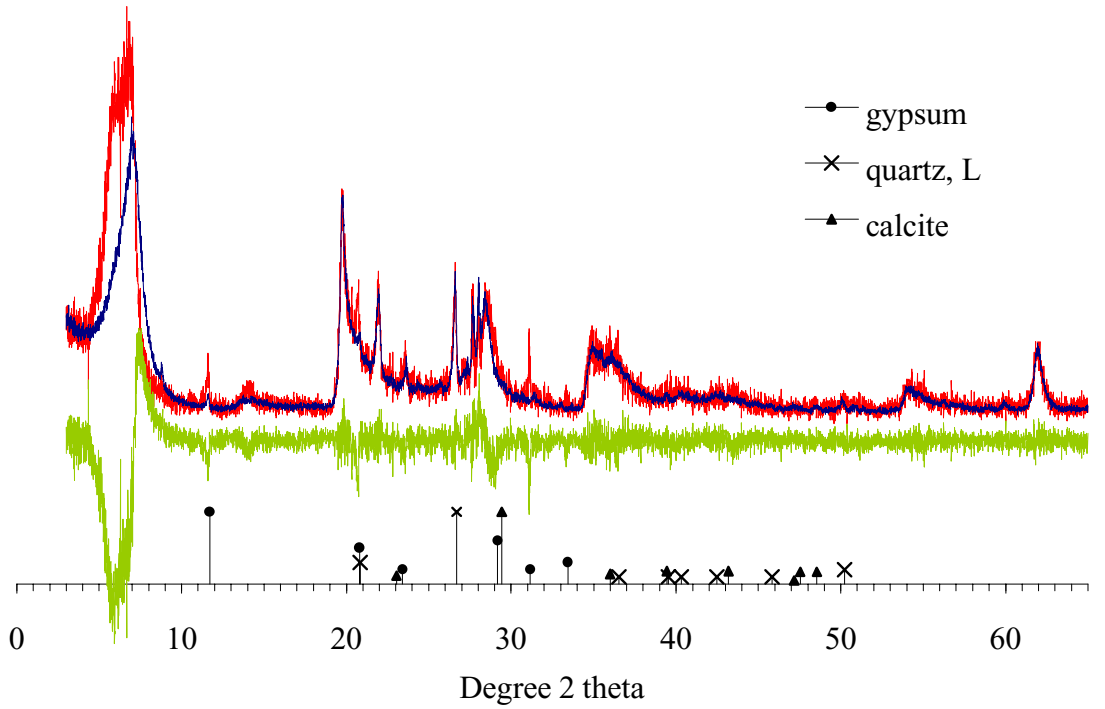

Figure 5-42 *XRD results from innermost position (red) in block 03 in the S1 parcel, reference material (dark blue) and calculated difference between the two (green). Vertical bars indicate peak positions for possible precipitation substances.*

Comparison between results from XRD analyses of parcel and reference material may be summarised in the following items:

- Indications of increase in montmorillonite basal distance,
- No significant change with respect to accessory minerals in the original test volume,
- No neoformed minerals,
- Significant increase in gypsum and calcite content in the interface between copper and bentonite,
- Significant increase of montmorillonite basal distance up to 14.5 Å close to the interface between copper and bentonite.

The increase of basal spacing in the montmorillonite is probably related to the high concentration of calcium, which also led to the precipitation of gypsum and calcite.

5.11 Electron microscopy analysis

5.11.1 Test principle and equipment

The particle size in swelling clays calls for electron microscopy techniques in order to get a sufficiently high magnification for microstructure studies. The resolution in SEM permits microstructure studies of accessory minerals but not of the montmorillonite component, which requires nanometre resolution. A transmission electron microscopy (TEM) study is planned for after the uptake of the A0 parcel, but has not been made on the present material.

The present scanning electron microscopy (SEM) analyses mainly aimed at identifying accessory minerals and element distribution in the material. Representative bentonite material from the hot and cold parts from the A1 and S1 parcels was analysed. The selection of material for analyses was similar to that in all other analyses, but the division in 5 individual specimens was not necessary since the technique admits continuous analyses from the interface with the copper to the interface with rock. The scale in SEM makes it possible to accidentally find almost anything in bentonite, and the way of working was therefore to scan relatively large areas and make a subjective evaluation of the general impression. E.g. the high content of gypsum revealed by XRD in the innermost hot parts was easily detected.

The SEM study was made by use of a Phillips 515 SEM microscope and the element microanalyses by use of a LINK 2000 at the EM-unit, University Hospital, Lund. The energy dispersive X-ray (EDX) detector was equipped with a beryllium window which limits the analyses to elements with $Z > 11$ (Na).

5.11.2 Sample preparation

Electron microscopy normally works under vacuum, which excludes the introduction of liquid water, and several techniques in order to remove water from specimens are available. Artefacts introduced by such preparations are a general problem and especially troublesome for swelling clays since the interaction between the liquid and

the clay mineral is the very cause of the in situ microstructure. Further, ordinary drying leads to transport of dissolved elements to the surface of the specimens. Cryo-examination and ”environmental EM” have been used in some studies, but no standard techniques are presently at hand. In the present SEM analyses the basic aim was to study element distribution and the prevention of redistribution was therefore most important. The microstructure was hereby altered, but the induced changes may in some respect be informative. The specimens were therefore prepared without replacing the water according to the following technique:

- Specimens were cut from undisturbed samples at test termination,
- Rapidly frozen in liquid nitrogen (N_{liq}),
- Freeze dried for 24 h at -20°C and <0.1 Pa,
- Broken, in order to expose fresh surfaces,
- Fixed to an aluminium stub by use of carbon glue,
- Specimens aimed for morphological study were sputter coated with gold to a thickness of 20 nm, and specimens aimed for element studies were coated by carbon or left uncovered.

5.11.3 Results

No significant changes were found with respect to clay minerals in the parcel material or to accessory mineral in the major part of the bentonite mass. However, both morphological evidence and element mapping supported the precipitation of gypsum in the volume close to the copper tube. An increase in calcium and sulphur were found close to the copper tube. Since carbon is not possible to analyse there were no element indication of calcite but morphological, and indirectly by the lack of plausible anions in structures rich in calcium (Figure 5-43). The dominating grain size of neoformed gypsum and calcite was up to 10 μm.

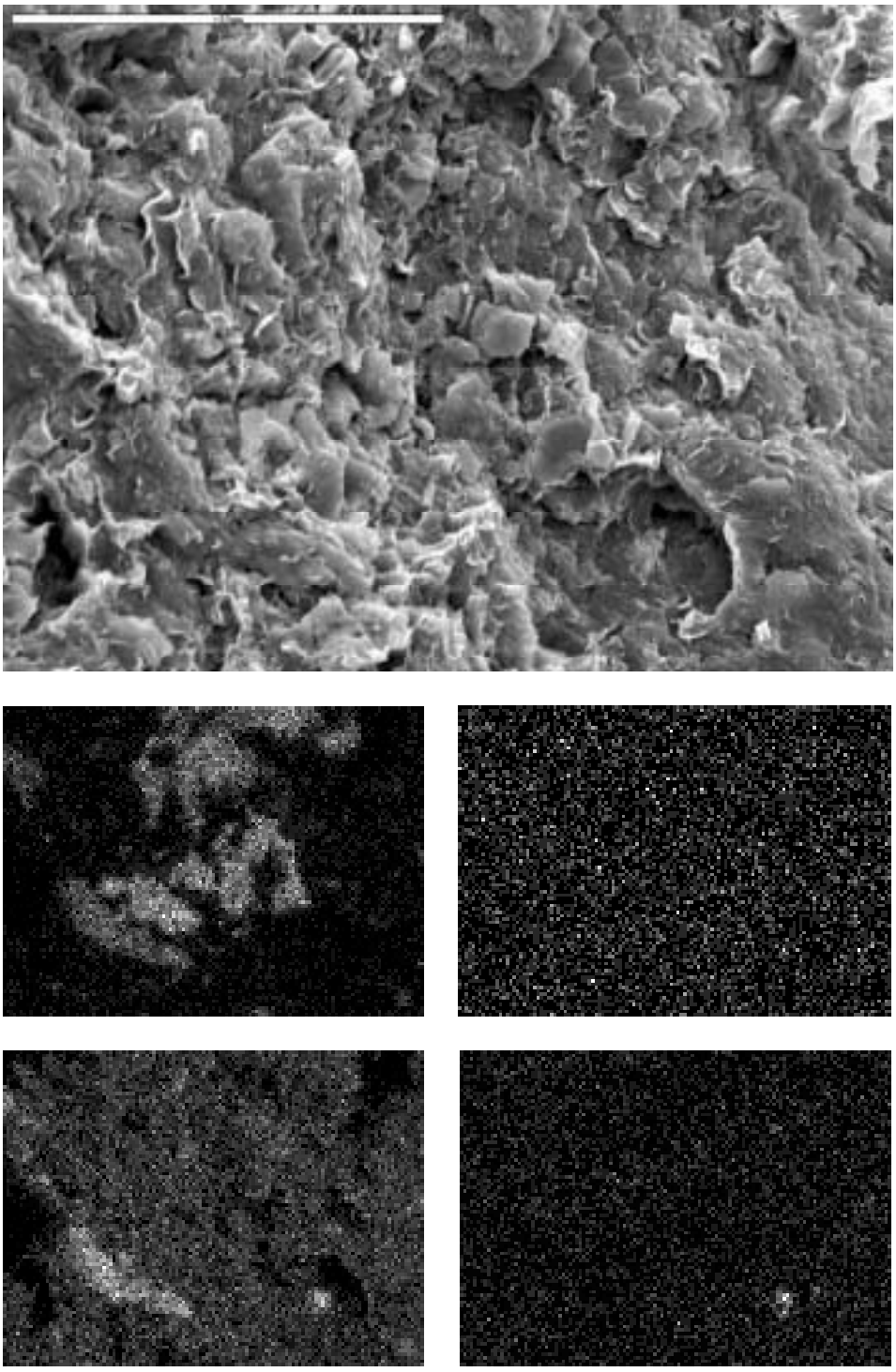

Figure 5-43 Bentonite from close to the copper tube (Cu 10-20 µm to the left). Space bar in upper picture shows 50 µm. The lower 4 pictures show the same view but with calcium (middle left), copper (middle right), sulphur (lower left) and iron content (lower right), respectively, as contrast.

References

Aagard P., Helgeson H.C., 1983. Activity/Composition Relations Among Silicates in Aqueous Solutions II. Clays and Clay Minerals 31 (1983) 207.

Abercrombie H.J., Hutcheon I. E., Bloch J.D. and de Caritat P., 1994. Silica activity and the smectite-to-illite reaction. Geology, v. 22, p 539-542

Arfvidsson J., Claesson J., Hökmark H., 2000. Method to verify numerical THM-models. SKB TR in print, SKB, Stockholm, Sweden.

Boles J.R. and Franks S.G., 1979. Clay diagenesis in the Wilcox Sandstones of southwest Texas. J. sed. Petrol. 49, 55-70.

Börgesson L., Johannesson L.-E., Sandén T., Hernelind J., 1995. Modelling of the physical behaviour of water saturated clay barriers. SKB TR 95-20, SKB, Stockholm, Sweden.

Börgesson L., Johannesson L.-E. 1995. Thermo-hydro-mechanical modelling of water unsaturated buffer material. SKB TR 95-32, SKB, Stockholm, Sweden

Chapman, H.D. & Pratt, P.F., 1961. Methods of soil analysis for soils, plants and waters. Div. of Agr. Sci. University of California, Berkeley

Coutour R.A., 1985. Steam rapidly reduces the swelling capacity of bentonite. Nature, 318, 50-52.

Eberl D.D., Velde B. and McCormic T., 1993. Synthesis of illite-smectite from smectite at earth surface temperatures and high pH. Clay Minerals 28, 49-60.

Grauer R., 1986. Bentonite as a backfill material in the high-level wast repository: chemical aspects. NAGRA, Technical Report 86-12E.

Hower J., Eslinger E.V., Hower M.E. and Perry E.A., 1976. Mechanism of burial metamorphism of argillaceous sediments. Geol.Soc. Amer. Bull. 87 725-737.

Huang W.-L., Longo J.M. and Pevear D.R., 1993. An experimentally derived kinetic model for smectite-to-illite conversion and its use as a geothermometer. Clays and Clay Minerals 41, 162-177.

Hökmark H., 1995. Smectite-to-illite conversion in bentonite buffers; application of a technique for modeling degradation processes. SKB Arbetsrapport AR 95-07, Stockholm.

Johannesson L.-E., Bögesson L., Sandén T., 1995. Compaction of bentonite blocks. SKB TR 95-19. SKB Stockholm, Sweden.

Karnland O., Pusch R. and Sandén T., 1994. Effects of cyclic hydration/dehydration on Na and K bentonites. SKB Arbetsrapport AR 94-40, Stockholm.

Karnland O., Warfvinge P., Pusch R., 1995. Smectite-to-illite conversion models. SKB AR 95-27. SKB Stockholm, Sweden.

Karnland O. 1995:2. Salt redistribution and enrichment in compacted bentonite exposed to a thermal gradient. SKB AR 95-31, SKB, Stockholm, Sweden.

Karnland O. 1997. Cement/bentonite interaction - Results from 16 months laboratory tests. SKB TR 97-32, SKB Stockholm, Sweden.

Meier P. and Kahr G. 1999. Determination of the cation exchange capacity (CEC) of clay minerals using the complexes of copper(II) ion with triethylenetetramine and tetraethylenepentamine. Clays and Clay Minerals, Vol. 47, No. 3, 386-388, 1999.

Motamedi M., Karnland O. and Pedersen K. 1995. Survival of bacteria in nuclear waste buffer materials - The influence of nutrients, temperature and water activity. SKB Technical Report 95-27. SKB Stockholm, Sweden.

Müller-Vonmoos M., Kahr G., 1983. Mineralogiche Untersuchungen von Wyoming Bentonit MX-80 und Montigel. NTB 83-12, Baden.

Nilsson A.-C., 1995. Compilation of the groundwater chemistry data from Äspö. Progress Report 25-95-02, SKB, Stockholm.

Perry E.A. and Hower J., 1970. Burial diagenesis in Gulf Coast pelitic sediments. Clays and Clay Minerals 18, 165-178.

Pusch R., Karnland O., Hökmark H., Sandén T., Börgesson L. 1991. Final Report of the Rock Sealing Project- Sealing Properties and Longevity of Smectitic Clay Grouts. SKB TR Stripa Project 91-30. SKB Stockholm, Sweden.

Pusch R., Karnland O., Lajudie A., Bouchet A. 1992. Hydrothermal field test with french candidate clay embedding steel heater in the Stripa mine. SKB TR 93-02. SKB Stockholm, Sweden.

Weaver C.E., 1959. The clay petrology of sediments. Clays and Clay Minerals 6, 154-187.

Wersin P., Spahiu K., Bruno J. (1994) Kinetic modelling of bentonite-canister interaction. Long-term predictions of coper canister corrosion under oxic and anoxic conditions. SKB Technical Report 94-25. SKB Stockholm, Sweden.

Wersin P., Bruno J., Spahiu K. (1993) Kinetic modelling of bentonite-canister interaction. Implications for Cu, Fe and Pb corrosion in a repository for spent nuclear fuel. SKB Technical Report 94-25. SKB Stockholm, Sweden.

6 Cation diffusion

Trygve E Eriksen, Mats Jansson, Susanna Wold and Kjell Svärdström.

6.1 Introduction

The migration of radionuclides in compacted bentonite has been studied rather extensively in laboratory with respect to the effects of sorption and ion exclusion on the apparent and effective diffusivities (Muurinen 1994, Eriksen and Jansson 1996, Yu and Neretnieks 1997). In-situ diffusion experiments with the cations Cs^+, Sr^{2+} and Co^{2+} have also been carried out in bentonite compacted to a dry density of 1800 kg/m^3 and saturated with Äspö groundwater using the CHEMLAB probe (Jansson and Eriksen 1998). The long term test of buffer material offered a possibility to study radionuclide migration in compacted bentonite saturated with natural groundwater under conditions quite different from those in laboratory experiments and more realistic with respect to conditions expected to prevail in a KBS3 repository; larger scale, initially dry bentonite subjected to water saturation, high temperature and temperature gradient across the buffer during the experiments. The cations Cs^+ and Co^{2+} with the tracers ^{134}Cs and ^{57}Co, respectively, were chosen for the experimental study. The choice of cations was based on the following criteria:

- Diffusion behaviour at different chemical conditions should be well characterised.
- Dependence of sorption behaviour and sorption mechanisms on ion composition and pH of water solutions should be known.
- The dominant sorption mechanism for the cations should preferably be different, i.e. ion exchange for Cs^+ and surface complexation for Co^{2+}.
- The half-life of the tracers should be long enough to allow a two-years experimental study.

6.2 Experimental performance

The experimental technique chosen was to add the diffusants (carriers and tracers), contained in prepared plugs of dry bentonite compacted to desired density, to well defined positions in the bentonite parcel immediately before lowering the parcel into the borehole. Four identical tracer doped plugs were prepared at KTH using 20 mm thick cylindrical plugs with 20 mm diameter compacted by Clay Technology, Lund. A 5 mm diameter hole was drilled into the centre of each plug and a few cubic millimetre of dry bentonite; ion exchanged to contain 1 MBq of each tracer was placed at the bottom of the hole. The top part of the hole was refilled with inactive bentonite and compacted to the original density. The distribution of the tracer within a plug is shown in Figure 6-1 by a dummy prepared using dyed bentonite.

Two diametrically situated holes were drilled from the mantle surface into the blocks S105 and A105, respectively. The diameter of the holes was 21 mm and the depth 80 mm. The doped plugs were inserted into the holes and the remaining outer parts of the holes sealed by inactive bentonite plugs immediately before lowering the bentonite

parcels into position. The diffusant containing volumes were initially 15 mm from the copper tube.

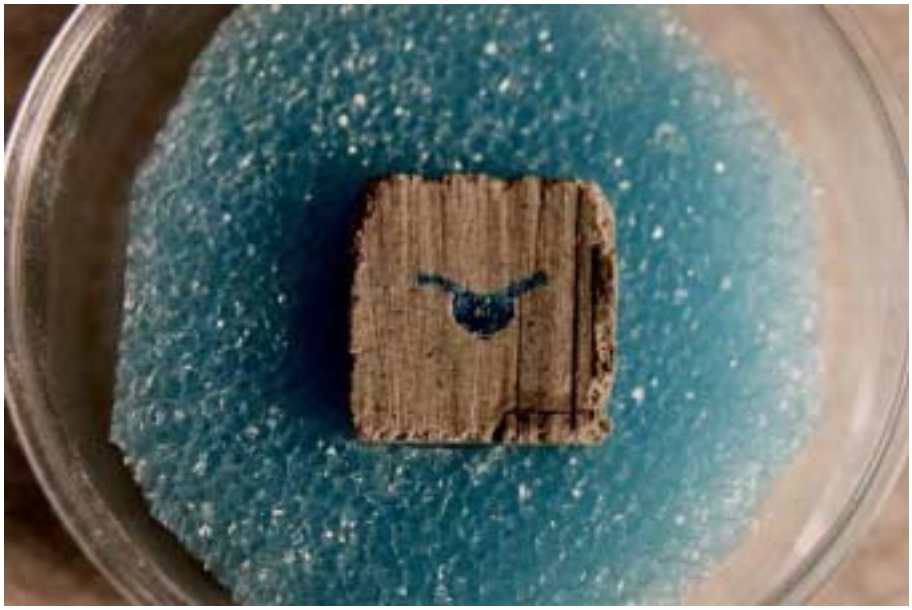

Figure 6-1 *A split dummy plug prepared with a dye instead of the radioactive tracers in order to verify the location of the introduced material. The "wings" are likely not present in the tracer samples. Photograph by Kjell Svärdström, KTH, Stockholm.*

The radionuclides were left in the bentonite parcel for the whole period, exposed to the heat treatment described in section 4.2. When groundwater reached the radionuclides the diffusion started and continued during the saturation process.

6.2.1 S-1 Experiment

Test parcel S-1 was placed October 10th, the heating cycle started October 30th, 1996 and ended December 10th, 1997. The temperature cycles in block 2 and 8 are shown in Figure 4-6. The overlapping core drilling started January 27th, and the bentonite parcel with a 10-15 cm thick envelope of the surrounding rock was removed from the experimental position February 9th, 1998. The rock was removed and the bentonite and copper tube was cut at the boundary between blocks 8 and 9. The lower part of the parcel (blocks 1 to 8), wrapped in plastic foil and placed in a container, was transported to KTH, Stockholm for activity distribution analysis.

6.2.2 A-1 Experiment

The test parcel was placed November 16th 1996, the heating started December 4th, 1996 and ended December 10th, 1997. The temperature cycles in block 2 and 8 are shown in Figure 4-8. The test parcel was removed from the experimental position March 17th, 1998 by overlapping core drilling. Whereas the bentonite in the central part of the test parcel was washed away during the drilling, the section containing the radionuclides was found to be nearly intact but with a soft 4-5 cm thick expanded outer layer with

high water content, Figure 6-2. The radionuclide containing section was wrapped in a plastic sheet, placed in a plastic barrel and transported to KTH for activity distribution measurements.

Figure 6-2 Lower part of test parcel A-1. The holes are due to sampling. Photograph by Kjell Svärdström, KTH, Stockholm.

6.3 Analysis

6.3.1 Parcel S-1

The bentonite appeared to be dry and cracked (Figure 4-13), making sampling rather difficult. Samples were taken from the bentonite using gouges with 15 mm diameter near the surface and 10 mm diameter near the original position of the tracer doped volume. The bentonite samples were analysed for ^{134}Cs and ^{57}Co using a Ge-detector and multi-channel analyser. The water content of the samples was determined by weighing the samples before and after drying at 105 °C.

The water ratio analysis revealed that the block containing radiotracers was far from fully water saturated at termination. The radiotracers had hardly migrated at all, confirming that the diffusive mobility of cations is very low in semi-dry bentonite. The concentration profile was not further evaluated.

6.3.2 Parcel A-1

The outer part of the clay in the high temperature experiment (A1) had high water content when it was removed from the borehole due to the free swelling. The clay was clearly expanded; the diameter was almost one and a half times larger than the original size. The viscosity of the outermost layer was relatively low, but the clay was more compact in the middle. The first samples were taken by drilling holes into the bentonite. The sample cores were sliced into segments and then counted for activity. The drilled holes can be seen in Figure 6-2. Closer to the initial position of the activity, the bentonite was peeled off layer by layer. Each layer was cut into approximately 1x1 cm pieces, which were weighed and analysed by γ-counting using a germanium detector and multi-channel analyser. Altogether, roughly 1000 samples were analysed.

6.4 Data evaluation

From the analysis of the A-1 experiment, activity levels of approximately 1000 points in the bentonite parcel were obtained. Since one doped bentonite plug was inserted on each side of the copper tube, the samples were divided into two groups depending on which side of the tube the sample was taken. The two groups were treated separately. A coordinate system was applied to each side of the copper tube, defining the origin where the activity maximum was found. The distance to origin was calculated for each point to create a one-dimensional activity profile. The profiles were then examined to see whether the profiles looked different in different directions from the origin or not. This was made by studying six 10 mm thick planes in different directions in space. The examination showed that the profile for each radionuclide looked the same in all planes on both sides of the copper tube. Scooping calculations showed that with diffusivities and K_d-values obtained from earlier diffusion studies at similar environmental conditions (Eriksen and Jansson 1996, Jansson and Eriksen 1998), the radionuclides would not diffuse out of the bentonite block. The system could therefore be described as diffusion from a source into an infinite medium. The cylinder containing the radionuclides was approximated to be a sphere. The concentration at distance r can then be obtained from equation 6-1 (Crank 1957).

$$C = \frac{1}{2} C_0 \left\{ \operatorname{erf} \frac{a+r}{2\sqrt{(Dt)}} + \operatorname{erf} \frac{a-r}{2\sqrt{(Dt)}} \right\} - \frac{C_0}{r} \sqrt{\left(\frac{Dt}{\pi} \right)} \left\{ \mathrm{e}^{\frac{(a+r)^2}{4Dt}} - \mathrm{e}^{\frac{(a-r)^2}{4Dt}} \right\} \qquad 6\text{-}1$$

where C_0 is the initial concentration, a is the radius of the sphere and D the diffusivity, or as in this case, the apparent diffusivity, D_a.

6.5 Results and discussion

6.5.1 Cobalt

The activity profiles for cobalt are presented in linear and logarithmic plots in figures 6-3a and b, respectively. From the plots it is obvious that the cobalt has not moved very much at all, which was to be expected from the relatively high K_d-values and low diffusivities found in previous investigations. As can be seen, the values fit well with

the calculated profiles, indicating that the apparent diffusivity, D_a, is about 2×10^{-9} cm^2 s^{-1}, which is in good agreement with apparent diffusivities obtained in laboratory experiments as well as in CHEMLAB experiments.

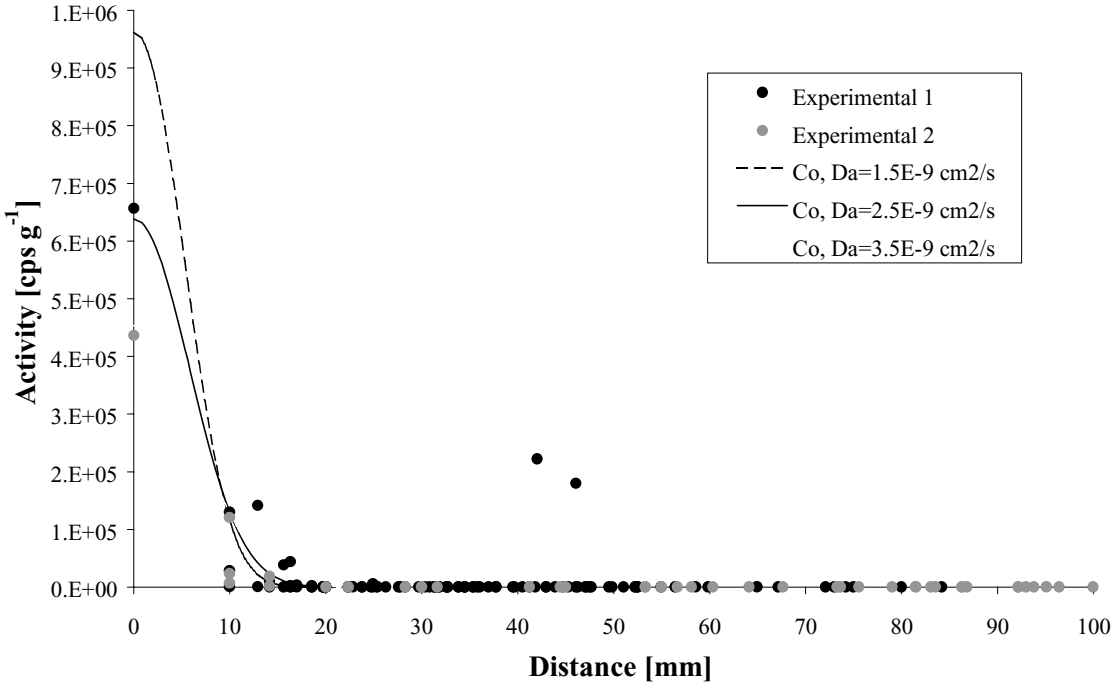

Figure 6-3a Experimentally determined and calculated results for cobalt. Experimental 1 and 2 are taken from each side of the copper tube.

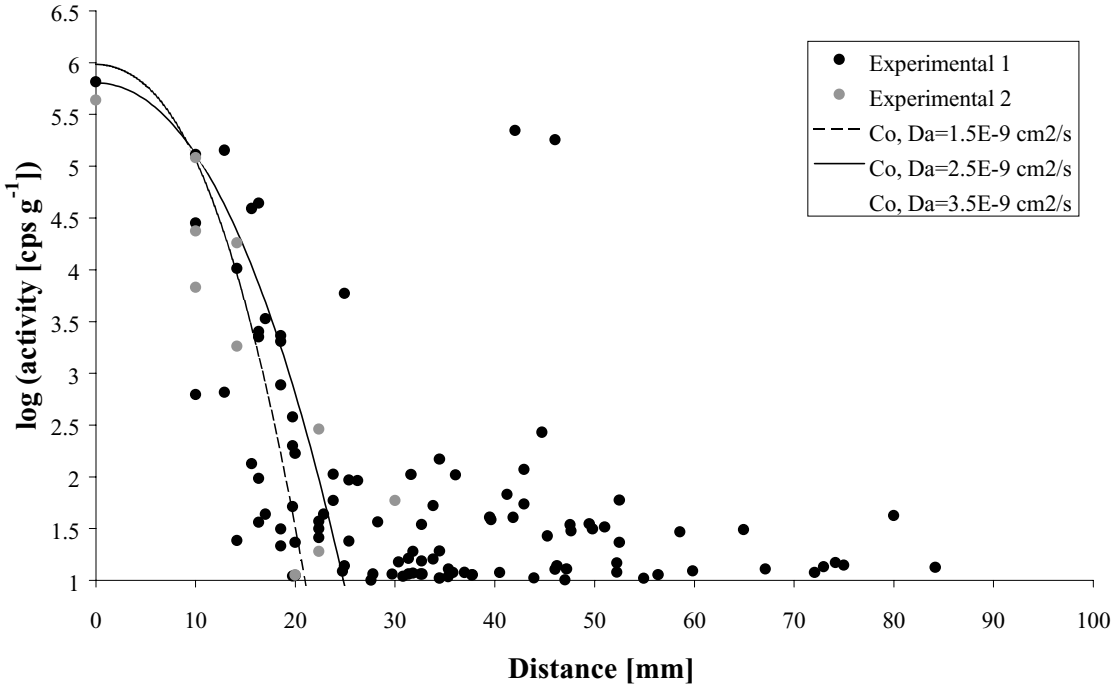

Figure 6-3b Logarithmic presentation of the results for cobalt. Experimental 1 and 2 are taken from each side of the copper tube.

6.5.2 Caesium

The activity profiles for caesium are presented in linear and logarithmic plots in figures 6-4a and 6-4b, respectively. It is not possible to accommodate the ^{134}Cs data using equation 6-1. Whereas the activity peak in the distance range 0 to 25 mm indicates an apparent diffusivity of 5×10^{-8} cm^2 s^{-1}, the widely spread level of 200-300 Bq/g clearly shows that part of the activity has been much more dispersed than expected. According to the data it cannot be completely dismissed that cobalt has undergone a similar process to that of caesium, although to a much lower extent

The profiles of Co^{2+} and Cs^{+} are for comparison shown in recovered activity versus distance plots in Figure 6-5.

The Cs^{+} result was quite unexpected. Different research groups have proposed several different explanations to the caesium behaviour, e.g.:

- High caesium vapour pressure,
- Intra-layer ionic diffusion,
- That there might have been a crack in the caesium containing plug in which the caesium rapidly moved and spread in the gap between the copper rod and bentonite,
- Water evaporating close to the copper tube dragging caesium away.
- Channel building in the clay during the analytic work.

One can probably rule out convective transport due to the heating of the system, since caesium appears to have moved isotropically. Most of the suggested explanations are rather far fetched, however, and no conclusions can be drawn from this single experiment.

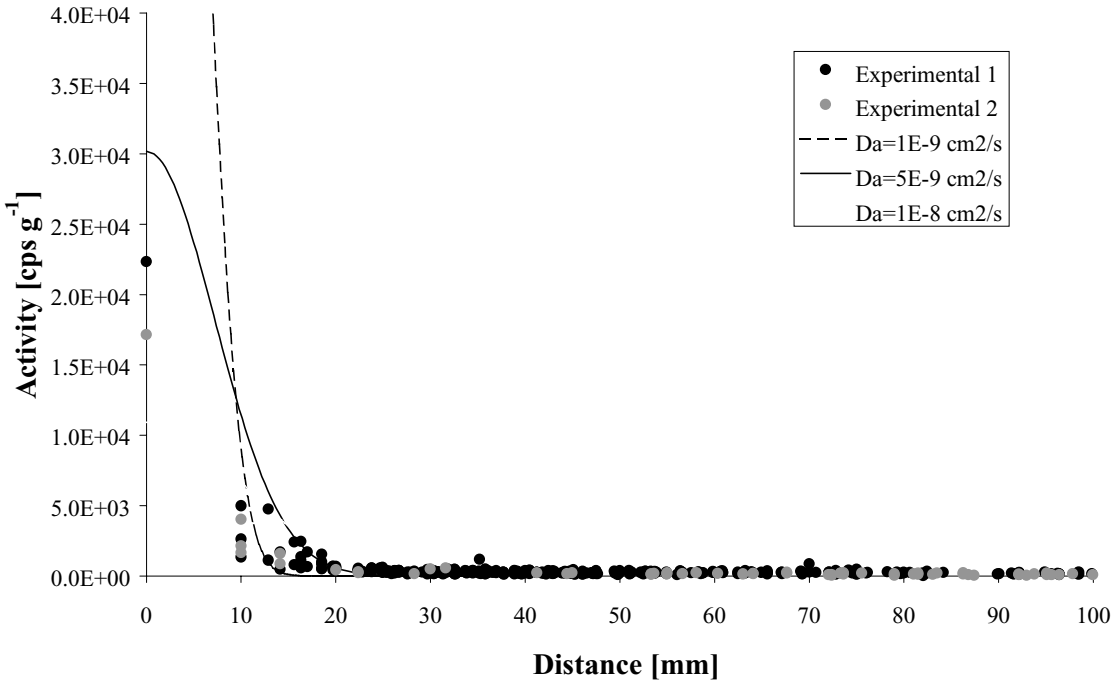

Figure 6-4a Experimentally determined and calculated results for caesium. Experimental 1 and 2 are taken from each side of the copper tube.

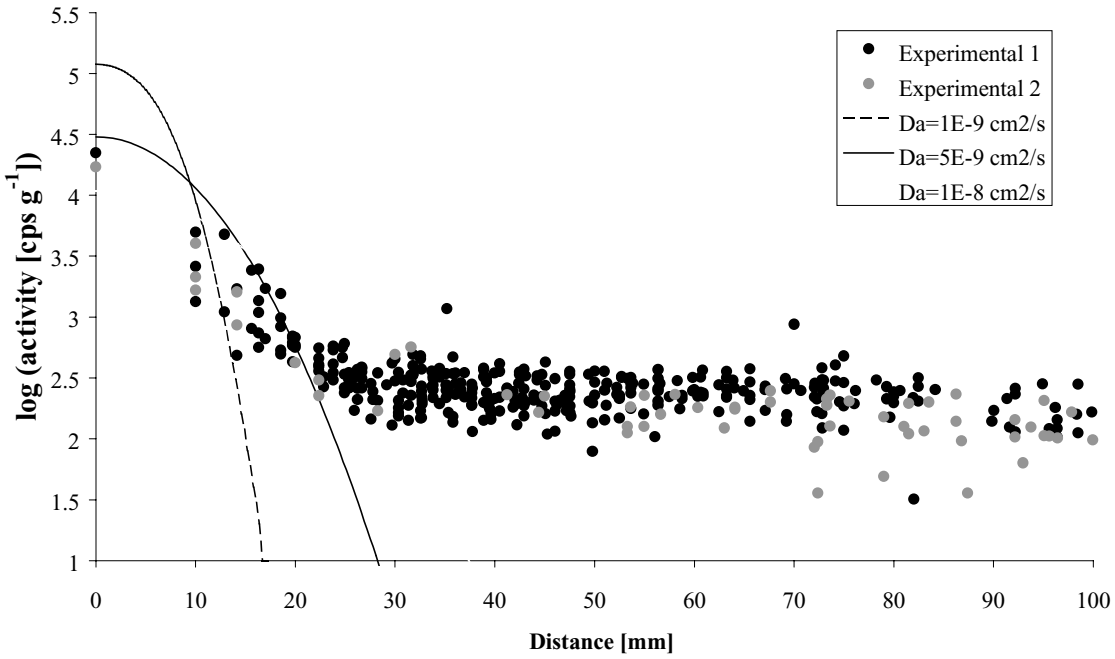

Figure 6-4b Logarithmic presentation of the results for caesium. Experimental 1 and 2 are taken from each side of the copper tube.

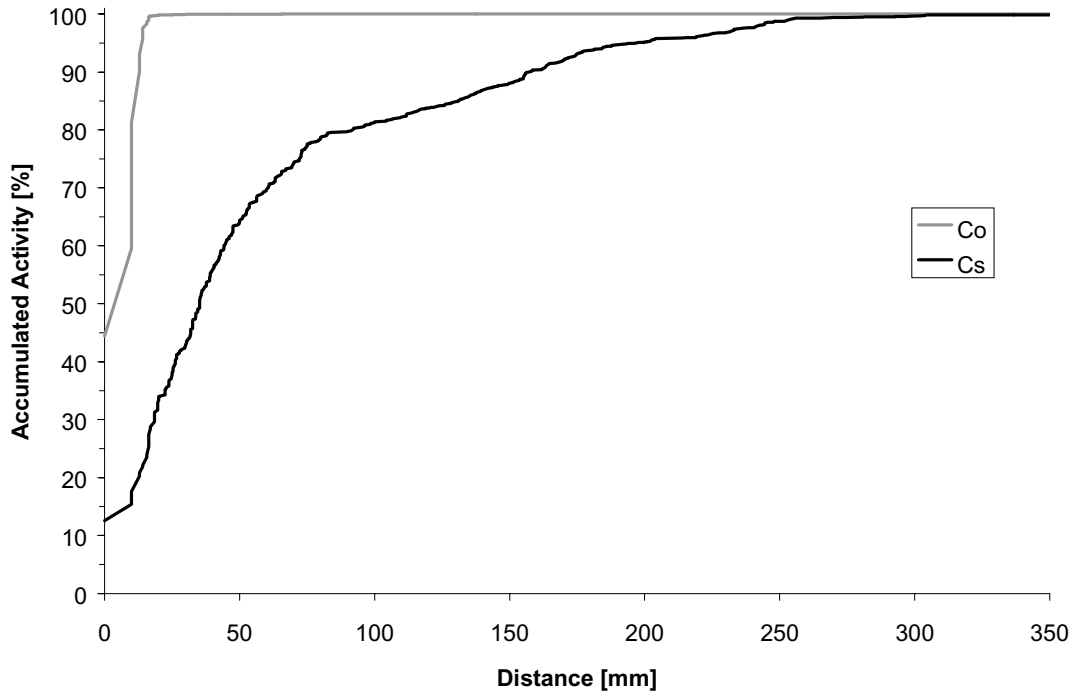

Figure 6-5 Recovered activity for cobalt (upper) and caesium (lower) versus distance.

References

Crank, J.: *The Mathematics of Diffusion,* 1st Ed, University Press, Oxford, p 27, 1957.

Eriksen, T.E. and Jansson, M. *Diffusion of I⁻, Cs^+ and Sr^{2+} in compacted bentonite - Anion exclusion and surface diffusion.* SKB Technical Report 96-16, 1996.

Jansson, M. and Eriksen, T.E.: *CHEMLAB-in situ Diffusion Experiments Using Radioactive Tracers.* Radiochimica Acta 82, 153-156, 1998.

Muurinen, A.: *Diffusion of anions and cations in compacted sodium bentonite*. Espoo, Technical Research Centrer of Finland, VTT Publications 168, 1994.

Yu, J.W., Neretnieks, I.: *Diffusion and sorption properties of radionuclides in compacted bentonite.* SKB Technical Report 97-12, 1997.

7 Bacteria test

Karsten Pedersen, Mehrdad Motamedi, Ola Karnland and Torbjörn Sandén

7.1 Introduction

Oxygen and sulphide are potential corrosive elements, which may threaten the integrity of the copper canisters. Oxygen is introduced during the open phase of a repository, but after closure, it is expected to be rapidly reduced by microorganisms in the groundwater (Banwart et al., 1996; Kotelnikova and Pedersen, 1999). By contrast, sulphide will be produced by a specific group of microorganisms, the sulphate-reducing bacteria (SRB), which are common in deep groundwater (Haveman et al., 1999). Sulphate-reducing bacteria will be active under anaerobic conditions after closure of a repository (Pedersen, 1999). The worst possible case scenario in copper canister corrosion would be if SRB formed biofilms on the canisters or grew intensively in the buffer close to the canister. The sulphide corrosion process would be controlled by the transport of sulphate to the SRB in the vicinity of the canisters, if enough hydrogen or degradable organic carbon were available for their growth. This could lead to considerably accelerated corrosion, since the transport of sulphate in the buffer is expected to be much faster than the transport of sulphide, owing to the fact that the sulphate concentration in the bentonite can be up to tens of mmol/dm^3.

The water content, availability of nutrient and energy sources, high temperatures, and radiation are factors which will influence the development of microbial populations in the buffer around nuclear waste storage canisters, an environment classified as extreme (Gascoyne, 1996; Kushner, 1978; Pedersen and Karlsson, 1995; West et al., 1985). In contrast to nutrient, energy, pressure and temperature constraints, few microorganisms can withstand desiccation. A full-scale Canadian field experiment showed that microorganisms in the studied sand/bentonite buffer mix (50/50%) did not survive at a water content below a certain value (Stroes-Gascoyne et al., 1997). In the Canadian experiment, SRB were not detected, possibly because the anaerobic and reduced conditions required by SRB did not develop during the time course of the experiment (approximately 2.5 years). Laboratory experiments with SRB were therefore subsequently started. The results showed that low water content was lethal to the SRB studied (Motamedi et al., 1996). It may, however, be argued that more desiccation-resistant SRB than those studied could survive and be active in a bentonite buffer, and also, that the laboratory batch conditions used may be more restrictive for SRB survival than the field conditions.

The main purpose of the present tests was to investigate the survival of introduced microorganisms in the clay, focusing on desiccation and high-temperature-tolerant species including SBR. In the S1 parcel a series of different bacteria, including three species of SRB, were mixed with bentonite clay and introduced into the bentonite blocks. The numbers of cultivable microorganisms were analysed in the start material, after mixing and compaction of the bentonite, and after the field exposure.

7.2 Material and methods

7.2.1 Bacterial species

Bacteria with varying relevant characteristics were chosen for the test and ordered from international culture collections as follows: aerobic bacteria included *Deinococcus radiophilus* (Deutsche Sammlung von Mikroorganismen (DSM) No. 20551), which bacterium can tolerate high doses of radiation and is very desiccation-resistant, the chemoheterotrophic bacterium *Pseudomonas aeruginosa* (Culture Collection of the University of Göteborg (CCUG) No. 241), which frequently occurs in soil, the chemo-organotrophic and chemolithotrophic (hydrogen-utilising) organism Ralstonia *eutrophus* (CCUG No. 1776), the chemoheterotrophic endospore-forming bacterium *Bacillus subtilis* (CCUG No. 163), and the thermophilic endospore-forming bacterium *Bacillus stearothermophilus* (CCUG No. 6241). Anaerobic bacteria included the SRB species *Desulfovibrio aespoeensis* (DSM No. 10631) isolated from deep Äspö HRL groundwater (Motamedi and Pedersen, 1998), the moderately halophilic SRB *Desulfovibrio salexigens* (DSM No. 2638), and the thermophilic, endospore-forming SRB *Desulfotomaculum nigrificans* (DSM No. 574). Detailed characteristics of the investigated species can be found in *Bergey's Manual of Systematic Bacteriology* (Holt, 1984–1989).

7.2.2 Determination of cultivable numbers of aerobic bacteria

The aerobic bacteria were pre-cultured in nutrient broth (NB) medium (Merck 1.7884) and in Petri dishes on a solid nutrient agar (NA) medium which was prepared by adding 1% w/w agar (Oxoid 800348-2) to the NB medium. The numbers of cultivable aerobic bacteria were determined by the plate count (PC) technique on nutrient agar medium, as described elsewhere (Koch, 1994). Briefly, the samples were serially diluted in a phosphate buffer to the inverse of the total number of cells ml^{-1} and spread in triplicate on the solid nutrient agar plates. One complete dilution series was prepared and incubated for each species at each determination and at its optimum temperature.

7.2.3 Determination of cultivable numbers of sulphate-reducing bacteria

D. aespoeensis and *D. salexigens* were cultivated in the anoxic mineral medium described by Widdel and Bak (1992) containing 0.13 M and 0.86 M NaCl, respectively. The medium was added, with 6 mM lactate as the carbon source and 14 mM sodium sulphate as the electron acceptor. Medium E (Postgate, 1984) was used for cultivation of *D. nigrificans*. The numbers of cultivable SRB were estimated by the most probable number (MPN) method (Koch, 1994). This involves the mathematical inference of the most probable cultivable count from the fraction of multiple cultures that fail to show growth in a series of dilution tubes containing SRB medium. For dilution of SRB, a brackish SRB medium without energy and carbon sources and electron acceptors was used. The samples were serially diluted to the inverse of the total number of cells ml^{-1} and five repetitions of each dilution were inoculated. The results were calculated with a computer program according to Kohno and Fukunaga (1998).

7.2.4 Estimation of the number of spores

The number of spores of spore-forming bacteria was analysed using a heat shock technique. A portion of a ca 10 ml sample was heated for 10 minutes to 80°C for *B. subtilis*, and to 100°C for *B. stearothermophilus* and *D. nigrificans*, and counted with the PC technique.

7.2.5 Preparation and installation of bacterial bentonite plugs

Bentonite clay was used in the preparation of the plugs containing the bacteria, to be installed in the test parcel S1. The clay was heat-dried in a laboratory oven at 100°C overnight before use. The number and types of naturally occurring bacteria in the bentonite clay were analysed before and after the heat treatment. The number of cultivable cells was investigated by the PC and MPN methods described above, at culturing temperatures of 30°C and 65°C. Growing bacteria were isolated and partially identified.

The acridine orange direct count (AODC) technique (Hobbie et al., 1977) was used to determine the total number of bacteria in the cultures used for the plug preparations. Nuclepore filters (0.2 µm pore size, 13 mm diameter) were pre-stained with a Sudan-black solution. Before use, the filters were thoroughly rinsed with de-ionised water. A portion of the sample was filtered onto a nuclepore filter at –20 KPa and stained for 7 minutes with acridine orange (AO). The total number of bacteria was then counted using blue light (with an excitation wavelength of 390–490 nm) under an epifluorescence microscope (barrier filter 515 nm, Zeiss, Göteborg, Sweden).

For the plug preparations, 25.0 ml of the aerobic bacterial culture mix was transferred to a sterilised spray glass bottle. The same volume of SRB culture mix was transferred to a second sterilised spray glass bottle. A tray (25 x 35 cm) with a sterilised, ethanol-washed glass Petri dish (15 cm in diameter) was placed on a balance and 11.86 g heat-treated clay were sieved onto the Petri dish. As the clay was heat-treated, it contained no water at the outset. Bacterial suspension (1.19 g) was sprayed on the clay. The tray was subsequently wiped with sterilised tissue and the edge of the Petri dish was wiped with a piece of sterilised cotton. Any bacterial suspension lost to the tray or removed by wiping was replaced with more bacterial culture sprayed on, until the required 1.19 g volume of bacterial suspension per plug was filled. The bacterial clay sample was thoroughly mixed. The clay at this stage contained 10% water, all of which came from the bacterial suspension sprayed. There were 34 preparations in total, 17 of aerobic bacteria and 17 of SRB. Before compacting the bacterial clay mixtures, samples were taken from four different preparations (two containing aerobic bacteria and two with SRB) to estimate the number of cultivable cells and spores present in the mixtures immediately after mixing the clay with the respective bacterial suspensions.

Using a laboratory compaction device, the samples were compacted to form plugs to a density corresponding to the test block density of 2000 kg/m^3 after full water saturation (section 3.4.5). The compaction was accordingly controlled by the final sample volume and not by the maximum compaction pressure. The plugs were cylindrical, with a 20 mm length and diameter. They were put in sterilised plastic tubes and caps were screwed on tightly to maintain the humidity until the placement (ca 72 hours later) in

the designated bentonite blocks at the test site. One plug containing aerobic bacteria and another containing SRB were used to estimate the number of cultivable cells after 72 hours.

Cylindrical holes were drilled from the four cardinal points into the mantle surface in blocks 17 and 29. The diameter of the holes was 21 mm and they were 80 mm deep, which meant that there was approximately 3 mm bentonite left to the inner radius of the circular block. Before inserting the plugs into the test holes the outer plugs were sprayed with a small amount of sterilised, distilled water in order to get the bentonite to start swelling and thus seal up the slots between the wall of the holes and the plugs. The positions of the plugs were marked with 1 mm thick titanium wires inserted into drilled holes placed 20 mm above the centre of the plugs. The northern position was marked with two titanium wires and the remaining positions, with one wire. The plugs were assembled into the bentonite blocks approximately half an hour before the S1 parcel was submerged into the rock. In total, 16 plugs (eight plugs inoculated with aerobic bacteria and eight inoculated with SRB) were inserted perpendicularly into each block. Block 17 was placed close to the centre of the parcel where the temperature was in the range of 50 to 80°C, while block 29 was placed in the upper part of the parcel which was exposed to a temperatures around 25°C (Figure 4-4).

7.2.6 Sampling of bacterial plugs at termination of the experiment

After uplift, the parcel was divided into the starting blocks using a saw, spatula and hammer. Blocks 17 and 29 were placed in plastic bags and delivered to a mobile field laboratory on ground equipped with an anaerobic box, with a mixture of 5% H_2, 5% CO_2 and 90% N_2. The blocks were placed in the box within 10 minutes after removal from the test parcel.

Inside the anaerobic box, the blocks were cut into pieces to extract the installed plugs (see Figure 7-1). Using sterilised spoons, clay samples of the bacterial plugs were taken and those containing aerobic bacteria were transferred to a phosphate buffer. Plugs containing SRB were transferred to a brackish SRB medium without an electron acceptor or energy and carbon sources. Sampling of aerobic bacteria was performed outside the anaerobic box. The clay was homogenised in the above mentioned dilution media and the number of cultivable bacteria was subsequently estimated, as described above. Two uninoculated blocks were sampled to estimate the remaining number of naturally occurring microorganisms. They were block 15, which had been exposed to high temperature, and block 35, which had not been exposed to a high temperature.

7.3 Results

7.3.1 Naturally occurring, cultivable bacteria

The number of cultivable aerobic bacteria in the heat-treated clay that was used in the plug preparation was determined at 30°C and at 65°C and was 1.1×10^2, and <100 cells per gram dry weight (gdw^{-1}) of clay, respectively. In the non-heat-treated clay, the number of cultivable cells was determined to be 3.4×10^4, and <100 cells gdw^{-1}, isolated at 30°C, and 65°C, respectively. The bacteria isolated from the clay included a new

species of *Bacillus* sp. (CCUG 36961), *Bacillus cereus* (CCUG 36963), *Pseudomonas stutzeri* (CCUG 36965), *Bacillus subtilis* (CCUG 36967) and *Breviabacillus brevis* (CCUG 36969). No SRB were found in the heat-treated or in the non-heat-treated clay. After termination of the experiment, the number of cultivable aerobic bacteria at 30°C and 65°C was below the detection limit, of 100 gdw^{-1}, in both blocks 15 (50–70 °C) and 35 (exposed to a temperature of 15–20°C). However, the blocks were not sterile because some bacteria could be enriched from them; there were bacteria present at numbers below the detection limit for the PC method (section 7.2.2). Block 35 carried the same new species, *Bacillus* sp. (CCUG 39164), as was isolated from the clay at the start of the experiment, *B. cereus* (CCUG 39161), and a species of the genus *Thermoactinomyces* (CCUG 39165). Sulphate-reducing bacteria could not be isolated from either block 15 or block 35.

Figure 7-1 Block 29 in the S1 parcel has been ruptured and a set of three plugs that were inoculated with bacteria become visible. The plugs were removed and analysed after 15 months' exposure. (Photograph: M. Motamedi)

7.3.2 Bacteria in the plugs at the start of the experiment

Up to 10% of the introduced aerobic bacteria could be cultured from the clay immediately after preparation (Table 7-1). The cultivability of SRB differed markedly, depending on the species. The best cultivability was observed for *D. nigrificans. D. salexigens* could not be cultivated from the clay and the number of *D. aespoeensis* was down to 7.5% of the initial population. Sampling after 72 hours showed that only *D. radiophilus* and the spore-forming species *B. subtilis*, *B. stearothermophilus* and *D. nigrificans* were cultivable at the time of emplacement of the test.

Table 7-1 Total number of cells, number of cultivable cells and number of spores of the tested species in the starting culture, and number of cultivable cells and spores in the plugs immediately and 72 hours after plug preparation.

Species	Cells ml^{-1} culture		Cultivable cells gdw^{-1} clay	
	Total number of bacteria[a]	Cultivable cells (plate counts[b] or MPN[c])	At preparation of the plugs	In the plugs after 72 h
D. radiophilus	4.1×10^8	3.1×10^8	5.2×10^7	3.0×10^7
P. aeruginosa	3.0×10^9	8.1×10^8	5.1×10^7	< 100
R. eutrophus	1.3×10^9	2.6×10^8	1.6×10^7	< 100
B. subtilis	4.6×10^8	4.3×10^8	3.0×10^7	2.8×10^7
B. subtilis (spores)	3.1×10^8	5.7×10^7	5.6×10^6	np[d]
B. stearothermo-philus	1.8×10^8	5.7×10^7	3.9×10^7	1.2×10^3
B. stearothermo-philus (spores)	3.8×10^7	2.1×10^4	4.2×10^4	np
D. salexigens	1.3×10^8	1.1×10^7	< 100	< 100
D. aespoeensis	1.5×10^8	1.1×10^5	8.2×10^3	< 100
D. nigrificans	4.5×10^7	np	3.3×10^6	1.7×10^6
D. nigrificans (spores)	np	np	4.9×10^5	np

a Counted by AOCD; b SD = 0.02–0.31; c SD = 0.21–0.25; d = not performed.

7.3.3 Bacteria in the plugs at termination of the experiment

All bacteria except for the spore-forming species were eliminated below the detection limits after 15 months' exposure of the plugs to the test conditions. The numbers of cultivable aerobic bacteria from the plugs of block 17 (with a temperature of 50–70°C) were below the detection limit (< 100 cells gdw^{-1}) for all investigated species. *B. subtilis* and *B. stearothermophilus* could be isolated from the plugs containing aerobic bacteria in block 29 (with a temperature of 20–30°) and *B. subtilis* was also cultivated from one of the plugs in block 17 (Figure 7-2a, b). In the plugs containing SRB, only *D. nigrificans* could be cultured (Figure 7-2c). Plug 12 was not found owing to extensive fracturing of block 17.

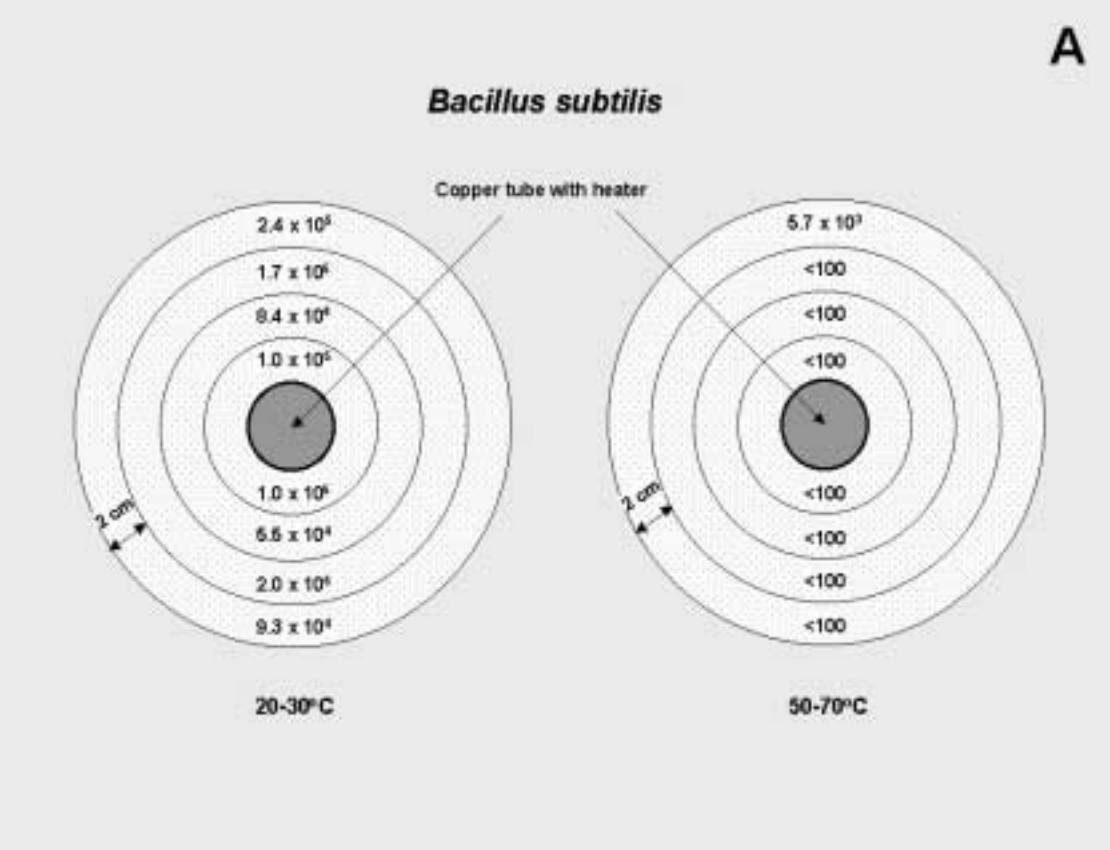

Figure 7-2a *Three different spore-forming bacteria survived after 15 months' exposure to different temperatures in the LOT experiment. They were exposed to gradients of the temperatures indicated, with the highest temperature closest to the heater. The numbers given are per gdw bentonite clay. (nf = not found.)*

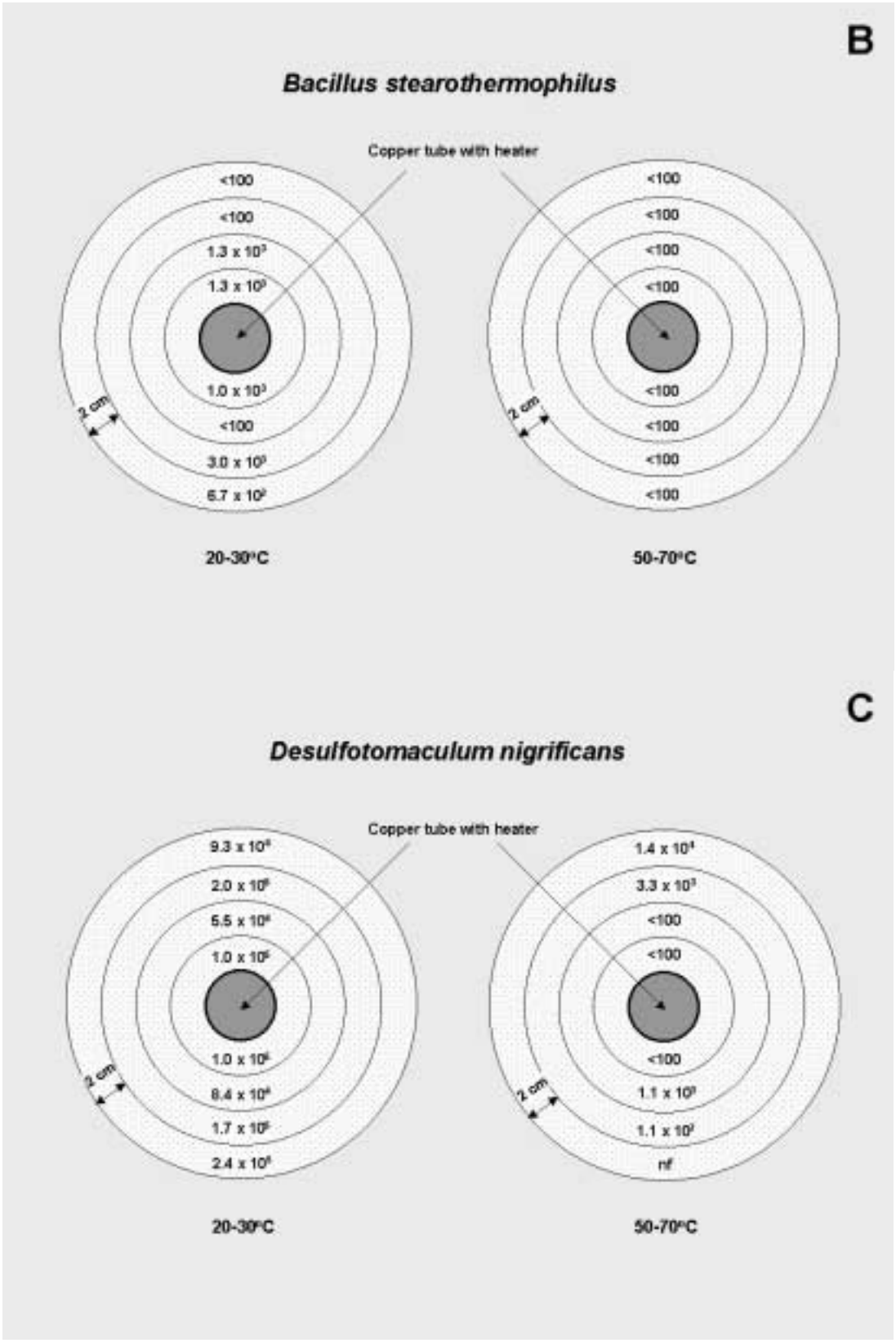

Figure 7-2b,c Three different spore-forming bacteria survived after 15 months' exposure to different temperatures in the LOT experiment. They were exposed to gradients of the temperatures indicated, with the highest temperature closest to the heater. The numbers given are per gdw bentonite clay. (nf = not found.)

7.4 Discussion

Results of laboratory experiments performed previously with SRB (Motamedi et al., 1996) showed that the environmental conditions in compacted bentonite clay reduce the number of cultivable SRB by many orders of degree over a 60-day test period. A high reduction rate of cultivable microorganisms was, therefore, expected in the studied LOT. The preparation of the LOT plugs was performed in the laboratory under exposure to oxygen in air, which mimicked realistic conditions of buffer block production. The tolerance of SRB to oxygen varies, but is generally low (Widdel and Hansen, 1992) and it was expected that the preparation procedure of the plugs would reduce the number of SRB. Large numbers of microorganisms, in the range of 10^7–10^9 cells gdw^{-1} clay (Table 7-1), were chosen as starting concentrations to counteract the harsh conditions in the clay and the hostile conditions during plug preparation.

The method used to measure presence of viable cells in the clay was cultivation, a conclusive method in the sense that cultivable microorganisms in the sample were viable. However, the method does not guarantee that all the non-cultivable bacteria were dead or had disappeared. The possibility that some of the investigated microorganisms had been inactivated and were unable to grow, though still potentially viable, cannot be fully excluded. Cultivable laboratory strains with cultivation media protocols that have been demonstrated to be suitable for successful cultivation of respective species were used to reduce this potential problem. There would, however, have been much higher uncertainty had only naturally occurring microorganisms had been used, since it is well known that available culturing methods commonly fail to cultivate up to 99% or more of environmental microorganisms (see, e.g., Amann et al., 1995).

A suitable measure of availability of water, or of water content, is the thermodynamic water activity (a_w) of a system in equilibrium (Potts, 1994). The water activity of a solution is related to the relative humidity of air in equilibrium with a solution or a water-containing bentonite clay. In other words, at a given temperature, a_w is the ratio between the vapour pressure of the solution (clay) (P_s) and that of water (P_0).

$$a_w = P_s / P_0 \qquad 7\text{-}1$$

Thus, water activity is a measure of the relative tendency of water to escape from the system, compared with pure water, and can adequately be described by the relative humidity that the system can maintain in equilibrium. Microorganisms can grow over a large range of a_ws (0.999–0.75), but most favour an a_w of seawater (0.98) or above. Bentonite that has been compacted to 2 kg/m^3, and which is water-saturated, has an a_w of 0.96 (Motamedi et al., 1996). This number illustrates that the water content will be low in a HLW bentonite buffer compared with most aquatic systems where microorganisms proliferate, such as lakes, the sea, and groundwater. The water content of the LOT plugs directly after preparation was, however, much lower; only 10% corresponded to an a_w of 0.76. The number of cultivable cells of aerobic bacteria decreased dramatically after preparation of the plugs (Table 7-1), most probably owing to the very desiccated and therefore harsh environmental conditions in the plugs. With the exception of *D. radiophilus*, only spore-forming bacteria could be detected after 72 hours, showing the intolerance of non-spore-forming bacteria to a low a_w. Table 7-1 shows that part of the bacterial populations mixed with the clay were spores, as

indicated by cultivability after heat treatment. The heat treatment should have killed all vegetative cells. Spore formation is a life process that requires energy for spore growth and the formation of spore components; this process takes several hours. Most probably, therefore, it was not possible for those spore-forming bacteria not already in a spore, to form spores once sprayed on the clay, since the desiccation effect rapidly would have inactivated them. This conclusion is supported by the data in Table 7-1 showing that the number of spores in the cultures exceeded, or was equal to, the number of cultivable cells after 72 hours in the plugs. It can therefore be anticipated that the plugs only carried spores and some vegetative cells of *D. radiophilus* at emplacement of the S1 test parcel.

D. radiophilus could be isolated from the plugs after 72 hours. This can be explained by the unique characteristics of *D. radiophilus*, which, in addition to tolerance of very high radiation doses, include survival in desiccated environments such as soil and in culturing media containing up to 5% NaCl (Murray, 1991). Therefore, this species stayed cultivable in the dry clay for a longer time than the other, less desiccation-resistant, non-spore-forming bacteria studied. The desiccation effect is most probably also an important reason for the reduction of cultivable cells of the non-spore-forming species *D. salexigens* and *D. aespoeensis* to <100 and 8200 cells gdw^{-1} clay, respectively, immediately following plug preparation (Table 7-1). This effect came in addition to the oxygen exposure effect discussed above. After 72 hours, only the spore-forming SRB *D. nigrificans* could be isolated, while the other two SRB were below detection.

Several species could be isolated directly from the clay before and after the heat treatment. Generally, with the exception of *P. stutzeri*, all other bacteria found were spore-forming ones. The ability of some non-spore-forming bacteria to withstand desiccating conditions over extensive periods, days or even years has been documented (McEldowney and Fletcher, 1988). *P. stutzeri* is a non-spore-forming bacterium that is widely distributed (Rossello et al., 1991). It is a non-fluorescent, denitrifying pseudomonad that can grow in a medium containing up to 7.5% NaCl and it utilises a wide variety of sugars and aromatic carbohydrates. *P. stutzeri* was frequently observed in different locations in the buffer/container experiment at the Atomic Energy of Canada Limited's (AECL) underground research laboratory (Stroes-Gascoyne et al., 1997) and it was also found in this investigation. It appears that this bacterium is tolerant to the extreme conditions that occur in compacted bentonite. Though it is not expected to be able to threaten the integrity of the HLW canisters, a focused investigation of this particular species may reveal new information about survival strategies of non-spore-forming bacteria in desiccating environments.

After emplacement, it took several months for the bentonite to become fully water-saturated in the borehole. The period of very desiccating conditions consequently continued for at least 60 more days, in addition to the first 3 days between plug preparation and emplacement. Additionally, some of the plugs experienced a significant increase in temperature. One basic requirement for the LOTs was to keep a defined high temperature in the central and lower part of the clay column, which would give a temperature gradient in the bentonite. Block No. 29 was not close to the heater and the temperature gradient in this block was between 30°C (inner part) and 20°C (outer part). *B. subtilis*, *B. stearothermophilus* and *D. nigrificans* could all be isolated from all the plugs of block 29 (Figure 7-1). The temperature gradient in block 17 was between 70°C

and 50°C. *Desulfotomaculum nigrificans* was cultivated from four, *B. subtilis* from one, and *B. stearothermophilus* from none of the plugs in this block. The high temperature of block 17 during 15 months obviously added a significant constraint to the cultivability of the introduced microorganisms, that is, the spores. Bacterial spores generally exhibit a high resistance to adverse physical conditions (e.g. temperature and desiccation) and to chemical agents. The survival of spores of different spore-forming species under similar conditions varies and depends on factors such as species, environmental constraints, and the time period that the spores are exposed to the environment (Acea et al., 1988; Briggs, 1960; Bruch and Smith, 1968; Donnelly and Busta, 1980; Molin, 1976). The heat resistance of bacterial spores depends on several factors (Angelotti et al., 1968):

- Species,
- Initial water content of the spores,
- Rate of spore desiccation during heating,
- Water retention capacity of the material in, or on, which spores are located,
- The relative humidity of the system at the test temperature.

In other words, the viability of bacterial spores will show a specific declination rate that may be large or negligible, as a function of a range of spore and environmental characteristics, as was found in this investigation. The results obtained in different studies, including this one, concerning survival and activity of microorganisms and a detailed discussion of the consequences for a HLW repository are given by Pedersen in SKB TR 00-04.

Acknowledgements

We would like to thank Farideh Taherinejad, Agneta Welin, Nadi Jahromi and Berit Ertman Ericsson for their laboratory assistance.

References

Acea, M.J., Moore, C.R., Alexander, M., 1988. Survival and growth of bacteria introduced into soil. Soil Biol. Biochem. 20, 509–515.

Amann, R.I., Ludwig, W., Schleifer K.-H., 1995. Phylogenetic identification and *in situ* detection of individual microbial cells without cultivation. Microbiol. Rev. 59, 143–169.

Angelotti, R., Maryanski, J.H., Butler, T.F., Peeler, J.T., Campbell, J.E., 1968. Influence of the spores moisture content on the dry-heat resistance of *Bacillus subtilis* var. *niger*. Appl. Microbiol. 16, 735–745.

Banwart, S., Tullborg, E.-L., Pedersen, K., Gustafsson, E., Laaksoharju, M., Nilsson, A.-C., Wallin, B., Wikberg, P., 1996. Organic carbon oxidation induced by large-scale shallow water intrusion into a vertical fracture zone at the Äspö Hard Rock Laboratory (Sweden). J. Cont. Hydrol. 21, 115–125.
Briggs, A., 1960. The resistance of spores of the genus *Bacillus* to phenol, heat and radiation. J. Appl. Bacteriol. 29, 490–504.
Bruch, M.K., Smith, F.W., 1968. Dry heat resistance of spores of *Bacillus subtilis* var. *nige*r on Kapton and teflon film at high temperature. Appl. Microbiol. 16, 1841–1846.
Donnelly, L.S., Busta, F.F., 1980. Heat resistance of *Desulfotomaculum nigrificans* spores in soy protein infant preparations. Appl. Environ. Microbiol. 40, 721–725.
Gascoyne, M., 1996. The geochemical environment of nuclear fuel waste disposal. Can. J. Microbiol. 42, 401–409.
Grim, R.E., Guven, N., 1978. Developments in Sedimentology. Elsevier. Amsterdam,
Haveman, S.H., Pedersen, K., Routsalainen, P., 1999. Distribution and metabolic diversity of microorganisms in deep igneous rock aquifers of Finland. Geomicrobiol. J. 16, 277–294.
Hobbie, J.E., Daley, R.J., Jasper, S., 1977. Use of nuclepore filters for counting bacteria by fluorescence microscopy. Appl. Environ. Microbiol. 33, 1225–1228.
Holt J. G., 1984–1989. Bergey's Manual of Systematic Bacteriology, vol. 1–4. Baltimore, MD: Williams & Wilkins, 2648 pp.
Karnland, O., 1997. Bentonite swelling pressure in strong NaCl solutions. Correlation between model calculations and experimentally determined data. SKB Technical Report 97-31. Swedish Nuclear Fuel and Waste Management Co., Stockholm, pp. 1–30. (Available from fax. +46 8 661 57 19.)
Karnland, O., Sandén, T., 1998. SKB Progress Report HRL-97-30. Swedish Nuclear Fuel and Waste Management Co., Stockholm. (Available from fax. +46 8 661 57 19.)
Koch, A.L., 1994. Growth measurement. In: Gerhardt, P., Murray, R.G.E., Wood, W.A., Krieg, N.R. (eds), Methods for General and Molecular Bacteriology. Washington, DC: American Society for Microbiology, pp. 249–296.
Kohno, T., Fukunaga, S., 1998. The "cut-off probability" as the measure of quantal improbability in the dilution method. Water Res. 32, 3099–3107.
Kotelnikova, S., Pedersen, K. (1999) The microbe-REX project. Microbial O_2 consumption in the Äspö tunnel. SKB Technical Report 99-17. Swedish Nuclear Fuel and Waste Management Co., Stockholm, pp. 1–73. (Available from fax. +46 8 661 57 19.)
Kushner, D.J., 1978. Microbial Life in Extreme Environments. London, UK: Academic Press.
McEldowney, S., Fletcher, M., 1988. The effect of temperature and relative humidity on the survival of bacteria attached to dry solid surfaces. Lett. Appl. Microbiol. 7, 83–86.
Molin, G., 1976. Inherent genetic differences in dry heat resistance of some *Bacillus* spores. In: Barker, A.N., Wolf, J., Eller, D.J., Dring, G.J., Gould, G.W. (eds), Spore Research. London, UK: Academic Press, pp. 487–500.
Motamedi, M., Pedersen, K., 1998. *Desulfovibrio aespoeensis* sp. nov., a mesophilic sulfate-reducing bacterium from deep groundwater at Äspö hard rock laboratory, Sweden. Int. J. Syst. Bacteriol. 48, 311–315.
Motamedi, M., Karnland, O., Pedersen, K., 1996. Survival of sulfate reducing bacteria at different water activities in compacted bentonite. FEMS Microbiol. Lett. 141, 83–87.
Murray, R.G.E., 1991. The family Deinococcaceae. In: Balows, A., Trüper, H.G., Dworkin, M., Schleifer, K.-H. (eds), The Prokaryotes. New York, NY: Springer-Verlag, pp. 3732–3744.

Pedersen K., 1999. Subterranean microorganisms and radioactive disposal in Sweden. Engineering Geol. 52, 163–176.
Pedersen, K., Karlsson, F., 1995. Investigations of subterranean bacteria. Their importance for performance assessment of radioactive waste disposal. SKB Technical Report 95-10. Swedish Nuclear Fuel and Waste Management Co., Stockholm, pp. 1–221. (Available from fax. +46 8 661 57 19.)
Postgate, J.R., 1984. The sulphate-reducing bacteria. Cambridge, UK: CambridgeUniversity Press.
Potts, M., 1994. Desiccation tolerance of prokaryotes. Microbiol. Rev. 58: 755–805.
Rossello, R., Garcia-Valdes, E., Lalucat, J., Ursing, J., 1991. Genotypic and phenotypic diversity of *Pseudomonas stutzeri*. Syst. Appl. Microbiol. 14, 150–157.
SKB AB, 1999a. Deep repository for spent nuclear fuel. SR-97 – Post-closure safety. SKB Technical Report 99-06. Stockholm: Swedish Nuclear Fuel and Waste Management Co., pp. 1–119. (Available from fax. +46 8 661 57 19.)
SKB AB, 1999b. Äspö Hard Rock Laboratory, annual report 1998. Technical Report TR-99-10. Stockholm: Svensk Kärnbränslehantering AB. (Available from fax. +46 8 661 57 19.)
Stroes-Gascoyne, S., Pedersen, K., Haveman, S.A., Dekeyser, K., Arlinger, J., Daumas, S., Ekendahl, S., Hallbeck, L., Hamon, C.J., Jahromi, N., Delaney, T.-L., 1997. Occurrence and identification of microorganisms in compacted clay-based buffer material designed for use in a nuclear fuel waste disposal vault. Can. J. Microbiol. 43, 1133–1146.
West, J.M., Christofi, N., McKinley, I.G., 1985. An overview of recent microbiological research relevant to the geological disposal of nuclear waste. Radioactive Waste Management 6, 79–95.
Widdel, F., Bak, F., 1992. Gram-negative mesophilic sulfate-reducing bacteria. In: Balows, A., Trüper, H.G., Dworkin, M., Harder, W., Schleifer, K.H. (eds), The Prokaryotes. New York, NY: Springer-Verlag, pp. 3352–3378.
Widdel, F., Hansen, T.A., 1992. The dissimilatory sulfate- and sulfur-reducing bacteria. In: Balows, A., Trüper, H.G., Dworkin, M., Harder, W., Schleifer, K.H. (eds), The Prokaryotes. New York, NY: Springer-Verlag, pp. 582–624.

8 Copper corrosion

Bo Rosborg and Ola Karnland

8.1 Introduction

Initially, a limited amount of air is left in a KBS3-type repository, which partly will be trapped by the low permeability rim of groundwater-saturated bentonite. The air will be pressurised in the unsaturated central volume due to the advancing waterfront. Parallel to the volume decrease, the air will diffuse outwards and eventually the oxygen content will be very low. In addition to diffusion also chemical reactions and bacterial activity are expected to contribute to the reduction of gaseous oxygen.

Pure metallic copper react relatively fast with oxygen, but is very stable under reducing conditions. In general the following uncertainties are identified for modeling of the copper corrosion rate of copper in bentonite (Wersin 1993):

- Model validity
- Time scale of oxic/anoxic transition
- Pitting factor
- Transport properties in the clay

Modeling which takes into account transport by diffusion in addition to flow, equilibrium reactions and kinetic processes at the bentonite-canister interface has been made (Wersin 1994). The results indicate conservative corrosion rates of 2×10^{-8} and 7×10^{-6} m/y for anoxic and oxic conditions, respectively. A sensitivity analysis indicates that the main uncertainties arise from the diffusion properties of the clay.

8.2 Experimental layout

The purpose with this study was to identify the type and extent of copper corrosion in the field test. Small copper coupons were used instead of the central copper tube, which was only to some extent inspected after the uplift. The reason for this strategy was to get:

- The same copper quality as proposed for the canisters.
- Well characterised test specimens.
- Simple sampling for subsequent analyses.

In total 12 copper coupons were used for the study, 4 were placed in parcel S1, 4 in parcel A1, and 4 were kept as reference. The coupons were delivered by Outokumpu Poricopper OY, Finland, with the nominal dimensions 50x23x1 mm. The copper quality (Table 8-1) was chosen in order to correspond to what is proposed as canister material, which is a very pure copper (99.992% Cu) with a small deliberate addition of phosphorus.

Table 8-1 Chemical analyses of the used copper material (from Outokumpu). All figures in ppm.

Element	Content	Element	Content	Element	Content
Ag	15	Mg	<0.5	Si	<1
Al	<1	Mn	<1	Sn	<3
As	<2	Ni	<3	Te	<2
Bi	<1	P	50	Zn	<1
Cd	<1	Pb	<1	Zr	<2
Co	<3	S	8		
Cr	<1	Sb	3	O_2	1.6
Fe	<2	Se	<1	H_2	0.42

The coupons were initially carefully weighed by use of an analysis balance (Table 8-2). The test coupons were placed in position in the prepared bentonite blocks according to Figure 8.1. The remaining four reference specimens were stored at room conditions (20°C, ~50%RH).

Table 8-2 The engraved marks of the copper coupons, bentonite block in which plates were placed, and the determined mass of the coupons.

coupon mark	block no	mass g	coupon mark	block no	mass g
A	S122	12.2044	G	A130	11.7964
B	S122	11.8130	H	A130	11.8053
C	S130	11.7257	I	R	12.1469
D	S130	12.0647	J	R	12.1186
E	A122	12.0412	K	R	12.3025
F	A122	12.2317	L	R	12.1424

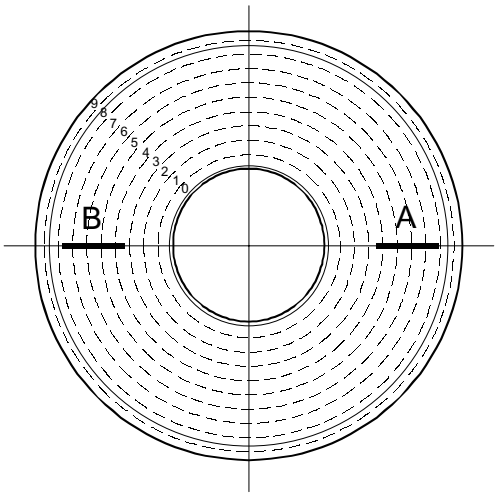

Figure 8-1 Schematic drawing of the upper surface of bentonite block S122 showing slot positions and coupon marks.

8.3 Analyses

8.3.1 Copper samples

The blocks containing the copper coupons were separated from the S1 parcel and transported to Studsvik for analyses. The samples were relatively well protected from air by the surrounding bentonite blocks, which in turn were protected by hermetically sealed plastic bags. The copper coupon containing blocks in parcel A1 were lost during the drilling operation, at uptake, and were consequently not analysed.

Coupon A from block S122 and coupon D from block S130, representing temperature conditions around 50°C and 25°C, respectively were analysed by two different techniques. Coupon A was released from bentonite by mechanical breaking, and coupon D and a few centimetres of covering bentonite was resin impregnated for SEM/EDX analyses.

Coupon A and reference coupon J were analysed in parallel, according to the following scheme:

- Photographing of the copper coupon A (Figure 8-2 left) and bentonite surfaces
- Weighing the copper coupons
- Exposure to deionised water overnight
- Drying, weighing and photographing
- Ultrasonic cleaning in deionised water for 5 minutes
- Drying, weighing and photographing
- Ultrasonic cleaning for 25 minutes in deionised water
- Drying, weighing and photographing
- Ultrasonic cleaning for 30 minutes (totally 60 minutes)
- Drying, weighing and photographing
- Ultrasonic cleaning for 30 minutes (totally 90 minutes)
- Drying, weighing and photographing
- Ultrasonic cleaning for 30 minutes (totally 120 minutes)
- Drying, weighing and photographing (Figure 8-2 centre)
- SEM analyses of coupons A, J and untreated coupon I
- Ultrasonic treatment in 10% H_2SO_4 solution for 10 minutes
- Drying, weighing
- Ultrasonic treatment in 10% H_2SO_4 solution for another 10 minutes
- Drying, weighing, and photographing (Figure 8-2 right)

8.3.2 Adjacent Bentonite

Bentonite in direct contact with copper coupon A was mechanically removed, dried in air and mounted on SEM sample holders in such a way that EDX element analyses could be made perpendicular to the copper-bentonite interface.

Figure 8-2 *Copper coupon A after removal from bentonite (left), after the final washing in water (centre), and coupon J after the last treatment with diluted H_2SO_4, (right). Coupons A and J had a similar appearance after the last treatment.*

8.4 Results

8.4.1 Copper samples

The visual inspection before cleaning did not reveal any significant differences between the surfaces on the copper tubes and the copper coupons.

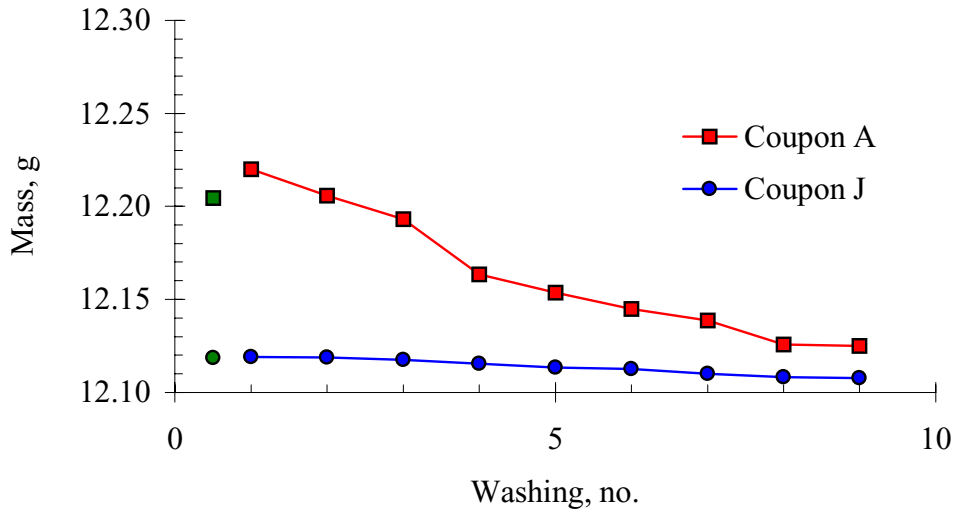

Figure 8-3 *Mass of coupons A (block S122) and J (reference) as a function of repeated washings. First individual dots indicate the original value measured prior to field exposure.*

The mass decrease of coupon A, due to the successive removal of bentonite and corrosion products, are shown in Figure 8-3. The mean corrosion rate ($\overline{R}_c$) was calculate to be 3 µm per year, based on the mass loss of the exposed coupon and reference coupon according to:

$$\overline{R}_c = \frac{\Delta m_e - \Delta m_r}{\rho_{Cu} \cdot A \cdot \frac{365}{t_{exp}}}, \qquad 8\text{-}1$$

where Δm_e is the mass loss of the field exposed coupon, Δm_r is the mass loss of the reference coupon, ρ_{Cu} is the density of copper, A is the exposed surface area of a coupon, and t_{exp} is the exposure time of the coupon expressed in days.

The evaluated mean corrosion rate is obviously not fully adequate to characterise the corrosion, since the corrosion attack may be uneven as Figure 8-2 depicts. However, the optical and SEM micrographs did not reveal any signs of pitting.

The corrosion pattern was rather complicated and several types of corrosion products were present e.g. Cuprite (Cu_2O), and Malachite, ($Cu_2CO_3(OH)_2$). A detailed XRD analysis is therefore planed for the coupons placed in the A0 parcel.

8.4.2 Adjacent bentonite

A higher copper content was noticed in the bentonite in the vicinity of both coupons A and D. Microscopic grains and thereby higher values were found around coupon D, which likely is a result of the impregnation and grinding preparation technique. No such artefacts were though possible around coupon A.

Figure 8-4 shows a cross section of bentonite where the removed copper coupon A originally was situated to the left. Element intensity scans were made for copper and, as reference, for silicon (Figure 8-5). A significant increase in copper content was found only a few microns from the copper surface, but indication of a minor increase compared to reference samples was found tens of microns from the plate.

The ICP/AES analyses of the solid total material (Section 5.8) showed a maximum copper content in the first centimetre of up to 100 ppm and a mean value of around 25 ppm at a distance of 3 cm from the tube.

The copper content in the clay fraction in the first centimetres was only slightly lower, down to 50 ppm, indicating that the copper was incorporated in the montmorillonite structure likely as exchangeable ions or as central ions in the octahedral layer. The ICP/AES analyses of the ion-exchanged solutions from the CEC analyses (Section 5.9) indicate that there was a minor increase in exchangeable copper in the parcel material, but the picture is not unequivocal.

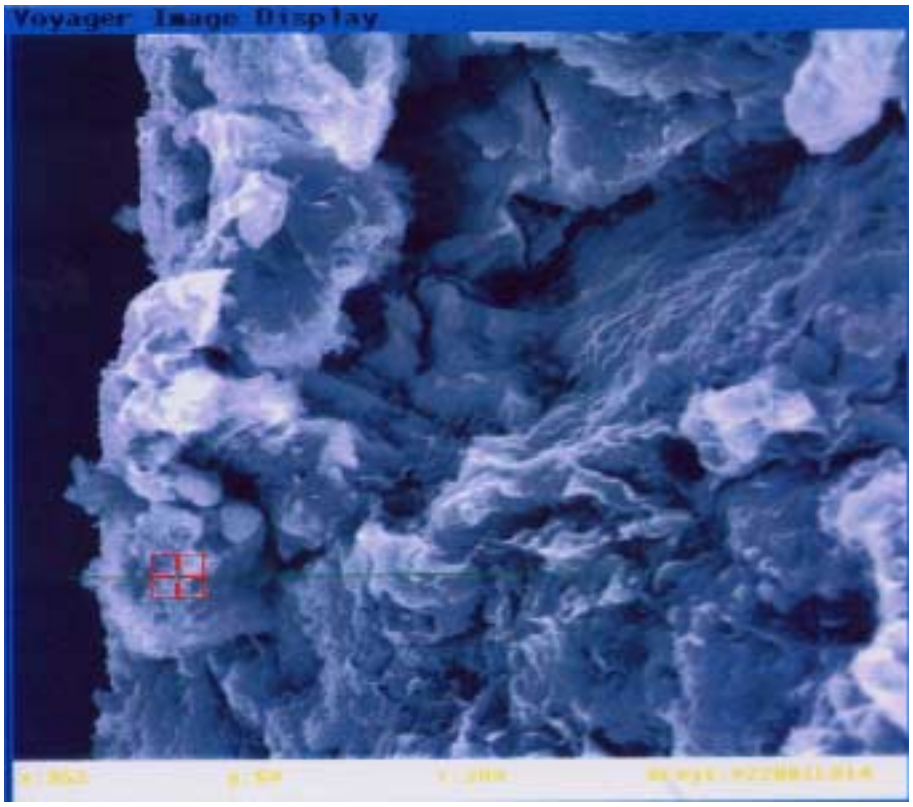

Figure 8-4 *SEM image of bentonite material adjacent to the Cu coupon A. The left side of the bentonite sample was in direct contact with the copper coupon.*

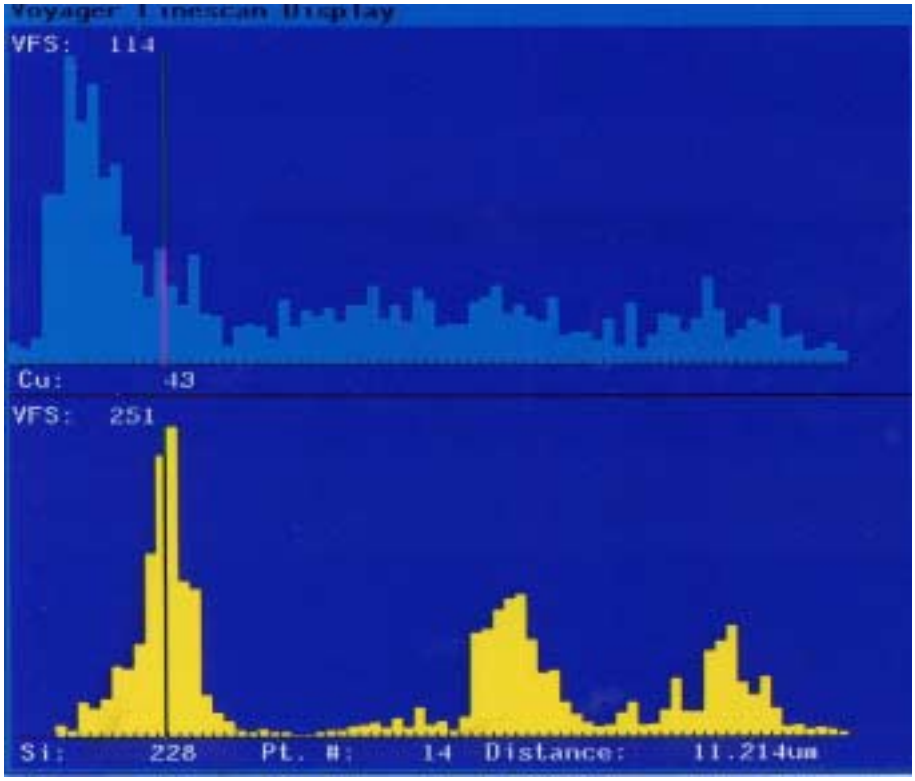

Figure 8-5 *Results of EDX line-scan analyses (as shown in Figure 8-4) of copper (upper) and silicon (lower) from bentonite adjacent to coupon A.*

Acknowledgements

Hans Eriksson has performed the weighing and the photography, and Jiaxin Chen, Camilla Hansson and Kurt Norrgård have performed the SEM work. Their contributions are gratefully acknowledged.

References

Wersin P., Spahiu K., Bruno J. (1994) Time evolution of dissolved oxygen and redox conditions in a HLW repository. SKB Technical Report 94-02. SKB Stockholm, Sweden.

Wersin P., Spahiu K., Bruno J. (1994) Kinetic modelling of bentonite-canister interaction. Long-term predictions of copper canister corrosion under oxic and anoxic conditions. SKB Technical Report 94-25. SKB Stockholm, Sweden.

Wersin P., Bruno J., Spahiu K. (1993) Kinetic modelling of bentonite-canister interaction. Implications for Cu, Fe and Pb corrosion in a repository for spent nuclear fuel. SKB Technical Report 94-25. SKB Stockholm, Sweden.

9 Summary of result and comments

9.1 General

The tests and analyses of the parcel material in the pilot tests were basically aimed at revealing systematic changes compared to the original material. Both water saturation and the long-term processes are expected to give relatively small effects on the buffer. A hypothetical result showing no systematic changes would have been pleasant from a repository point of view, but not from the perspective of the LOT project, since the difference between no actual changes and to crude analyses would then not be clear. Much effort has consequently been spent on improving accuracy, precision and generality of tests and analyses, and to interpret the results. Fortunately, the results concerning parcel material do in several tests and analyses show small but significant changes compared to reference material, which in most cases were expected.

The following sections shortly describe the most interesting results. The bentonite data are in principle considered to be results of the water saturation process and no conclusions concerning the effects of long-term exposure to repository conditions can be drawn before data from the ongoing long-term tests are at hand.

9.2 Bentonite

The data from the original material show that the natural variation of the reference material was small, except for content variations in illite/mica, feldspar and quartz shown by the XRD analyses, which partly are due to the relatively large grains of accessory minerals compared to the XRD samples. Further, the accuracy of the CEC analyses made by ammonium ion exchange technique turned out to be insufficient, and the copper-trien method was therefore used as a complement. On the other hand, the results from swelling pressure and hydraulic conductivity tests are examples where the results were significantly better than in previous test series (section 5.5). In general, the quality and number of analyses from the original reference material are sufficient and the results are believed to give a solid background for comparison with parcel material.

The most important finding concerning the parcel material is that the major part of the bentonite may be described as almost unaffected by the water saturation process under natural conditions and against a temperature gradient, with respect to mineralogy and thereby also to physical properties at full water saturation. However, small but significant changes were found in parts of the parcel material. The main results concerning the bentonite may be summarised in the following items:

- No signs of montmorillonite alteration.
- No significant changes of physical properties.
- Minor redistribution of elements along the temperature gradient, e.g. silicon and magnesium.
- Minor increase/decrease of elements in general, sodium, calcium and potassium, indicating an ion-exchange process.
- Precipitation, mainly gypsum, on the copper tube in the warmest section.

- Increase of minerals, mainly gypsum, in the innermost millimetres of the bentonite in the warmest section.

Observations, which were not related to basic aims with the project:

- The bentonite water saturation process seems qualitatively to have taken place in accordance with previously laboratory experiments.
- The rock around the core-drilled test-holes did not effectively distribute water for saturation as shown by the unsaturated lower part of S1 parcel.

9.3 Cation diffusion

The diffusion test volume in the S1 parcel had at test termination approximately the initial water content, i.e. the bentonite was relatively dry with a water activity of around 0.6. The diffusion under such conditions is expected to be very slow and the experiment confirmed that both caesium and cobalt were in principle immobile under such conditions.

The A1 parcel was fully water saturated and the results significantly different. The cobalt transport was limited, which was to be expected from the relatively high K_d-values and low diffusivities found in previous investigations. The measured distribution values fit well with the calculated profiles, indicating that the apparent diffusivity, D_a, is about 2×10^{-9} cm^2 s^{-1}, which is in good agreement with apparent diffusivities obtained in laboratory experiments as well as in CHEMLAB experiments.

The caesium results, on the other hand, were not possible to accommodate to a diffusion profile. Whereas the activity peak in the distance range 0 to 25 mm indicates an apparent diffusivity of 5×10^{-8} cm^2 s^{-1}, the widely spread level of 200-300 Bq/g clearly shows that part of the activity has been much more dispersed than expected. Convective transport as due to the heating of the system, can probably be ruled out since caesium appears to have moved isotropically. Several different possible explanations to the caesium distribution have been proposed, e.g. high caesium vapour pressure, intra-layer ionic diffusion, mechanical and geometrical conditions in the bentonite, water evaporating close to the copper tube dragging away caesium. Most of these explanations are rather far fetched, and no final conclusions should be drawn from this single experiment.

The results from the S1 parcel confirmed that diffusion in unsaturated bentonite is insignificant, and the results from the A1 parcel confirmed lower mobility of Cobalt compared to caesium, verifying different sorption mechanisms for the cations, i.e. ion exchange for caesium and surface complexation for cobalt. The unexpectedly large dispersion of caesium may be related to the no intentional free swelling, which took place during the excavating drilling. The experiment is therefore repeated in the A0 parcel which is presently run parallel to the ongoing long-term parcels, and in addition, laboratory experiments have been started in order to study the diffusion at elevated temperature in detail under more controlled conditions.

9.4 Bacteria

Microorganisms can grow over a large range of water activities (a_w) down to 0.75, but most favour an a_w of seawater (0.98) or above. The final conditions after water saturation in the LOT bentonite was calculated to have an a_w of 0.96. The water content of the LOT plugs directly after preparation was, however, much lower; only 10% corresponding to an a_w of around 0.75.

Results of laboratory experiments performed previously with Sulphide Reducing Bacteria (Motamedi et al., 1996) showed that the environmental conditions in compacted bentonite clay reduce the number of cultivable SRB by many orders of degree over a 60-day test period. A high reduction rate of cultivable microorganisms was, therefore, expected in the LOT experiment.

The original bentonite material, used to produce the bacteria doped plugs, was heat-treated before mixing with bacteria. The clay was analyses before the treatment in order to determine the natural occurring bacteria and after the treatment to get the test starting numbers. The following major results were obtained:

- The natural occurring numbers of cultivable cells were 3.4 x10^4, and <100 cells per gram dry weight (gdw^{-1}), isolated at 30°C, and 65°C, respectively. The bacteria isolated from the clay included a new species of *Bacillus* sp. (CCUG 36961), *Bacillus cereus* (CCUG 36963), *Pseudomonas stutzeri* (CCUG 36965), *Bacillus subtilis* (CCUG 36967) and *Breviabacillus brevis* (CCUG 36969).
- The number of cultivable aerobic bacteria in the heat-treated clay was 1.1 x 10^2, and <100 cells gdw^{-1} determined at 30°C and at 65°C, respectively.
- No Sulphate Reducing Bacteria (SRB) were found, neither in the heat-treated, nor in the non-heat-treated clay.

Large numbers of microorganisms, in the range of 10^7–10^9 cells gdw^{-1} clay, were introduced into block 17 and block 29 as starting concentrations to counteract the harsh conditions in the clay and the hostile conditions during plug preparation. The material was analysed immediately after mixing and the plugs after 72 hours. The following test start conditions were measured:

- Up to 10% of the introduced aerobic bacteria could be cultured from the clay immediately after preparation.
- The cultivability of SRB differed markedly, depending on the species. The best cultivability was observed for *D. nigrificans. D. salexigens* could not be cultivated from the clay and the number of *D. aespoeensis* was down to 7.5% of the initial population.
- Sampling after 72 hours showed that only *D. radiophilus* and the spore-forming species *B. subtilis*, *B. stearothermophilus* and *D. nigrificans* were cultivable.

The number of cultivable cells of aerobic bacteria consequently decreased dramatically after preparation of the plugs, most probably due to the very desiccated and therefore harsh environmental conditions in the plugs. With the exception of *D. radiophilus*, only spore-forming bacteria could be detected after 72 hours, showing the intolerance of non-spore-forming bacteria to a low a_w.

During the experiment block 17 and block 29 were exposed to temperatures ranging from 50–80 °C and around 25°C, respectively. The water activity start value was 0.75 and the final value was around 0.97. Temperature and water activity co-operated to give a harsher environment in the inner part of the blocks, since water uptake started from the outer mantel surface. After termination of the experiment the following results were measured:

- All bacteria except for the spore-forming species were eliminated below the detection limits.
- The numbers of cultivable aerobic bacteria from the plugs of block 17 were below the detection limit (< 100 cells gdw^{-1}) for all investigated species.
- *B. subtilis* and *B. stearothermophilus* could be isolated from the plugs originally containing aerobic bacteria in block 29 and *B. subtilis* was also cultivated from one of the plugs in block No. 17.
- In the plugs containing SRB, only *D. nigrificans* could be cultured.

The high temperature in block 17 obviously added a significant constraint to the cultivability of the introduced microorganisms, that is, the spores.

The viability of bacterial spores generally show a specific declination rate that may be large or negligible, as a function of a range of spore and environmental characteristics. The results in this study have given detailed information on the interaction between bacteria and the buffer material under repository like conditions.

9.5 Copper corrosion

The visual inspection before the cleaning treatment did not reveal any significant differences between the surfaces of the copper tubes and the copper coupons, with the exception of mineral precipitation on the warmest parts of the tubes. The following basic observations were made concerning the coupons:

- The entire plate surface was affected.
- The corrosion attack was uneven.
- The optical and SEM micrographs did, however, not reveal any signs of pitting.

The mean corrosion rate was calculated to be 3×10^{-6} m/y, based on the mass loss of an exposed sample and a reference sample after removal of corrosion products. This is well in accordance with previous modeling indicating conservative corrosion rates of 2×10^{-8} and 7×10^{-6} m/y for anoxic and oxic conditions, respectively.

The corrosion pattern was rather complicated and several types of corrosion products were present e.g. Cuprite (Cu_2O), and Malachite, ($Cu_2CO_3(OH)_2$). A detailed XRD analysis is therefore planned for on the coupons placed in the A0 parcels.

A higher copper content was noticed in the bentonite in the vicinity the copper coupons A and D. High content were found a few microns from the copper surface. Indication of an increase compared to reference samples was found tens of microns from the plate A according to SEM analyses. The ICP/AES analyses of the solid total material showed a

maximum copper content in the first centimetre of up to 100 ppm and a mean value of around 25 ppm at a distance of 3 cm from the tube.

The copper content increase in the clay fraction indicates that copper was incorporated in the montmorillonite structure, likely as exchangeable ions or as central ions in the octahedral layer. Regardless of the position of the copper, the measured content is too low to result in changes of the clays physical properties. A hypothetical general value of 100 ppm in a KBS3 buffer would correspond to approximately 2 kg copper, which in turn corresponds to a uniform reduction of a canister copper thickness by around 10 μm. An uptake of copper into the bentonite, of the order found in this study, is consequently negligible both with respect to the canister, if the release of copper is evenly distributed, and to the bentonite.

9.6 Additional

Valuable experiences concerning the construction and handling of the test system have been gained during the pilot tests, which now are used in the long-term tests and in the planning of the full-scale tests, i.e. the Canister Retrieval Test and the Prototype Repository Test. The most important findings may be summarised in the following way:

- Unintentionally the large-scale effect of high salinity and reduced mechanical support for the bentonite was experienced in the release operation of the A1 parcel, which led to loss of material during the drilling operation.
- Technique for preparation, handling and instrumentation of bentonite blocks has been developed.
- The Datascan hardware and Orchestrater software data collection system have been adapted to the needs and found sufficient for most instruments and for alarm functions.
- A system for data handling and presentation of field data has been developed.
- Corrosion was a major problem for the sensors in the parcels; e.g. the Inconel 600 material in the thermocouple jacketing did in a few cases not survive the entire test period. Copper was relatively unaffected but is sparsely used in the long-term parcels because of the interest for possible copper uptake into the bentonite from the central tube and the coupons. No effect was found on the titanium components and titanium is therefore chosen in general for the long-term and full-scale tests.

ISSN 1404-0344

CM Digitaltryck AB, Bromma, 2000